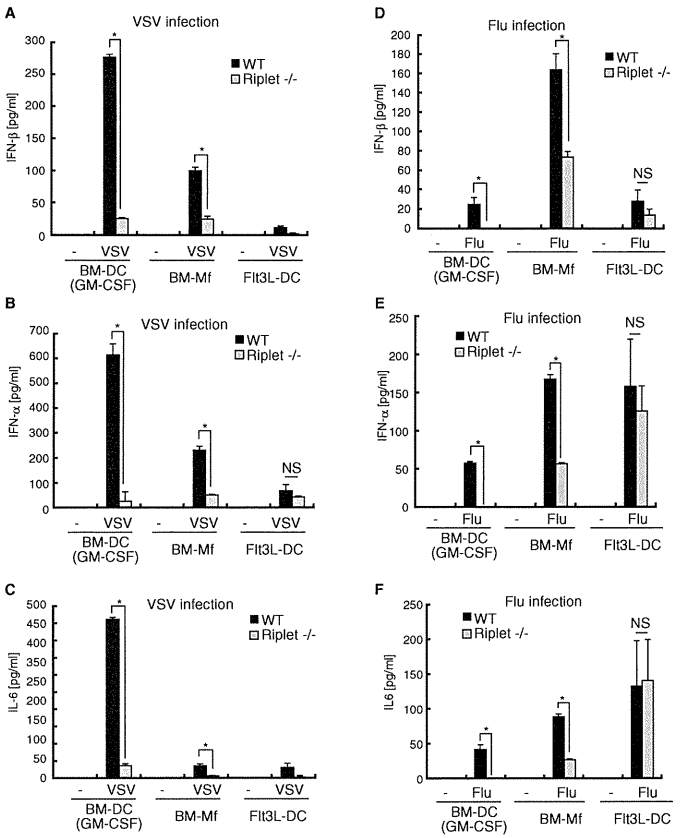

Figure 6. Role of Riplet in Responses to VSV or Flu Infection in Bone Marrow-Derived Cells

GM-DCs, BM-Mf, or Flt3L-DCs were induced from BM-derived cells in the presence of GM-CSF, M-CSF, or Flt3L and infected with VSV or influenza A virus at moi = 1. Twenty-four hours after viral infection, amounts of IFN-β (A and D), -α (B and E), and IL-6 (C and F) in culture supernatants were measured by ELISA. Data are shown as means ±SD and are representative of two independent experiments. *$p < 0.05$ (Student's t test). NS indicates not statistically significant.
See also Figure S4.

by overexpression of Riplet was also abolished by the 5KA mutation. These data support our model. However, we do not exclude the possibility that other Lys residues of RIG-I are ubiquitinated by Riplet, because we have not yet directly detected polyubiquitinated residues of RIG-I CTD by mass spectrometory analysis. Further in vitro studies are required to determine the polyubiquitination sites and to reveal precise RIG-I regulatory mechanisms by Riplet-mediated Lys63-linked polyubiquitation.

In general, E3 ubiquitin ligase targets several types of proteins. Therefore, it is possible that Riplet targets other proteins. Previous work has shown that Riplet binds to the Trk-fused gene (TFG) protein (Suzuki et al., 2001). The TFG protein interacts with TANK and NEMO, which are involved in the NF-κB pathway (Miranda et al., 2006). Although NEMO is involved in IPS-1-mediated signaling, RIG-I CARDs- or MDA5-mediated signaling was normal in *Riplet*$^{-/-}$ MEFs. Therefore, interaction between Riplet

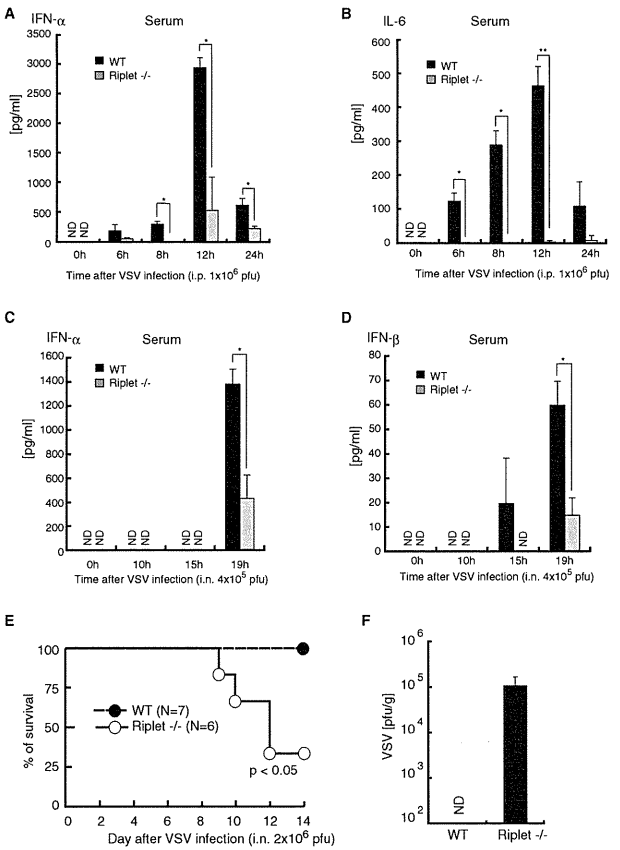

Figure 7. Role of Riplet in Antiviral Responses In Vivo

(A and B) Wild-type or *Riplet*$^{-/-}$ mice were injected intraperitoneally with 1 × 10^6 pfu of VSV. Amounts of IFN-α (A) and IL-6 (B) in mouse serum were measured by ELISA. Data are shown as mean ±SD of samples obtained from three wild-type and three Riplet −/− mice at each time point. *$p < 0.05$ (Student's t test). "ND" indicates not detected.

(C and D) Wild-type and *Riplet*$^{-/-}$ mice were infected intranasally with 4 × 10^5 pfu of VSV. Amounts of IFN-α (C) and IFN-β (D) in mouse serum were measured by ELISA.

(E) Wild-type and *Riplet*$^{-/-}$ mice were infected intranasally with 2 × 10^6 pfu of VSV and mice mortality was observed for 14 days (*$p < 0.05$ between wild-type and *Riplet*$^{-/-}$ mice, log rank test).

(F) Wild-type and *Riplet*$^{-/-}$ mice were infected intranasally with 2 × 10^6 pfu of VSV, and sacrificed for their tissues on day 7 after infection. Titers in brain were determined by the plaque assay. Viral titers in brains of wild-type mice were below 100 pfu/g, and thus not detected (ND). Data are shown as means ±SD ($n = 3$).
See also Figure S5.

and TFG protein is not required for RIG-I-mediated signaling. However, since TFG is involved in tumorigenesis (Miranda et al., 2006), Riplet may be involved in human tumorigenesis.

Several viral proteins inhibit RIG-I-mediated signaling. For example, Flu NS1 inhibits TRIM25 and HCV NS3/4A cleaves IPS-1 (Meylan et al., 2005; Gack et al., 2009). Therefore, Riplet may be inhibited by viral proteins. Indeed, our pilot study indicated that the Riplet protein is disrupted in human hepatocyte cell lines carrying a full-length HCV replicon. RIG-I is involved in innate immune responses against various viruses. In this study, we showed that Riplet is required for innate immune responses against VSV, Flu, and SeV. Therefore, Riplet is also expected to be involved in innate immune responses against other viruses that are recognized by RIG-I.

EXPERIMENTAL PROCEDURES

Generation of Riplet-Deficient Mice

The Riplet gene was amplified by PCR using genomic DNA extracted from ESCs by PCR. The targeting vector was constructed by replacing the second and third exons with a neomycine-resistance gene cassette (Neo), and a herpes simplex virus thymidine kinase (HSV-TK) driven by PGK promoter was inserted into the genomic fragment for negative selection. After the targeting vector was transfected into 129/Sv mice-derived ESCs, G418 and gancyclovir doubly resistant colonies were selected and screened by PCR. The targeted cell line was injected in C57BL/6 blastocysts, resulting in the birth of male chimeric mice. These mice were then crossed with 129/Sv mice to obtain heterozygous mutants. The heterozygous mutants were intercrossed to obtain homozygous *Riplet*$^{-/-}$ mice.

Cells, Viruses, and Reagents

Wild-type and *Riplet*$^{-/-}$ MEFs were prepared from day 12.5–13.5 embryos. *Riplet*$^{-/-}$ MEFs were immortalized with large T antigen and named R3T cell line. BM cells were prepared from 5- to 10-week-old mice. VSV Indiana strain was provided by A. Takada (Hokkaido University). VSV was amplified using Vero cells and the viral titer was determined by the plaque assay. Flu (PR8 strain) and SeV (HVJ strain) was provided by Y. Sakoda (Hokkaido University). HSV-1 strain was provided by K. Kondo (The JIKEI University). Anti-mouse IRF3 antibody was purchased from Zymed. Anti-phospho-STAT1 antibody was purchased from Cell Signaling and anti-STAT1 antibody from Santa Cruz. Salomon sperm dsDNA was purchased from Invitrogen. To determine the viral titer in the brain, the mice were sacrificed, and the brain was aseptically removed and frozen at −80°C. The brain was homogenized in 1 ml of PBS on ice, and the titer was determined by plaque assay.

Preparation of Viral Double-Stranded RNA

cDNA of the HCV 3′UTR region was amplified from total RNA of the HCV genotype 1b full-length replicon using primers HCV-F1 and HCV-R1, and then cloned in the pGEM-T Easy Vector. The primer set sequences were HCV-F1, CTCCAGGTGAGATCAATAGG; and HCV-R1, CGTGACTAGGGCTAAGATGG. RNA was synthesized using T7 and SP6 RNA polymerases. Template DNA was digested by DNase I, and RNA was purified using TRIZOL (Invitrogen) according to manufacturer's instructions.

Quantitative PCR

For qPCR, total RNA was extracted with TRIZOL (Invitrogen) and 0.5 μg of RNA was reverse-transcribed using the High Capacity cDNA Transcription Kit (ABI) with random primers according to the manufacturer's instructions. qPCR was performed using the Step One Real-Time PCR system (ABI). Primer sequences used for qPCR are listed in Table S1.

Measurement of Cytokines

In brief, 5 × 10^5 cells in a 24-well plate were either infected with VSV or Flu, stimulated with LPS, or transfected with HCV 3′UTR dsRNA or poly(I:C). Twenty-four hours after infection, stimulation, or transfection, culture supernatants were collected and analyzed for IFN-α, -β, and IL-6 production by ELISA. Cytokine levels were measured in mouse serum obtained from the mouse tail vein. ELISA kits for mouse IFN-α and -β were purchased from PBL Biomedical Laboratories. ELSA kit for mouse IL-6 was purchased from Invitrogen.

Preparation of Dendritic Cells and Macrophages

BM cells were prepared from the femur and tibia. The cells were cultured in RPMI1640 medium supplemented with 10% FCS, 100 μM 2-Me, and 100 ng/ml human Flt3 ligand (Pepro Tech), and 10 ng/ml murine GM-CSF or culture supernatant NIH 3T3 expressing M-CSF. After 6 days, cells were collected and used as Flt3L-DC, GM-DC, or BM-Mf. In the case of GM-DC or BM-Mf, the medium was changed every 2 days.

Native PAGE Analysis

Approximately 1 × 10^6 MEFs were infected with VSV at moi = 1 for 9 hr and then lysed. Cell lysates in native PAGE sample buffer (62.5 mM Tris-HCl [pH 6.8], 15% glycerol, and BPB) were separated using native PAGE and then immunoblotted with anti-murine IRF3 antibody (Zymed).

Luciferase Assay

Expression plasmids for mouse RIG-I N-terminal CARDs, full-length RIG-I, or full-length MDA5 were constructed in pEF-BOS. The cDNA fragment encoding the ORF of RIG-I or MDA5 was amplified by RT-PCR using total RNA prepared from MEFs. The Riplet dRING mutant protein lacks 1–69 aa region. Wild-type and mutant (Riplet dRING) Riplet-expression vectors were described previously (Oshiumi et al., 2009). Wild-type or *Riplet*$^{-/-}$ MEFs were transiently transfected in 24-well plates with reporter constructs containing the IFN-β promoter and Renilla luciferase (internal control) together with the empty vector (control), RIG-I CARDs, full-length RIG-I, or MDA5 expression vectors. Twenty-four hours after transfection, cells were lysed and subjected to the luciferase assay using the Dual-Luciferase Reporter Assay system (Promega).

Statistical Analyses

Statistical significance of differences between groups was determined by the Student's t test, and survival curves were analyzed by the log rank test using Prism 4 for Macintosh software (GraphPad Sofware, Inc.). Chi-square goodness-of-fit tests and Student's t tests were performed using MS-Excel software and a chi-square distribution table.

SUPPLEMENTAL INFORMATION

Supplemental Information includes five figures, one table, and Supplemental Experimental Procedures and can be found with this article at doi:10.1016/j.chom.2010.11.008.

ACKNOWLEDGMENTS

We thank Dr. John P. Atkinson (Washington University) and Dr. Ralph Steinman (Rockefeller University) for critical discussions, Yoko Esaki and Kiyo Kawata for technical support in generating Riplet KO mice, N. Irie for a pilot study of B-DNA stimulation assay, and Sakoda Y. for technical instructions for the experiments using Flu and SeV. This work was supported in part by the Mitsubishi Foundation; Mochida Foundation; Akiyama Life Science Foundation; and Grants-in-Aid from Ministry of Education, Science, and Culture and Ministry of Health, Labor, and Welfare of Japan.

Received: June 4, 2010
Revised: August 18, 2010
Accepted: November 5, 2010
Published: December 15, 2010

REFERENCES

Akira, S., Uematsu, S., and Takeuchi, O. (2006). Pathogen recognition and innate immunity. Cell *124*, 783–801.

Arimoto, K., Takahashi, H., Hishiki, T., Konishi, H., Fujita, T., and Shimotohno, K. (2007). Negative regulation of the RIG-I signaling by the ubiquitin ligase RNF125. Proc. Natl. Acad. Sci. USA *104*, 7500–7505.

Chiu, Y.H., Macmillan, J.B., and Chen, Z.J. (2009). RNA polymerase III detects cytosolic DNA and induces type I interferons through the RIG-I pathway. Cell *138*, 576–591.

Cui, S., Eisenacher, K., Kirchhofer, A., Brzozka, K., Lammens, A., Lammens, K., Fujita, T., Conzelmann, K.K., Krug, A., and Hopfner, K.P. (2008). The C-terminal regulatory domain is the RNA 5′-triphosphate sensor of RIG-I. Mol. Cell *29*, 169–179.

Diebold, S.S., Kaisho, T., Hemmi, H., Akira, S., and Reis e Sousa, C. (2004). Innate antiviral responses by means of TLR7-mediated recognition of single-stranded RNA. Science *303*, 1529–1531.

Douglas, J., Cilliers, D., Coleman, K., Tatton-Brown, K., Barker, K., Bernhard, B., Burn, J., Huson, S., Josifova, D., Lacombe, D., et al. (2007). Mutations in RNF135, a gene within the NF1 microdeletion region, cause phenotypic abnormalities including overgrowth. Nat. Genet. *39*, 963–965.

Gack, M.U., Shin, Y.C., Joo, C.H., Urano, T., Liang, C., Sun, L., Takeuchi, O., Akira, S., Chen, Z., Inoue, S., and Jung, J.U. (2007). TRIM25 RING-finger E3 ubiquitin ligase is essential for RIG-I-mediated antiviral activity. Nature *446*, 916–920.

Gack, M.U., Kirchhofer, A., Shin, Y.C., Inn, K.S., Liang, C., Cui, S., Myong, S., Ha, T., Hopfner, K.P., and Jung, J.U. (2008). Roles of RIG-I N-terminal tandem CARD and splice variant in TRIM25-mediated antiviral signal transduction. Proc. Natl. Acad. Sci. USA *105*, 16743–16748.

Gack, M.U., Albrecht, R.A., Urano, T., Inn, K.S., Huang, I.C., Carnero, E., Farzan, M., Inoue, S., Jung, J.U., and Garcia-Sastre, A. (2009). Influenza A virus NS1 targets the ubiquitin ligase TRIM25 to evade recognition by the host viral RNA sensor RIG-I. Cell Host Microbe *5*, 439–449.

Gao, D., Yang, Y.K., Wang, R.P., Zhou, X., Diao, F.C., Li, M.D., Zhai, Z.H., Jiang, Z.F., and Chen, D.Y. (2009). REUL is a novel E3 ubiquitin ligase and stimulator of retinoic-acid-inducible gene-I. PLoS ONE *4*, e5760. 10.1371/journal.pone.0005760.

Honda, K., Yanai, H., Takaoka, A., and Taniguchi, T. (2005). Regulation of the type I IFN induction: a current view. Int. Immunol. *17*, 1367–1378.

Honda, K., Takaoka, A., and Taniguchi, T. (2006). Type I interferon [corrected] gene induction by the interferon regulatory factor family of transcription factors. Immunity *25*, 349–360.

Horner, S.M., and Gale, M., Jr. (2009). Intracellular innate immune cascades and interferon defenses that control hepatitis C virus. J. Interferon Cytokine Res. *29*, 489–498.

Hornung, V., Ellegast, J., Kim, S., Brzozka, K., Jung, A., Kato, H., Poeck, H., Akira, S., Conzelmann, K.K., Schlee, M., et al. (2006). 5′-Triphosphate RNA is the ligand for RIG-I. Science *314*, 994–997.

Ishii, K.J., Coban, C., Kato, H., Takahashi, K., Torii, Y., Takeshita, F., Ludwig, H., Sutter, G., Suzuki, K., Hemmi, H., et al. (2006). A Toll-like receptor-independent antiviral response induced by double-stranded B-form DNA. Nat. Immunol. *7*, 40–48.

Ishii, K.J., Kawagoe, T., Koyama, S., Matsui, K., Kumar, H., Kawai, T., Uematsu, S., Takeuchi, O., Takeshita, F., Coban, C., and Akira, S. (2008). TANK-binding kinase-1 delineates innate and adaptive immune responses to DNA vaccines. Nature *451*, 725–729.

Ishikawa, H., and Barber, G.N. (2008). STING is an endoplasmic reticulum adaptor that facilitates innate immune signalling. Nature *455*, 674–678.

Ishikawa, H., Ma, Z., and Barber, G.N. (2009). STING regulates intracellular DNA-mediated, type I interferon-dependent innate immunity. Nature *461*, 788–792.

Kato, H., Sato, S., Yoneyama, M., Yamamoto, M., Uematsu, S., Matsui, K., Tsujimura, T., Takeda, K., Fujita, T., Takeuchi, O., and Akira, S. (2005). Cell type-specific involvement of RIG-I in antiviral response. Immunity *23*, 19–28.

Kato, H., Takeuchi, O., Sato, S., Yoneyama, M., Yamamoto, M., Matsui, K., Uematsu, S., Jung, A., Kawai, T., Ishii, K.J., et al. (2006). Differential roles of MDA5 and RIG-I helicases in the recognition of RNA viruses. Nature *441*, 101–105.

Kawai, T., Takahashi, K., Sato, S., Coban, C., Kumar, H., Kato, H., Ishii, K.J., Takeuchi, O., and Akira, S. (2005). IPS-1, an adaptor triggering RIG-I- and Mda5-mediated type I interferon induction. Nat. Immunol. *6*, 981–988.

Kumagai, Y., Takeuchi, O., Kato, H., Kumar, H., Matsui, K., Morii, E., Aozasa, K., Kawai, T., and Akira, S. (2007). Alveolar macrophages are the primary interferon-alpha producer in pulmonary infection with RNA viruses. Immunity *27*, 240–252.

Kumar, H., Kawai, T., Kato, H., Sato, S., Takahashi, K., Coban, C., Yamamoto, M., Uematsu, S., Ishii, K.J., Takeuchi, O., and Akira, S. (2006). Essential role of IPS-1 in innate immune responses against RNA viruses. J. Exp. Med. *203*, 1795–1803.

Meylan, E., Curran, J., Hofmann, K., Moradpour, D., Binder, M., Bartenschlager, R., and Tschopp, J. (2005). Cardif is an adaptor protein in the RIG-I antiviral pathway and is targeted by hepatitis C virus. Nature *437*, 1167–1172.

Miranda, C., Roccato, E., Raho, G., Pagliardini, S., Pierotti, M.A., and Greco, A. (2006). The TFG protein, involved in oncogenic rearrangements, interacts with TANK and NEMO, two proteins involved in the NF-kappaB pathway. J. Cell. Physiol. *208*, 154–160.

Nakhaei, P., Genin, P., Civas, A., and Hiscott, J. (2009). RIG-I-like receptors: sensing and responding to RNA virus infection. Semin. Immunol. *21*, 215–222.

Onoguchi, K., Yoneyama, M., Takemura, A., Akira, S., Taniguchi, T., Namiki, H., and Fujita, T. (2007). Viral infections activate types I and III interferon genes through a common mechanism. J. Biol. Chem. *282*, 7576–7581.

Oshiumi, H., Matsumoto, M., Hatakeyama, S., and Seya, T. (2009). Riplet/RNF135, a RING finger protein, ubiquitinates RIG-I to promote interferon-beta induction during the early phase of viral infection. J. Biol. Chem. *284*, 807–817.

Pichlmair, A., Schulz, O., Tan, C.P., Naslund, T.I., Liljestrom, P., Weber, F., and Reis e Sousa, C. (2006). RIG-I-mediated antiviral responses to single-stranded RNA bearing 5′-phosphates. Science *314*, 997–1001.

Rehwinkel, J., Tan, C.P., Goubau, D., Schulz, O., Pichlmair, A., Bier, K., Robb, N., Vreede, F., Barclay, W., Fodor, E., and Reis e Sousa, C. (2010). RIG-I detects viral genomic RNA during negative-strand RNA virus infection. Cell *140*, 397–408.

Saito, T., Hirai, R., Loo, Y.M., Owen, D., Johnson, C.L., Sinha, S.C., Akira, S., Fujita, T., and Gale, M., Jr. (2007). Regulation of innate antiviral defenses through a shared repressor domain in RIG-I and LGP2. Proc. Natl. Acad. Sci. USA *104*, 582–587.

Saito, T., Owen, D.M., Jiang, F., Marcotrigiano, J., and Gale, M., Jr. (2008). Innate immunity induced by composition-dependent RIG-I recognition of hepatitis C virus RNA. Nature *454*, 523–527.

Seth, R.B., Sun, L., Ea, C.K., and Chen, Z.J. (2005). Identification and characterization of MAVS, a mitochondrial antiviral signaling protein that activates NF-kappaB and IRF 3. Cell *122*, 669–682.

Shigemoto, T., Kageyama, M., Hirai, R., Zheng, J., Yoneyama, M., and Fujita, T. (2009). Identification of loss of function mutations in human genes encoding RIG-I and MDA5: implications for resistance to type I diabetes. J. Biol. Chem. *284*, 13348–13354.

Sun, Q., Sun, L., Liu, H.H., Chen, X., Seth, R.B., Forman, J., and Chen, Z.J. (2006). The specific and essential role of MAVS in antiviral innate immune responses. Immunity *24*, 633–642.

Suzuki, H., Fukunishi, Y., Kagawa, I., Saito, R., Oda, H., Endo, T., Kondo, S., Bono, H., Okazaki, Y., and Hayashizaki, Y. (2001). Protein-protein interaction panel using mouse full-length cDNAs. Genome Res. *11*, 1758–1765.

Takahasi, K., Yoneyama, M., Nishihori, T., Hirai, R., Kumeta, H., Narita, R., Gale, M., Jr., Inagaki, F., and Fujita, T. (2008). Nonself RNA-sensing mechanism of RIG-I helicase and activation of antiviral immune responses. Mol. Cell *29*, 428–440.

Takeuchi, O., and Akira, S. (2010). Pattern recognition receptors and inflammation. Cell *140*, 805–820.

Xu, L.G., Wang, Y.Y., Han, K.J., Li, L.Y., Zhai, Z., and Shu, H.B. (2005). VISA is an adapter protein required for virus-triggered IFN-beta signaling. Mol. Cell *19*, 727–740.

Yoneyama, M., and Fujita, T. (2009). RNA recognition and signal transduction by RIG-I-like receptors. Immunol. Rev. *227*, 54–65.

Yoneyama, M., and Fujita, T. (2010). Recognition of viral nucleic acids in innate immunity. Rev. Med. Virol. *20*, 4–22.

Yoneyama, M., Kikuchi, M., Natsukawa, T., Shinobu, N., Imaizumi, T., Miyagishi, M., Taira, K., Akira, S., and Fujita, T. (2004). The RNA helicase RIG-I has an essential function in double-stranded RNA-induced innate antiviral responses. Nat. Immunol. *5*, 730–737.

Zeng, W., Sun, L., Jiang, X., Chen, X., Hou, F., Adhikari, A., Xu, M., and Chen, Z.J. (2010). Reconstitution of the RIG-I pathway reveals a signaling role of unanchored polyubiquitin chains in innate immunity. Cell *141*, 315–330.

OPEN ACCESS Freely available online

PLoS one

Hepatitis C Virus Core Protein Abrogates the DDX3 Function That Enhances IPS-1-Mediated IFN–Beta Induction

Hiroyuki Oshiumi[1], Masanori Ikeda[2], Misako Matsumoto[1], Ayako Watanabe[1], Osamu Takeuchi[3], Shizuo Akira[3], Nobuyuki Kato[2], Kunitada Shimotohno[4], Tsukasa Seya[1]*

1 Department of Microbiology and Immunology, Hokkaido University Graduate School of Medicine, Sapporo, Japan, **2** Department of Tumor Virology, Okayama University Graduate School of Medicine, Dentistry, and Pharmaceutical Sciences, Okayama, Japan, **3** Laboratory of Host Defense, WPI Immunology Frontier Research Center, Research Institute for Microbial Diseases, Osaka University, Suita, Japan, **4** Research Institute, Chiba Institute of Technology, Narashino, Japan

Abstract

The DEAD box helicase DDX3 assembles IPS-1 (also called Cardif, MAVS, or VISA) in non-infected human cells where minimal amounts of the RIG-I-like receptor (RLR) protein are expressed. DDX3 C-terminal regions directly bind the IPS-1 CARD-like domain as well as the N-terminal hepatitis C virus (HCV) core protein. DDX3 physically binds viral RNA to form IPS-1-containing spots, that are visible by confocal microscopy. HCV polyU/UC induced IPS-1-mediated interferon (IFN)-beta promoter activation, which was augmented by co-transfected DDX3. DDX3 spots localized near the lipid droplets (LDs) where HCV particles were generated. Here, we report that HCV core protein interferes with DDX3-enhanced IPS-1 signaling in HEK293 cells and in hepatocyte Oc cells. Unlike the DEAD box helicases RIG-I and MDA5, DDX3 was constitutively expressed and colocalized with IPS-1 around mitochondria. In hepatocytes (O cells) with the HCV replicon, however, DDX3/IPS-1-enhanced IFN-beta-induction was largely abrogated even when DDX3 was co-expressed. DDX3 spots barely merged with IPS-1, and partly assembled in the HCV core protein located near the LD in O cells, though in some O cells IPS-1 was diminished or disseminated apart from mitochondria. Expression of DDX3 in replicon-negative or core-less replicon-positive cells failed to cause complex formation or LD association. HCV core protein and DDX3 partially colocalized only in replicon-expressing cells. Since the HCV core protein has been reported to promote HCV replication through binding to DDX3, the core protein appears to switch DDX3 from an IFN-inducing mode to an HCV-replication mode. The results enable us to conclude that HCV infection is promoted by modulating the dual function of DDX3.

Citation: Oshiumi H, Ikeda M, Matsumoto M, Watanabe A, Takeuchi O, et al. (2010) Hepatitis C Virus Core Protein Abrogates the DDX3 Function That Enhances IPS-1-Mediated IFN–Beta Induction. PLoS ONE 5(12): e14258. doi:10.1371/journal.pone.0014258

Editor: Jörn Coers, Duke University Medical Center, United States of America

Received May 28, 2010; **Accepted** November 16, 2010; **Published** December 8, 2010

Funding: This work was supported in part by the Program of Founding Research Centers for Emerging and Reemerging Infectious Diseases, MEXT, Sapporo Biocluster "Bio-S", the Knowledge Cluster Initiative of the MEXT, Grants-in-Aid from the Ministry of Education, Science, and Culture (Specified Project for Advanced Research) and the Ministry of Health, Labor, and Welfare of Japan, Mochida Foundation, Yakult Foundation, NorthTec Foundation and Waxman Foundation. The funders had no role in study design, data collection and analysis, decision to publish, or preparation of the manuscript.

Competing Interests: The authors have declared that no competing interests exist.

* E-mail: seya-tu@pop.med.hokudai.ac.jp

Introduction

The retinoic acid inducible gene-I (RIG-I) and the melanoma differentiation-associated gene 5 (MDA5) encode cytoplasmic RNA helicases [1–3] that signal the presence of viral RNA through the adaptor, IPS-1/Mitochondrial antiviral signaling protein (MAVS)/Caspase recruitment domain (CARD) adaptor inducing interferon (IFN)-beta (Cardif)/Virus-induced signaling adaptor (VISA) to produce IFN-beta [4–7]. IPS-1 is localized to the mitochondrial outer membrane through its C-terminus [6]. Increasing evidence suggests that the DEAD-box RNA helicase DDX3, which is on the X chromosome, participates in the regulation of type I IFN induction by the RIG-I pathway.

DDX3 acts on the IFN-inducing pathway by a complex mechanism. Early studies reported that DDX3 up-regulates IFN-beta induction by interacting with IKKepsilon [8] or TBK1 [9] in a kinase complex. Both TBK1 and IKKepsilon are IRF-3-activating kinases with NF-kappaB- and IFN-inducible properties. DDX3 has been proposed to bind IKKepsilon, and IKKepsilon is generated after NF-kappaB activation [10]. Yeast two-hybrid studies demonstrated that DDX3 binds IPS-1, and both are constitutively present prior to infection (Fig. 1). Ultimately, DDX3 forms a complex with the DEAD-box RNA helicases RIG-I and MDA5 [11], which are present at only low amounts in resting cells, and are up-regulated during virus infection. Previously we used gene silencing and disruption, to show that the main function of DDX3 is to interact with viral RNA and enhance RIG-I signaling upstream of NAP1/TBK1/IKKepsilon [11]. Hence, DDX3 is involved in multiple pathways of RNA sensing and signaling during viral infection.

DDX3 resides in both the nucleus and the cytoplasm [12], and has been implicated in a variety of processes in gene expression regulation, including transcription, splicing, mRNA export, and translation [13]. A recent report suggested that the N-terminus of hepatitis C virus (HCV) core protein binds the C-terminus of DDX3 (Fig. S1) [14,15], and this interaction is required for HCV replication [16]. Although DDX3 promotes efficient HCV infection by accelerating HCV RNA replication, the processes

A

Two representative polyI:C-binding proteins identified by mass-spectrometric analysis

dsRNA-binding protein	ID	Mr (kDa)	polyI:C	polyU	gene name
dsRNA-activated protein kinase	IPI00019463	63 kDa	37	2	PKR
ATP-dependent RNA helicase	IPI00215637	73 kDa	19	12	DDX3

B

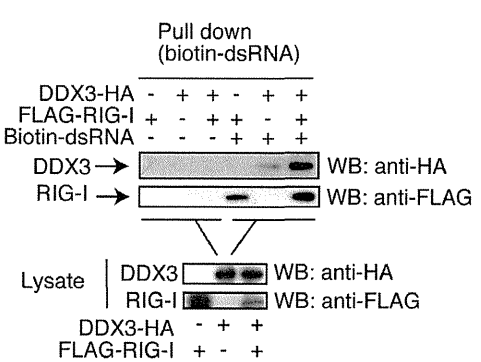

Figure 1. DDX3 is a RNA-binding protein. (A) DDX3 is a polyU- and polyI:C-binding protein. Mass spectrometry analyses indicated that DDX3 binds polyI:C- and polyU-Sepharose, although PKR binds polyI:C but not polyU. The rough data from MASCOT and one representative of six trials are shown. (B) DDX3 binds dsRNA, RIG-I and HCV core protein. Expression vectors for Flag-tagged RIG-I and HA-tagged DDX3 were transfected into HEK293 cells using lipofectamine 2000. Twenty-four hours after the transfection, extract from transfected cells were mixed with biotin-conjugated dsRNA. RNA-protein complex were recovered by pull-down assay using streptavidin-Sepharose. The protein within the pull-down fraction was analyzed by western blotting. The results are representative of two independent experiments.
doi:10.1371/journal.pone.0014258.g001

appear independent of its interaction with the viral core protein [15]. HCV seems to co-opt DDX3, and require DDX3 for replication. In addition, the association between DDX3 and core protein implicates DDX3 in HCV-related hepatocellular carcinoma progression [17]. Therefore, DDX3 could be a novel target for the development of drugs against HCV [18].

A number of reports have demonstrated the formation of the DDX3-core protein complex in the cytoplasm, but the functional relevance of DDX3-core protein interaction is not known. In this report, we show evidence that the HCV core protein participates in suppression of DDX3-augmented IPS-1 signaling for IFN-β induction. Several possible functions of DDX3 are discussed, focusing on its core protein association and IPS-1-regulatory properties.

Materials and Methods

Cell culture and reagents

HEK293 cells and HEK293FT cells were maintained in Dulbecco's Modified Eagle's low or high glucose medium (Invitrogen, Carlsbad, CA) supplemented with 10% heat-inactivated FCS (Invitrogen) and antibiotics. Huh7.5 cells were maintained in MEM (Nissui, Tokyo, Japan) supplemented with 10% heat-inactivated FCS. Hepatocyte sublines with HCV replicon (O cells) and without replicon (Oc cells) were established as described previously [19]. O cells with core-less subgenomic replicon (sO cells) were also generated in Dr. Kato's laboratory [16,19]. RIG-I −/− mouse embryonic fibroblasts (MEF) were gifts from Drs. Takeuchi and Akira [1]. Anti-FLAG M2 monoclonal Ab and anti-HA polyclonal Ab were purchased from Sigma. A mitochondria marker (Mitotracker) and Alexa Fluor®-conjugated secondary antibodies were purchased from Molecular probe. Anti-HCV core mAb (C7-50) [20] and anti-human DDX3 pAb were from Affinity BioReagents, Inc and Abcam, Cambridge MA, respectively.

Plasmids

DDX3 cDNA encoding the entire ORF was cloned into pCR-blunt vector using primers, DDX3N F-Xh (CTC GAG CCA CCA TGA GTC ATG TGG CAG TGG AA) and DDX3C R-Ba (GGA TCC GTT ACC CCA CCA GTC AAC CCC) from human lung cDNA library. To make an expression plasmid, HA tag was fused at the C-terminal end of the full length DDX3 (pEF-BOS DDX3-HA). pEF-BOS DDX3 (1-224aa) vector was made by using primers, DDX3 N-F-Xh and DDX3D1 (GGA TCC GGC ACA AGC CAT CAA GTC TCT TTT C). pEF-BOS DDX3-HA (225-662) was made by using primers, DDX3D2-3 (CTC GAG CCA CCA TGC AAA CAG GGT CTG GAA AAA C) and DDX3C R-Ba. To make pEF-BOS DDX3-HA (225-484) and pEF-BOS DDX3-HA (485-663), the primers, DDX3D2 R-Ba (GGA TCC AAG GGC CTC TTC TCT ATC CCT C) and DDX3D3 F-Xh (CTC GAG CCA CCA TGC ACC AGT TCC GCT CAG GAA AAA G) were used, respectively. HCV core expressing plasmids, pcDNA3.1 HCVO core or JFH1 core, were previously reported by N. Kato (Okayama University Japan) [16]. Another 1b genotype of the core was cloned from a HCV patient in Osaka Medical Center (Osaka) according to the recommendation of the Ethical Committee in Osaka. We obtained written informed consent from each patient for research use of their samples. Reporter and internal control plasmids for reporter gene assay are previously described [21,22].

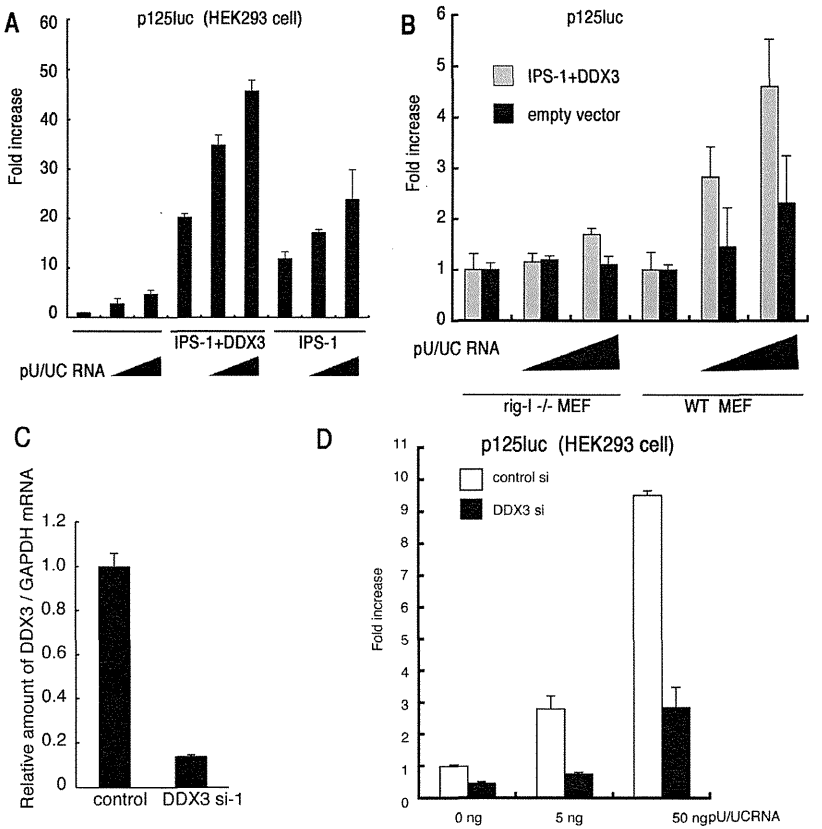

Figure 2. DDX3 is a positive regulator of IPS-1-mediated IFN promoter activation. (A) IFN-β induction by polyU/UC is augmented by DDX3. IPS-1 (100 ng), DDX3 (100 ng) and p125luc reporter (100 ng) plasmids were transfected into HEK293 cells in 24-well plates with or without the HCV 3′ UTR poly U/UC region (PU/UC) RNA (0, 25 or 50 ng/well), synthesized *in vitro* by T7 RNA polymerase. HCV RNA-enhancing activation of IFN-beta promoter was assessed by reporter assay in the presence or absence of the DDX3-IPS-1 complex. (B) RIG-I is essential for the DDX3/IPS-1-mediated IFN-promoter activation. MEF from wild-type and RIG-I −/− mice were transfected with plasmids of IPS-1, DDX3 and p125luc as in panel A, and stimulated with polyU/UC (0, 25 or 50 ng/well). Reporter activity was determined as in panel A. (C) Knockdown of DDX3. Negative control or DDX3 targeting siRNA (20 pmol), DDX3 si-1, was transfected into HEK293 cells, and after 48 hrs, expression of endogenous DDX3 mRNA was examined by real-time RT-PCR. DDX3 si-1-mediated down-regulation of the DDX3 protein was also confirmed by Western blotting (data not shown). (D) DDX3 enhances RIG-I-mediated IFN-beta promoter activation induced by polyU/UC. DDX3 si-1 or control siRNA was transfected into HEK293 cells with reporter plasmids (100 ng). After 48 hrs, cells were stimulated with polyU/UC (5~50 ng/ml) with lipofectamin 2000 reagent for 6 hrs, and activation of the reporter p125luc was measured. The results are representative of at least two independent experiments, each performed in triplicate.
doi:10.1371/journal.pone.0014258.g002

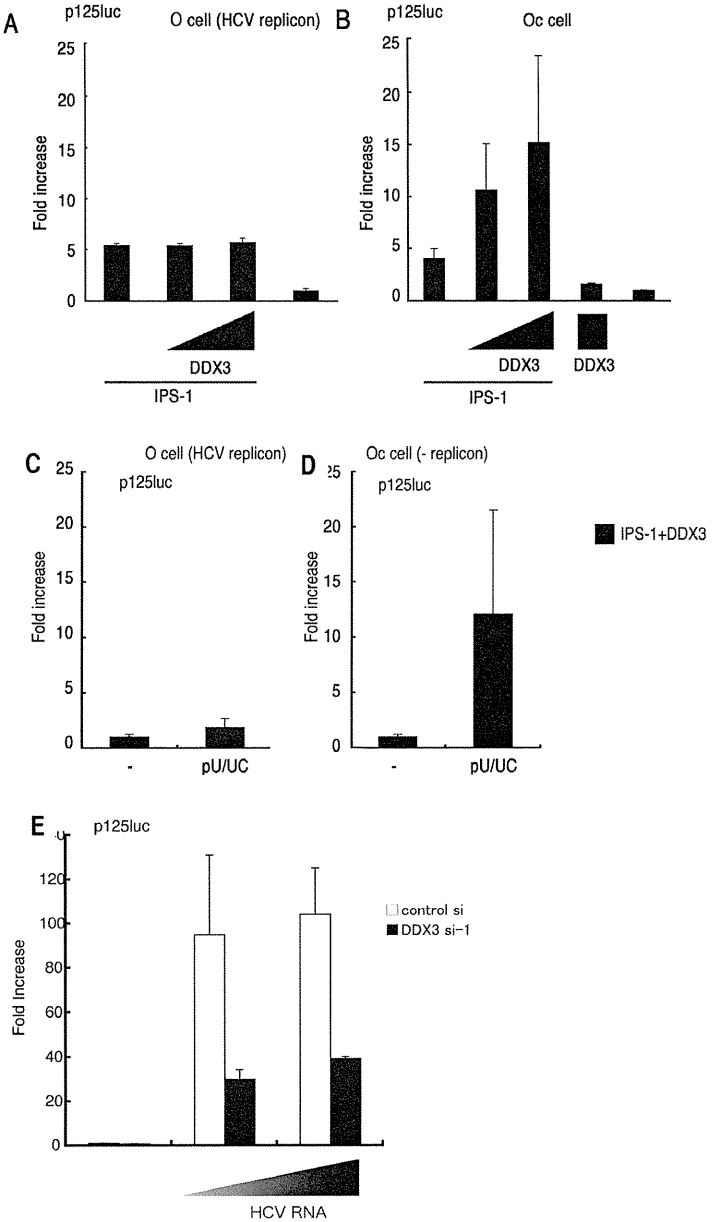

Figure 3. The HCV replicon suppresses IPS-1/DDX3-mediated augmentation of IFN promoter activation. (A,B) O cells with the HCV replicon fail to activate an IFN-β reporter in response to IPS-1/DDX3. O cells contain the full-length HCV replicon, and Oc cells do not [16]. O cells (A) or Oc cells (B) were transfected with IPS-1, DDX3 or p125luc reporter plasmids. At timed intervals (24 hrs), reporter activity was determined as in Fig. 2. (C,D) The HCV replicon suppresses IFN-promoter activation by polyU/UC. O cells and Oc cells expressing IPS-1 and DDX3 were stimulated with polyU/UC. At 48 hrs, reporter activity was determined as in panel A. (E) DDX3 is required for enhanced activation of IFN-beta promoter by O cell HCV 3′UTR. HCV 3′ UTR cDNA was amplified by RT-PCR from RNA extracted from O cells containing full-length HCV replicon. The HCV 3′ UTR RNA was synthesized *in vitro* using T7 RNA polymerase. DDX3 siRNA or control siRNA was transfected into HEK293 cells with the p125luc reporter. After 24 hrs, cells were transfected with HCV RNA, and incubated for 24 hrs. The IFN-beta promoter activation was assessed by luciferase reporter assay. One representative of at least three independent experiments, each performed in triplicate, is shown.
doi:10.1371/journal.pone.0014258.g003

Preparation of HCV polyU/UC RNA

The HCV genotype 1b polyU/UC RNA (from 9421 to 9480, Accession number: EU867431) [23] was synthesized by T7 RNA polymerase *in vitro*. The template dsDNA sequences were; Forward: TAA TAC GAC TCA CTA TAG GGT TCC CTT TTT TTT TTT CTT TTT TTT TTT TTT TTT TTT TTT TTT TTT TTT CTC CTT TTT TTT TC, Reverse: GAA AAA AAA AGG AGA AAA AAA AAA AAA AAA AAA AAA AAA AGA AAA AAA AGG GAA CCC TAT AGT GAG TCG TAT TA. The synthesized RNA was purified by TRIZOL reagent (Invitrogen). cDNA of HCV 3′ UTR region was amplified from total RNA of O cells using primers HCV-F1 and HCV-R1, and then cloned into pGEM-T easy vector. The primer set sequences were HCV-F1: CTC CAG GTG AGA TCA ATA GG and HCV-R1: CGT GAC TAG GGC TAA GAT GG. RNA was synthesized using T7 and SP6 RNA polymerases. Template DNA was digested by DNase I, and RNA was purified using TRIZOL (Invitrogen) according to manufacturer's instructions.

RNAi

Knockdown of DDX3 was carried out using siRNA, DDX3 siRNA-1: 5′-GAU UCG UAG AAU AGU CGA ACA-3′, siRNA-2: 5′-GGA GUG AUU ACG AUG GCA UUG-3′, siRNA-3: 5′-GCC UCA GAU UCG UAG AAU AGU-3′ and control siRNA: 5′-GGG AAG AUC GGG UUA GAC UUC-3′. 20 pmol of each siRNA was transfected into HEK293 cells in 24-well plate with Lipofectamin 2000 according to manufacture's protocol. Knockdown of DDX3 was confirmed 48 hrs after siRNA transfection. Experiments were repeated twice for confirmation of the results.

Reporter assay

HEK293 cells (4×10^4 cells/well) cultured in 24-well plates were transfected with the expression vectors for IPS-1, DDX3 or empty vector together with the reporter plasmid (100 ng/well) and an internal control vector, phRL-TK (Promega) (2.5 ng/well) using FuGENE (Roche) as described previously [23]. The p-125 luc reporter containing the human IFN-beta promoter region (−125 to +19) was provided by Dr. T. Taniguchi (University of Tokyo, Tokyo, Japan). The total amount of DNA (500 ng/well) was kept constant by adding empty vector. After 24 hrs, cells were lysed in lysis buffer (Promega), and the *Firefly* and *Renella* luciferase activities were determined using a dual-luciferase reporter assay kit (Promega). The *Firefly* luciferase activity was normalized by *Renella* luciferase activity and is expressed as the fold stimulation relative to the activity in vector-transfected cells. Experiments were performed three times in duplicate (otherwise indicated in the legends).

PolyI:C or polyU/UC stimulation

PolyI:C was purchased from GE Healthcare company, and solved in milliQ water. For polyI:C treatment, polyI:C was mixed with DEAE-dextran (0.5 mg/ml) (Sigma) in the culture medium, and the cell culture supernatant was replaced with the medium containing polyI:C and DEAE-dextran. Using DEAE-dextran, polyI:C is incorporated into the cytoplasm to activate RIG-I/MDA5.

HCV 3′ UTR poly U/UC region (PU/UC) RNA (0~50 ng/well), which is synthesized *in vitro* by T7 RNA polymerase, transfected into HEK293 cells in 24-well plate by lipofectamin 2000 (Invitrogen) with other plasmids. Cells were allowed to stand for 24~48 hrs and HCV RNA-enhancing activation of IFN-beta promoter was assessed by reporter assay.

Immunoprecipitation (i.p.)

HEK293FT cells were transfected in a 6-well plate with plasmids encoding DDX3, IPS-1, RIG-I or MDA5 as indicated in the figures. 24 hrs after tranfection, the total cell lysate was prepared by lysis buffer (20 mM Tris-HCl [pH 7.5] containing 125 mM NaCl, 1 mM EDTA, 10% Glycerol, 1% NP-40, 30 mM NaF, 5 mM Na_3Vo_4, 20 mM IAA and 2 mM PMSF), and the protein was immunoprecipitated with anti-HA polyclonal (SIGMA) or anti-FLAG M2 monoclonal Ab (SIGMA). The precipitated samples were resolved on SDS-PAGE, blotted onto a nitrocellulose sheet and stained with anti-HA (HA1.1) monoclonal (SIGMA), anti-HA polyclonal or anti-FLAG M2 monoclonal Ab.

Pull-down assay

The pull-down assay was performed according to the method described in Saito T et al. [24]. Briefly, the RNA used for the assay was purchased from JBioS, Co. Ltd (Saitama, Japan). The RNA sequences are (sense strand) AAA CUG AAA GGG AGA AGU GAA AGU G, (antisense strand)CAC UUU CAC UUC UCC CUU UCA GUU U. The biotin is conjugated at U residue at the 3′ end of antisence strand (underlined). Biotinylated double-stranded (ds)RNA were incubated for 1 hr at 25°C with 10 μg of protein from the cytoplasmic fraction of cells that were transfected with Flag-tagged RIG-I and HA-tagged DDX3 expressing vectors. The mixture was transferred into 400 μl of lysis buffer containing 25 μl of streptavidine Sepharose beads, rocked at 4°C for 2 h, collected by centrifugation, washed three times, resuspended in SDS sample buffer.

Proteome analysis of RNA-binding proteins

RNA-binding proteins were identified by affinity chromatography and Mass spectrometry. Briefly, cell lysate was prepared from human HEK293 or Raji cells as will be described elsewhere (Watanabe and Matsumoto, manuscript submitted for publication). The lysate was first applied to polyU-Sepharose and then the pass-through fraction was applied to PolyI:C-Sepharose. The eluted proteins were analyzed on Mass spectrometry using the MASCOT software.

Confocal analysis

HCV replicon-positive (O) or –negative (Oc) cells were plated onto cover glass in a 24-well plate. In the following day, cells were transfected with indicated plasmids using Fugene HD (Roch). The

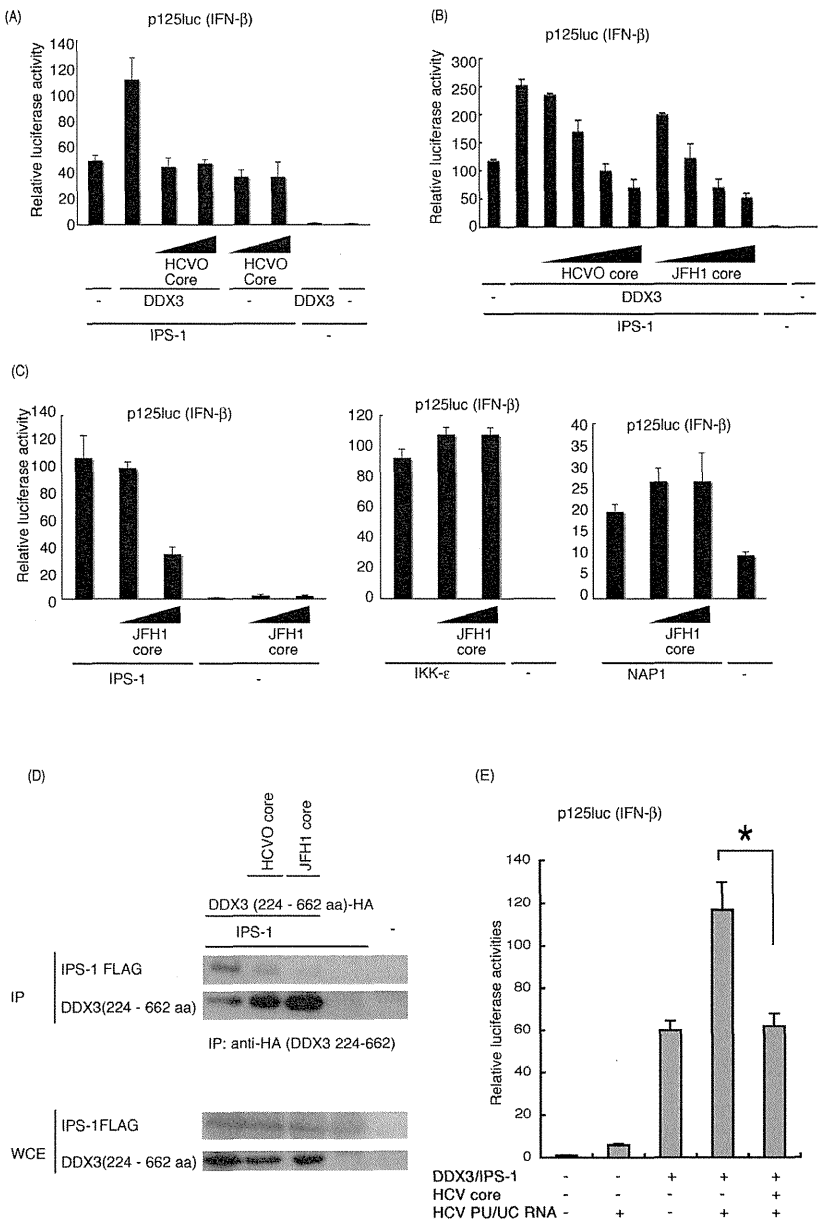

Figure 4. HCV core protein inhibits DDX3 promotion of IPS-1-mediated IFN-beta induction. (A) Expression plasmids for IPS-1 (100 ng), DDX3 (200 ng) and/or HCVO core (50 or 100 ng) were transfected into HEK293 cells in 24-well plates with reporter plasmids, and reporter activity was examined. (B) Expression plasmids for IPS-1 (100 ng), DDX3 (100 ng), and/or HCVO or JFH1 core (10, 25, 50 or 100 ng) were transfected into HEK293 cells, and reporter gene expression was analyzed. (C) IPS-1-, IKKepsilon- or NAP1-expressing plasmids were transfected into HEK293 cells with HCV JFH1 core-expressing plasmids (25 or 100 ng), for reporter gene analysis. (D) Plasmids for expression of FLAG-tagged IPS-1 (400 ng), HA-tagged DDX3 partial fragment (400 ng) and HCVO or JFH1 core (400 ng) were transfected into HEK293FT cells. 24 hrs later cells were lyzed and the lysate was incubated with anti-HA Ab for immunoprecipitation. The DDX3 (224-662)-bound IPS-1 was blotted onto a sheet and probed with anti-Flag Ab. Whole cell lysate was also stained with anti-tag Abs. (E) IPS-1 (100 ng), DDX3 (100 ng), JFH1 core (50 ng) and/or p125 luc reporter (100 ng) plasmids were transfected with HEK293 cells, with HCV 3'UTR poly-U/UC (PU/UC) RNA (25 ng), synthesized *in vitro*. Cell lysates were prepared after 24 hrs, and luciferase activities measured. One representative of at least three independent experiments is shown except for panel D, which is a representative of two sets of the experiments.
doi:10.1371/journal.pone.0014258.g004

amount of DNA was kept constant by adding empty vector. After 24 hrs, cells were fixed with 3% of paraformaldehyde in PBS for 30 minutes, and then permeabilized with PBS containing 0.2% of Triton X-100 for 15 min. Permeabilized cells were blocked with PBS containing 1% BSA, and were labeled with anti-Flag M2 mAb (Sigma) or anti-HA pAb (Sigma) in 1% BSA/PBS for 1 hr at room temperature [25]. In some cases, endogenous proteins were directly stained with anti-core (C7-50) mAb (Affinity BioReagents, Inc) or anti-DDX3 pAbs (Abcam, Cambridge MA). The cells were then washed with 1% BSA/PBS and treated for 30 min at room temperature with Alexa-conjugated antibodies (Molecular Probes). Thereafter, micro-cover glass was mounted onto slide glass using PBS containing 2.3% DABCO and 50% of glycerol. The stained cells were visualized at ×60 magnification under a FLUOVIEW (Olympus, Tokyo, Japan).

Results

DDX3 binds RNA species

We have performed proteome analyses of RNA-binding fractions in human dendritic cell lysate eluted from polyU and polyI:C Sepharose. 127 cytoplasmic proteins were reproducibly identified as polyI:C-binding proteins (Watanabe and Matsumoto, unpublished data). Four of them are DEAD/H box helicases. In this setting, we found DDX3 is a RNA-binding protein (Fig. 1A). DDX3 in cell lysate bound both polyU and polyI:C, while the control PKR bound only to polyI:C.

Using biotinylayed dsRNA, RNA-binding properties of DDX3 and RIG-I were tested by pull-down assay. DDX3 or RIG-I protein was co-precipitated with dsRNA in HEK293 cells expressing either alone of DDX3 or RIG-I (Fig. 1B). Strikingly, higher amounts of DDX3 and RIG-I were precipitated with dsRNA in cells expressing both proteins (Fig. 1B). This, taken together with previous results [11,14,16], indicates that DDX3 assembles in some RNA, RIG-I, IPS-1 and HCV core protein in its C-terminal domain (Fig. S1).

PolyU/UC but not replicon enhances IFN-β induction via IPS-1/DDX3

A polyU/UC sequence is present in the 3'-region of the HCV genome, and serves as a ligand for RIG-I in IPS-1 pathway activation [23]. We produced the polyU/UC RNA and tested its IFN-beta-inducing activity in the presence or absence of DDX3 and IPS-1 (Fig. 2A). HCV polyU/UC promoted IPS-1-mediated IFN-beta induction, and this was further enhanced by forced expression of DDX3/IPS-1 (Fig. 2A). Similar results were obtained with wild-type mouse embryonic fibroblasts (MEF) (Fig. 2B). We also investigated whether DDX3 enhanced IPS-1-mediated IFN-β promoter activation in a RIG-I −/− MEF background (Fig. 2B). In IPS-1/DDX3-expressing MEF cells, polyU/UC IFN-induction was almost totally abrogated by the lack of RIG-I, suggesting that the trace RIG-I protein in the IPS-1 complex is required for DDX3 enhancement of the polyU/UC-mediated IFN response.

DDX3 mRNA (Fig. 2C) and protein [11] were depleted in HEK293 cells by gene silencing with si-1 siRNA, so this was used for DDX3 loss-of-function analysis. Control or DDX3-silinced cells were transfected with increasing amounts of polyU/UC and IFN-beta promoter activation was determined by luciferase assay. DDX3 loss-of-function resulted in a decrease of promoter activation by intrinsic polyU/UC (Fig. 2D). The result was confirmed with cells over-expressing RIG-I and exogenous polyI:C stimulation. HEK293 cells were transfected with a plasmid for the expression of RIG-I and stimulated with polyI:C, an activator of the IPS-1 pathway (Fig. S2A). IFN-beta reporter activation was suppressed in si-1-treated cells that expressed RIG-I, since polyI:C lots often contain short size duplexes that can activate RIG-I [26]. In addition, DDX3 augmented the IFN-beta response in cells expressing MDA5/IPS-1 (Fig. S2B). Thus, DDX3 was also crucial for IPS-1-mediated IFN-beta promoter activation.

We next determined whether the HCV replicon triggers IPS-1/DDX3 IFN promoter activation, using human hepatocyte lines with the HCV replicon (O cells) or without it (Oc cells). In O cells with the HCV replicon, IPS-1/DDX3 expression showed minimal enhancement of IFN-beta promoter activation (Fig. 3A), while in control Oc cells with no replicon, DDX3 facilitated IFN-beta promoter activation (Fig. 3B). Similarily, an augmented IFN promoter response to polyU/UC was observed in control Oc cells, but not in O cells (Figs. 3C and 3D). HCV RNA was prepared from O cells, and its ability to activate the IFN-beta reporter was tested in HEK293 cells (Fig. 3E). The HCV RNA of O cells had a high potency to induce reporter activation, and this activity was largely abrogated by si-1 siRNA treatment. Therefore, DDX3 augments IPS-1-mediated IFN-beta promoter activation in hepatocyte O cells, and HCV RNA, presumably the 3'UTR, participates in this induction. However, no IFN-beta reporter activation was detected in O cells which harbor HCV replicon. Therefore, an unidentified viral factor appeared to participate in suppressing virus RNA-mediated IFN-beta induction, which occurred in O cells overexpressing DDX3/IPS-1.

HCV core protein inhibits IPS-1 signaling through DDX3

What HCV proteins participate in IFN-beta induction was tested in a pilot study using protein expression analysis. We found that expression of HCV core protein as well as NS3/4A led to suppression of IFN-beta reporter activity in Oc cells (data not shown). The HCV core protein physically binds DDX3 [14,16], and co-localizes with DDX3 in the cytoplasm of HeLa cells transfected with HCV core protein [14]. Furthermore, we showed that DDX3 binds IPS-1, which resides on the mitochondrial outer membrane, and assembles into RNA-sensing receptors. Since some populations of the HCV core protein localize on the mitochondrial outer membrane [27], we tested if HCV core

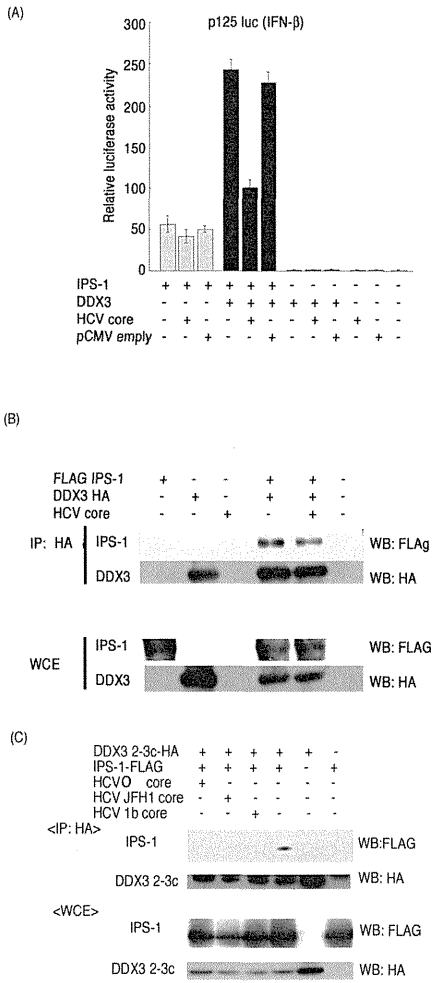

Figure 5. Properties of a 1b-type core protein in the IPS-1 pathway. (A) A core protein derived from an HCV patient suppressed DDX3-mediated activation of IPS-1 signaling. The 1b-type core protein was cloned into the pCMV vector from a patient with hepatitis C. IPS-1 (100 ng), DDX3 (100 ng) and HCV core (100 ng) expression vectors were transfected into HEK293 cells with a reporter plasmid (p125luc), for analysis as in Figure 4. (B) The core protein reduced interaction between full-length DDX3 and IPS-1. The plasmids encoding core protein (400 ng), DDX3-HA (400 ng) and FLAG-IPS-1 (400 ng) were transfected into HEK293FT cells. After 24 hrs, cell lysates were prepared and immunoprecipitation was carried out using anti-HA (DDX3-HA). (C) The core protein blocked interaction between the C-terminal fragment of DDX3 and IPS-1. The C-terminal region of DDX3 (199–662 aa) called DDX3 2-3c, IPS-1, HCV (O) and JFH1 or 1b core expression plasmids were transfected into HEK293FT cells. After 24 hrs, cell lysates were prepared and immunoprecipitation was carried out with anti-HA (DDX3 2–3c). Immunoprecipitates were analyzed by SDS-PAGE and Western blotting with anti-HA or FLAG antibodies. The results are representative of two independent experiments.

doi:10.1371/journal.pone.0014258.g005

protein affects IPS-1 signaling by binding to DDX3. The cDNAs for HCV core proteins, genotype 1b (HCVO) and 2a (JFH1) [16], were co-transfected into HEK293 together with IPS-1, DDX3, and reporter plasmids, and core protein interference with IPS-1/DDX3-mediated IFN-beta promoter activation was examined. We found that the core proteins of HCVO and JFH1 suppressed IPS-1/DDX3-augmented IFN-beta-induction in a dose-dependent manner (Fig. 4A and 4B). Without DDX3 transfection, core protein had no effect on IPS-1-mediated IFN-beta promoter activation (Fig. 4A). JFH1 core slightly more efficiently inhibited IPS-1/DDX3-augmented IFN-beta-induction than HCVO core (Fig. 4B).

Although some endogenous DDX3 was present in the cytoplasm without DDX3 transfection, only IPS-1 transfection permitted minimal induction of IFN-beta. It is notable that high doses of the HCV JFH1 core protein was needed to inhibit the IPS-1-mediated IFN-beta-induction signal (Fig. 4C, left panel). Since the imaging profile of DDX3 is not always monotonous in human cells, its distribution may be biased in the cytoplasm, which may reason that only a high dose of HCV core involves preoccupied DDX3 protein to inhibit the IPS-1 pathway. This is consistent with earlier reports on an NS3-independent mechanism to block IFN induction using HCV-infected Huh 7 cells [28].

IPS-1 transduces a RNA replication signal to result in IFN-beta output using downstream proteins, such as NAP1 and IKKeysilon. If the HCV core protein interferes with IPS-1 function through DDX3, the core should not inhibit over-expressed downstream molecules. As predicted, HCV core protein did not suppress the IKKepsilon- or NAP1-mediated IFN-beta-inducing signal (Fig. 4C, center and right panels). Hence, the core protein blocks the action of endogenous DDX3 and overexpressed IPS-1 to facilitate minimal IFN-beta promoter activation, and this IFN-beta blocking function of core does not target IKKepsilon or NAP1 (Fig. 4C). An upstream molecule of IKKepsilon and NAP1 is predicted to be the target of the HCV core protein, which is in line with the fact that the HCV core protein interacts with DDX3 [14,16].

To further confirm this model, we examined whether the HCV core protein inhibits the physical interaction between IPS-1 and DDX3. Full length IPS-1 and the C-terminal fragment of DDX3, which binds to the IPS-1 CARD-like region, were transfected into HEK293 cells, with or without the HCV core protein, and the DDX3 fragment was immunoprecipitated. Expression of HCV core proteins strongly inhibited interaction between the DDX3 C-terminal fragment and IPS-1 (Fig. 4D). JFH1 core appeared to show greater inhibition to DDX3-IPS-1 interaction than HCVO. We then examined this IFN-beta blocking function of JFH1 core in a similar cell condition plus polyU/UC. DDX3/IPS-1-enhanced p125luc reporter activity in cells stimulated with polyU/UC (Fig. 4E) was decreased in cells expressing HCV core. The results suggest that the role of the core in HCV-infected cells is to remove DDX3 from IPS-1, and facilitate its interaction with HCV replication complex (Fig. S1).

PolyU/UC HCV RNA activates the IFN-beta promoter (Fig. 2A), and this activity was inhibited by expression of the HCV core protein (Fig. 4E). PolyI:C/RIG-I-mediated IFN-β promoter activation was similarly suppressed by the core protein

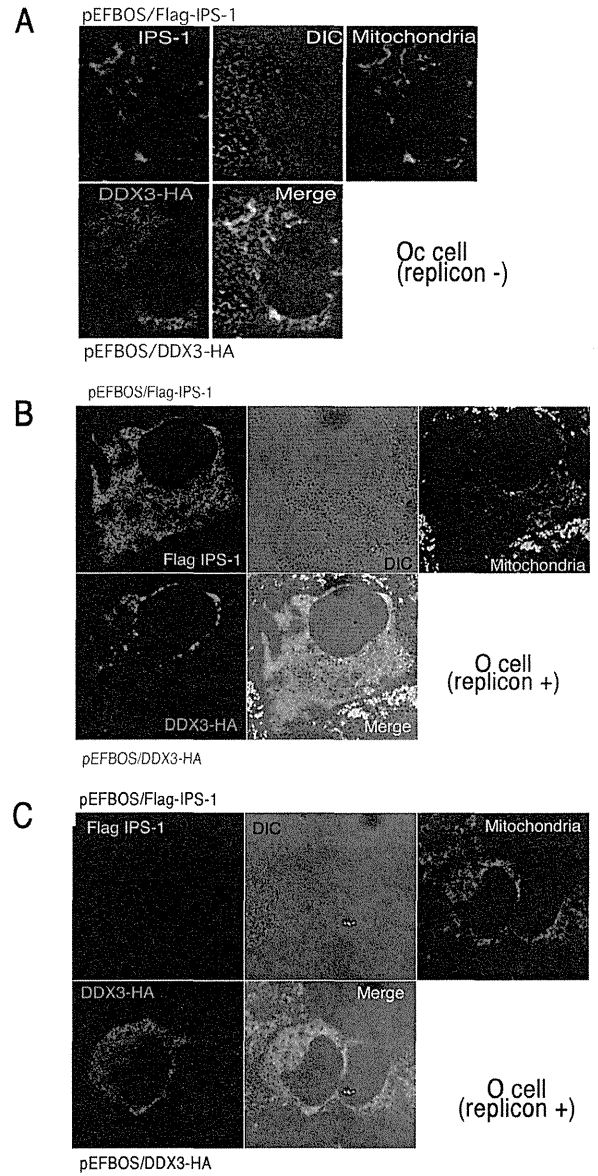

Figure 6. Distribution of DDX3 and IPS-1. (A) DDX3 colocalizes with IPS-1 on the mitochondria in Oc cells. HA-tagged DDX3 and FLAG-tagged IPS-1 were co-transfected into Oc cells. After 24 hrs, cells were fixed with formaldehyde and stained with anti-HA polyclonal and FLAG monoclonal Abs. Alexa488 (DDX3-HA) or Alexa633 antibody was used for second antibody. Mitochondria were stained with Mitotracker Red. Similar IPS-1-DDX3 merging profiles were observed in Huh7.5.1 cells (Fig. S3). (B,C) O cells with the HCV replicon poorly formed the DDX3-IPS-1 complex. Plasmids carrying IPS-1 (100 ng) or DDX3 (150 or 300 ng) were transfected into O (HCV replicon +) as in Oc cells (no replicon, panel A). After 24 hrs, localization of IPS-1 and DDX3 was examined by confocal microscopy. Two representatives which differ from the conventional profile (as in panel A) are shown. Similar sets of experiments were performed four times to confirm the results.
doi:10.1371/journal.pone.0014258.g006

(Fig. S2A). MDA5-dependent IFN-beta promoter activation was also suppressed by the core expression (Fig. S2B). The inhibitory effect of the core protein on DDX3-IPS-1 interaction was further confirmed using an 1b core isoform isolated from a patient. This HCV core protein also reduced interaction as well as IPS-1-mediated IFN-beta promoter activation (Fig. 5A). The blocking effect was relatively weak in cells expressing IPS-1 and full-length DDX3 (Fig. 5B). We presume that this is because there are multiple binding sites for IPS-1 in the DDX3 whole molecule [11]. For binding assay, we used DDX3 2-3c (across a.a. 199~662, longer than 224~662) instead of the whole DDX3. In fact, DDX3(199-662)-IPS-1 interaction was blocked by the additional expression of core protein (HCVO, JFH1 or 1b core) in Fig. 5C. Ultimately, HCV core protein suppresses IPS-1 signaling by blocking the interaction between the C-terminal region of DDX3 and the CARD-like region of IPS-1, and this inhibition apparently causes the disruption of the active RIG-I/DDX3/IPS-1 complex that efficiently induces IFN-beta production signaling.

Localization of DDX3 and HCV core protein in O cells

We attempted to confirm this finding by tag-expressed proteins and imaging analysis. In Huh7.5 cells IPS-1 colocalized with DDX3 around the mitochondria (Fig. S3), and so did in the hepatocyte lines Oc cells with no HCV replicon (Fig. 6A). In Oc and Huh7.5.1 cells with no HCV replicon, abnormal distribution of IPS-1 was barely observed (Fig. 6A, Fig. S3). In O cells expressing DDX3 and IPS-1, by contrast, two distinct profiles of IPS-1 were observed in addition to the Fig. 6A pattern of IPS-1: diminution or spreading of the IPS-1 protein over mitochondria (Fig. 6B,C). IPS-1 may be degraded by NS3/4A in some replicon-expressing O cells as reported previously [5,28]. We counted number of cells having the pattern represented by Fig. 6 panel B and those similar to Fig. 6 panel C, and in most cases the latter patterns were predominant.

What happens in the O cells with replicon when the core protein is expressed was next tested. Using O and Oc cells, we tested the localization of the core protein and DDX3 in comparison with IFN-inducing properties (Fig. 3). In O cells with full-length HCV replicon, DDX3 was localized proximal to the lipid droplets (LD) (Fig. 7A top panel) around which HCV particles assembled [29]. HCV core protein and DDX3 were partly colocalized in the HCV replicon-expressing cells (Fig. 7A center panel). The results were confirmed with HCV replicon-expressing O cells where endogenous core and DDX3 were stained (Fig. 7B upper panel). Partial merging between core and DDX3 was reproduced in this case, too. In contrast, sO cells, which possess a subgenomic replicon lacking the cording region of the core protein, showed no merging profile of DDX3 and LD (Fig. 7A bottom panel). Likewise, Oc cells barely formed assembly consisting of LD (where the core assembles) and overexpressed DDX3 (Fig. 7A bottom panel) or endogenous DDX3 (Fig. 7B lower panel). O cells expressing DDX3 tended to form large spots compared to Oc cells (with no replicon) and sO cells (core-less replicon) with DDX3.

Overexpressed DDX3 allowed the Oc cells to induce IPS-1-mediated IFN-beta promoter activation (Fig. 3B), while this failed to happen in O cells having HCV replicon (Fig. 3A). Ultimately, overexpressed IPS-1 did not facilitate efficient merging with DDX3 in O cells with replicon (Fig. 6B,C) compared to Oc cells or Huh7.5 cells with no replicon (Fig. 6A, Fig. S3). The results on the functional and immnoprecipitation analyses, together with the imaging profiles, infer that the IPS-1-enhancing function of DDX3 should be blocked by both NS3/4A-mediated IPS-1 degradation and the HCV core which translocates DDX3 from the IPS-1 complex to the proximity of LD in HCV replicon-expressing cells.

Discussion

We investigated the effect of the HCV core protein on the cytosolic DDX3 that forms a complex with IPS-1 to enhance the RIG-I-mediated RNA-sensing pathway. We demonstrated that the core protein removes DDX3 from the IFN-β-inducing complex, leading to suppression of IFN-β induction. DDX3 is functionally complex, since its protective role against viruses may be modulated by the synthesis of viral proteins. DDX3 acts on multiple steps in the IFN-inducing pathway [30]. In addition, DDX3 interacts with the HCV core protein in HCV-infected cells and promotes viral replication [16]. This alternative function is accelerated by the HCV core protein, resulting in augmented HCV propagation [14,16]. More recently, Patal et al., reported that interaction of DDX3 with core protein is not critical for the support of viral replication by DDX3, although DDX3 and core protein colocalize with lipid droplet [15]. If this is the case, what function is revealed by the interaction between DDX3 and HCV core protein remain unsettled. At least, HCV replication is not blocked by this molecular interaction [15].

It remains unclear in Fig. 4C why higher doses of JFH1 core protein are required to inhibit enhancement of IPS-1 signaling by endogenous DDX3 than by exogenously overexpressed DDX3. One possibility is that endogenous DDX3 is preoccupied in a molecular complex other than the IPS-1 pathway since DDX3 is involved in almost every step of RNA metabolism and its localization affects its functional profile [18,30].

Together with these findings, the results presented here suggest that the HCV core inactivates IPS-1 in a mode different from NS3/4A [5,31]. The core protein may switch DDX3 from an antiviral mode to an HCV propagation mode. The core protein localizes to the N-terminus of the HCV translation product, and is generated in infected cells before NS3/4A proteolytically liberates non-structural proteins and inactivates IPS-1. Our results on how the HCV core protein interferes with the interaction between DDX3 and IPS-1 add several possibilities to notions about the HCV function on the IFN-beta-inducing pathway [18].

DDX3 appears to be a prime target for viral manipulation, since at least three different viruses, including HCV [14], Hepatitis B virus [32], and poxviruses [8], encode proteins that interact with DDX3 and modulate its function. These viruses seem to co-opt DDX3, and also require it for replication. The viruses are all oncogenic, and may confer oncogenic properties to DDX3.

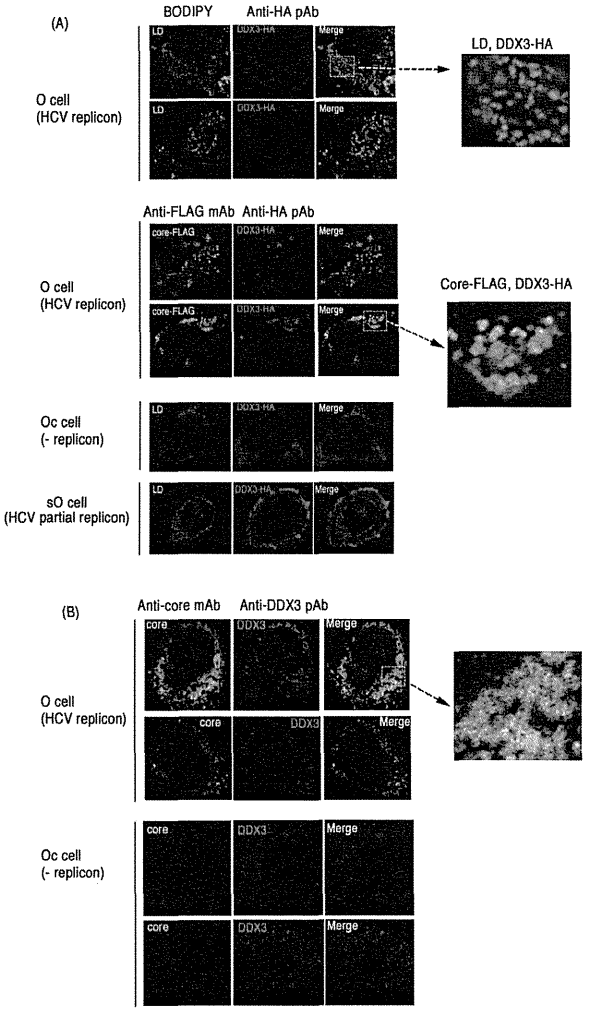

Figure 7. Partial association of endogenous and overexpressed DDX3 with HCV core protein in hepatocyte lines. (A) O cells with the HCV replicon form DDX3-containing speckles in the cytoplasm. O cells contain full-length HCV replicon, and Oc cells do not [16]. O cells were transfected with a plasmid expressing HA-tagged DDX3 (top panel). In other experiments, O cells were transfected with plasmids expressing HA-tagged DDX3 and FLAG-tagged HCV core protein (center panel). After 24 hrs, cells were stained with anti-HA or FLAG antibodies. Proteins were visualized with Alexa488 or 564 second antibodies and the LD was stained with BODIPY493/503. In the bottom panel, Oc cells (no replicon) and sO cells with the core-less subgenomic replicon [16] were transfected with a plasmid expressing HA-tagged DDX3. After 24 hrs, cells were stained with anti-HA antibodies. LD was stained with BODIPY493/503. (B) Endogenous DDX3-HCV core association in O cells. O or Oc cells were cultured to amplify the HCV replicon. Cells were stained with anti-core mAb and anti-DDX3pAb and secondary antibodies. Similar sets of experiments were performed three times to confirm the results.
doi:10.1371/journal.pone.0014258.g007

DDX3 is also involved in human immunodeficiency virus RNA translocation [33]. The DDX3 gene is conserved among eukaryotes, and includes the budding yeast homolog, Ded1 [34]. The Ded1 helicase is essential for initiation of host mRNA translation, and human DDX3 complements the lethality of Ded1 null yeast [14,35]. Another function of DDX3 is to bind viral RNA to modulate RNA replication and translocation. Constitutive expression of the HCV core or other DDX3-binding proteins may impede IFN induction and promote cell cycle progression. These reports are consistent with the implication of DDX3 in various steps of RNA metabolism in cells that contain both host and viral RNAs.

A continuing question is the physiological role of the molecular complex of DDX3 and IPS-1 during replication of HCV in hepatocytes. HCV proteins generated in host hepatocytes usually induce an HCV-permissive state in patients, for example in the IFN-inducing pathways. NS3/4A protease induces rapid degradation of IPS-1 [5,31] and TICAM-1/TRIF [36]. NS5A interferes with the MyD88 function [37]. Viral replication ultimately blocks the STAT1-mediated IFN-amplification pathway [38]. PKR may be an additional factor by which HCV controls type I IFN production [39]. Our results add to our knowledge of the mechanism of how HCV circumvents IFN induction in host cells: HCV core protein suppresses the initial step of IFN-beta induction by interfering with DDX3-IPS-1 association. Indeed, the core protein functions as the earliest IFN suppressor, since it is generated first in HCV-infected cells, and rapidly couples with DDX3 to retract it from the IPS-1 complex, resulting in localization of DDX3 near the LD (Fig. 7). It is HCV that hijacks this protein for establishing infection. Although gene disruption of DDX3 makes mice lethal, this issue will be further tested using IPS-1 −/− hepatocytes expressing human CD81 and occludin [40], in which HCV replication would proceed.

DDX3 primarily is an accelerating factor for antiviral response through IPS-1-binding. Many host proteins other than DDX3 may positively regulate HCV replication in hepatocytes in association with the IPS-1 pathway. In this context, we know LGP2 [41] and STING [42] act as positive regulators in virus infection. Peroxisomes serve as signaling platforms for recruiting IPS-1 with a different signalosome than mitochondria [43]. It appears rational that HCV harbors strategies to circumvent these positive regulators in the relevant steps of the IFN-inducing pathway.

Imaging studies suggest that the complex of IPS-1 involving the membrane of mitochondrial/peroxisomes differ from that free from the membrane. Although IPS-1 is liberated from the membrane by NS3/4A having largely intact cytosolic domain, it loses the IFN-inducing function [5,31]. Our results could offer the possibility that the clipped-out form of IPS-1 immediately fails to form the conventional complex for IRF-3 activation any more [44] or is easily degraded further to be inactive (Fig. 6C). Indeed, there are a number of mitochondria-specific molecules which assemble with IPS-1 [45]. Formation of the molecular complex on the mitochondria rather than simple association between IPS-1 and DDX3 may be critical for the DDX3 function.

Evidence is accumulating that HCV checks many steps in the IFN-inducing pathway throughout the early and late infection stages, and suppresses IFN production by multiple means. Disruption of IPS-1 function by both NS3/4A and core protein may be crucial in HCV-infected Huh7.5 cells, even though the cells harbor dysfunctional RIG-I [46]. Type I IFN suppresses tumors by causing expression of p53 and other tumor-suppressing agents [47]. These unique features of the HCV core protein require further confirmation, and should be minded in investigation of HCV persistency, chronic infection and progression to cirrhosis and carcinoma.

Supporting Information

Figure S1 The IPS-1 complex. IPS-1 and HCV core bind C-terminal regions of DDX3. DDX3 captures dsRNA at the C-terminal domain. This figure is constructed from [11], [14] and [16].
Found at: doi:10.1371/journal.pone.0014258.s001 (0.41 MB TIF)

Figure S2 DDX3 enhances RIG-I-mediated IFN-β promoter activation induced by polyI:C. (A) DDX3 si-1 or control siRNA was transfected into HEK293 cells with reporter plasmids and RIG-I-expression plasmid or control plasmid (100 ng). After 48 hrs, cells were stimulated with polyI:C (20 μg/ml) with dextran for 4 hrs, and activation of the reporter p125luc was measured. (B) MDA5 (25 ng), IPS-1 (100 ng), DDX3 (100 ng), JFH1 core (50 ng) and/or p125 luc reporter (100 ng) plasmids were transfected with HEK293 cells. Cell lysates were prepared after 24 hrs, and luciferase activities measured. The results are representative of two independent experiments, each performed in triplicate.
Found at: doi:10.1371/journal.pone.0014258.s002 (0.17 MB TIF)

Figure S3 DDX3 colocalizes with IPS-1 on the mitochondria in Huh7.5.1 cells. HA-tagged DDX3 and FLAG-tagged IPS-1 were co-transfected into Huh7.5.1 cells. After 24 hrs, cells were fixed with formaldehyde and stained with anti-HA polyclonal and FLAG monoclonal Abs. Alexa488 (DDX3-HA) or Alexa633 antibody was used for second antibody. Mitochondria were stained with Mitotracker Red. A representative result from three independent experiments is shown.
Found at: doi:10.1371/journal.pone.0014258.s003 (0.92 MB TIF)

Acknowledgments

We thank Drs. Y. Matsuura (Osaka Univ.), Kyoko Mori (Okayama Univ.), and M. Sasai (Yale Univ.) for invaluable discussions. Thanks are also due to Drs. T. Ebihara, K. Funami, A. Matsuo, A. Ishii, and M. Shingai in our laboratory for their critical discussions.

Author Contributions

Conceived and designed the experiments: HO MM TS. Performed the experiments: HO MM. Analyzed the data: HO MM KS TS. Contributed reagents/materials/analysis tools: MI AW OT SA NK KS. Wrote the paper: HO TS.

References

1. Yoneyama M, Kikuchi M, Natsukawa T, Shinobu N, Imaizumi T, et al. (2004) The RNA helicase RIG-I has an essential function in double-stranded RNA-induced innate antiviral responses. Nat Immunol 5: 730–737.
2. Yoneyama M, Kikuchi M, Matsumoto K, Imaizumi T, Miyagishi M, et al. (2005) Shared and unique functions of the DExD/H-box helicases RIG-I, MDA5, and LGP2 in antiviral innate immunity. J Immunol 175: 2851–2858.
3. Kato H, Takeuchi O, Sato S, Yoneyama M, Yamamoto M, et al. (2006) Differential roles of MDA5 and RIG-I helicases in the recognition of RNA viruses. Nature 441: 101–105.
4. Kawai T, Takahashi K, Sato S, Coban C, Kumar H, et al. (2005) IPS-1, an adaptor triggering RIG-I- and Mda5-mediated type I interferon induction. Nat Immunol 6: 981–988.
5. Meylan E, Curran J, Hofmann K, Moradpour D, Binder M, et al. (2005) Cardif is an adaptor protein in the RIG-I antiviral pathway and is targeted by hepatitis C virus. Nature 437: 1167–1172.
6. Seth RB, Sun L, Ea CK, Chen ZJ (2005) Identification and characterization of MAVS, a mitochondrial antiviral signaling protein that activates NF-kappaB and IRF 3. Cell 122: 669–682.
7. Xu LG, Wang YY, Han KJ, Li LY, Zhai Z, et al. (2005) VISA is an adapter protein required for virus-triggered IFN-beta signaling. Mol Cell 19: 727–740.
8. Schroder M, Baran M, Bowie AG (2008) Viral targeting of DEAD box protein 3 reveals its role in TBK1/IKKepsilon-mediated IRF activation. Embo J 27: 2147–2157.
9. Soulat D, Bürckstümmer T, Westermayer S, Goncalves A, Bauch A, et al. (2008) The DEAD-box helicase DDX3X is a critical component of the TANK-binding kinase 1-dependent innate immune response. Embo J 27: 2135–2146.
10. Kravchenko VV, Mathison JC, Schwamborn K, Mercurio F, Ulevitch RJ (2003) IKKi/IKKepsilon plays a key role in integrating signals induced by pro-inflammatory stimuli. J Biol Chem 278: 26612–26619.
11. Oshiumi H, Sakai K, Matsumoto M, Seya T (2010) DEAD/H BOX 3 (DDX3) helicase binds the RIG-I adaptor IPS-1 to up-regulate IFN-beta inducing potential. Eur J Immunol 40: 940–948.
12. Chao CH, Chen CM, Cheng PL, Shih JW, Tsou AP, et al. (2006) A DEAD box RNA helicase with tumor growth-suppressive property and transcriptional regulation activity of the p21waf1/cip1 promoter, is a candidate tumor suppressor. Cancer Res 66: 6579–6588.
13. Rocak S, Linder P (2004) DEAD-box proteins: the driving forces behind RNA metabolism. Nat Rev Mol Cell Biol 5: 232–241.
14. Owsianka AM, Patel AH (1999) Hepatitis C virus core protein interacts with a human DEAD box protein DDX3. Virology 257: 330–340.
15. Angus AGN, Dalrymple D, Boulant S, McGivern DR, Clayton RF, et al. (2010) Requirement of cellular DDX3 for hepatitis C virus replication is unrelated to its interaction with the viral core protein. J Gen Virol 91: 122–132.
16. Ariumi Y, Kuroki M, Abe K, Dansako H, Ikeda M, et al. (2007) DDX3 DEAD-box RNA helicase is required for hepatitis C virus RNA replication. J Virol 81: 13922–13926.
17. Chang PC, Chi CW, Chau GY, Li FY, Tsai YH, et al. (2006) DDX3, a DEAD box RNA helicase, is deregulated in hepatitis virus-associated hepatocellular carcinoma and is involved in cell growth control. Oncogene 25: 1991–2003.
18. Schroder M (2010) Human DEAD-box protein 3 has multiple functions in gene regulation and cell cycle control and is a prime target for viral manipulation. Biochem Pharmacol 79: 297–306.
19. Ikeda M, Abe K, Dansako H, Nakamura T, Naka K, et al. (2005) Efficient replication of a full-length hepatitis C virus genome, strain O, in cell culture, and development of a luciferase reporter system. Biochem Biophys Res Commun 329: 1350–1359.
20. Lin W, Kim SS, Yeung E, Kamegaya Y, Blackard JT, et al. (2006) Hepatitis C virus core protein blocks interferon signaling by interaction with the STAT1 SH2 domain. J Virol 2006 Sep; 80(18): 9226–35.
21. Sasai M, Shingai M, Funami K, Yoneyama M, Fujita T, et al. (2006) NAK-associated protein 1 participates in both the TLR3 and the cytoplasmic pathways in type I IFN induction. J Immunol 177: 8676–8683.
22. Oshiumi H, Matsumoto M, Funami K, Akazawa T, Seya T (2003) TICAM-1, an adaptor molecule that participates in Toll-like receptor 3-mediated interferon-beta induction. Nat Immunol 4: 161–167.
23. Saito T, Owen DM, Jiang F, Marcotrigiano J, Gale M, Jr. (2008) Innate immunity induced by composition-dependent RIG-I recognition of hepatitis C virus RNA. Nature 454: 523–527.
24. Saito T, Hirai R, Loo YM, Owen D, Johnson CL, et al. (2007) Regulation of innate antiviral defenses through a shared repressor domain in RIG-I and LGP2. Proc Natl Acad Sci U S A 104: 582–587.
25. Matsumoto M, Funami K, Tanabe M, Oshiumi H, Shingai M, et al. (2003) Subcellular localization of Toll-like receptor 3 in human dendritic cells. J Immunol 171: 3154–3162.
26. Oshiumi H, Matsumoto M, Hatakeyama S, Seya T (2009) Riplet/RNF135, a RING finger protein, ubiquitinates RIG-I to promote interferon-beta induction during the early phase of viral infection. J Biol Chem 284: 807–817.
27. Schwer B, Ren S, Pietschmann T, Kartenbeck J, Kaehlcke K, et al. (2004) Targeting of hepatitis C virus core protein to mitochondria through a novel C-terminal localization motif. J Virol 78: 7958–7968.
28. Cheng G, Zhong J, Chisari FV (2006) Inhibition of dsRNA-induced signaling in hepatitis C virus-infected cells by NS3 protease-dependent and -independent mechanisms. Proc Natl Acad Sci U S A 103: 8499–8504.
29. Miyanari Y, Atsuzawa K, Usuda N, Watashi K, Hishiki T, et al. (2007) The lipid droplet is an important organelle for hepatitis C virus production. Nat Cell Biol 9: 1089–1097.
30. Mulhern O, Bowie AG (2010) Unexpected roles for DEAD-box protein 3 in viral RNA sensing pathways. Eur J Immunol 40: 933–935.
31. Li XD, Sun L, Seth RB, Pineda G, Chen ZJ (2005) Hepatitis C virus protease NS3/4A cleaves mitochondrial antiviral signaling protein off the mitochondria to evade innate immunity. Proc Natl Acad Sci U S A 102: 17717–17722.
32. Wang H, Kim S, Ryu WS (2009) DDX3 DEAD-Box RNA helicase inhibits hepatitis B virus reverse transcription by incorporation into nucleocapsids. J Virol 83: 5815–5824.
33. Yedavalli VS, Neuveut C, Chi YH, Kleiman L, Jeang KT (2004) Requirement of DDX3 DEAD box RNA helicase for HIV-1 Rev-RRE export function. Cell 119: 381–392.
34. Chuang RY, Weaver PL, Liu Z, Chang TH (1997) Requirement of the DEAD-Box protein ded1p for messenger RNA translation. Science 275: 1468–1471.
35. Mamiya N, Worman HJ (1999) Hepatitis C virus core protein binds to a DEAD box RNA helicase. J Biol Chem 274: 15751–15756.
36. Li K, Foy E, Ferreon JC, Nakamura M, Ferreon AC, et al. (2005) Immune evasion by hepatitis C virus NS3/4A protease-mediated cleavage of the Toll-like receptor 3 adaptor protein TRIF. Proc Natl Acad Sci U S A 102: 2992–2997.
37. Abe T, Kaname Y, Hamamoto I, Tsuda Y, Wen X, et al. (2007) Hepatitis C virus nonstructural protein 5A modulates the toll-like receptor-MyD88-dependent signaling pathway in macrophage cell lines. J Virol 81: 8953–8966.
38. Heim MH, Moradpour D, Blum HE (1999) Expression of hepatitis C virus proteins inhibits signal transduction through the Jak-STAT pathway. J Virol 73: 8469–8475.
39. Arnaud N, Dabo S, Maillard P, Budkowska A, Kalliampakou KI, et al. (2010) Hepatitis C virus controls interferon production through PKR activation. PLoS One 5: e10575.
40. Ploss A, Evans MJ, Gaysinskaya VA, Panis M, You H, et al. (2009) Human occludin is a hepatitis C virus entry factor required for infection of mouse cells. Nature 457: 882–886.
41. Satoh T, Kato H, Kumagai Y, Yoneyama M, Sato S, et al. (2010) LGP2 is a positive regulator of RIG-I- and MDA5-mediated antiviral responses. Proc Natl Acad Sci U S A 107: 1512–1517.
42. Ishikawa H, Ma Z, Barber GN (2009) STING regulates intracellular DNA-mediated, type I interferon-dependent innate immunity. Nature 461: 788–793.
43. Dixit E, Boulant S, Zhang Y, Lee ASY, Odendall C, et al. (2010) Peroxisomes are signaling platforms for antiviral innate immunity. Cell 141: 668–681.
44. Yasukawa K, Oshiumi H, Takeda M, Ishihara N, Yanagi Y, et al. (2009) Mitofusin 2 inhibits mitochondrial antiviral signaling. Sci Signal 2: ra47.
45. Scott I (2010) The role of mitochondria in the mammalian antiviral defense system. Mitochondrion 10: 316–320.
46. Binder M, Kochs G, Bartenschlager R, Lohmann V (2007) Hepatitis C virus escape from the interferon regulatory factor 3 pathway by a passive and active evasion strategy. Hepatology 46: 1365–1374.
47. Takaoka A, Yanai H, Kondo S, Duncan G, Negishi H, et al. (2005) Integral role of IRF-5 in the gene induction programme activated by Toll-like receptors. Nature 434: 243–249.

European Journal of Immunology

DEAD/H BOX 3 (DDX3) helicase binds the RIG-I adaptor IPS-1 to up-regulate IFN-β-inducing potential

Hiroyuki Oshiumi, Keisuke Sakai, Misako Matsumoto and Tsukasa Seya

Department of Microbiology and Immunology, Hokkaido University Graduate School of Medicine, Kita-ku, Sapporo, Japan

Retinoic acid-inducible gene-I (RIG-I)-like receptors (RLR) are members of the DEAD box helicases, and recognize viral RNA in the cytoplasm, leading to IFN-β induction through the adaptor IFN-β promoter stimulator-1 (IPS-1) (also known as Cardif, mitochondrial antiviral signaling protein or virus-induced signaling adaptor). Since uninfected cells usually harbor a trace of RIG-I, other RNA-binding proteins may participate in assembling viral RNA into the IPS-1 pathway during the initial response to infection. We searched for proteins coupling with human IPS-1 by yeast two-hybrid and identified another DEAD (Asp-Glu-Ala-Asp) box helicase, DDX3 (DEAD/H BOX 3). DDX3 can bind viral RNA to join it in the IPS-1 complex. Unlike RIG-I, DDX3 was constitutively expressed in cells, and some fraction of DDX3 is colocalized with IPS-1 around mitochondria. The 622-662 a.a DDX3 C-terminal region (DDX3-C) directly bound to the IPS-1 CARD-like domain, and the whole DDX3 protein also associated with RLR. By reporter assay, DDX3 helped IPS-1 up-regulate IFN-β promoter activation and knockdown of DDX3 by siRNA resulted in reduced IFN-β induction. This activity was conserved on the DDX3-C fragment. DDX3 only marginally enhanced IFN-β promoter activation induced by transfected TANK-binding kinase 1 (TBK1) or I-kappa-B kinase-ε (IKKε). Forced expression of DDX3 augmented virus-mediated IFN-β induction and host cell protection against virus infection. Hence, DDX3 is an antiviral IPS-1 enhancer.

Key words: DDX3 · IFN-β · IPS-1 · RIG-I-like receptors · Viral infection

See accompanying Commentary by Mulhern and Bowie

Introduction

Retinoic acid-inducible gene-I (RIG-I) and melanoma differentiation-associated gene 5 (MDA5) are cytoplasmic RNA helicases [1–3], which signal the presence of viral RNA through the adaptor, IFN-β promoter stimulator-1 (IPS-1) (also known as mitochondrial antiviral signaling protein/caspase recruitment domain (CARD) adaptor inducing IFN-β (Cardif)/virus-induced signaling adaptor) to produce IFN-β [4–7]. IPS-1 localizes on the outer membrane of the mitochondria *via* its C-terminus [6]. Its N-terminus consists of a CARD domain, which interacts with the CARD domains of RIG-I and MDA5. Viral RNA resulting from penetration or replication are believed to assemble in the CARD-interacting helicase complex to activate the cytoplasmic IFN-inducing pathway. Although non-infected cells usually express minimal amounts of RIG-I/MDA5, the final output of type I IFN is efficiently induced at an early stage of infection to protect host cells from viral spreading.

Once IPS-1 is activated, the kinase complex consisting of TANK-homologous proteins and virus-activated kinases induce nuclear translocation of IFN regulatory factor-3 (IRF-3) to activate the IFN promoter [8]. NAK-associated protein 1, TANK-binding kinase 1 (TBK1) and I-kappa-B kinase-ε (IKKε) are components of the kinase complex that phosphorylates IRF-3 to induce type I IFN [9, 10]. RIG-I recognizes products of various RNA viruses, while MDA5 recognizes products of picornaviruses [1, 11]. RIG-I and MDA5 share the helicase domain, which is classified into the DEAD (Asp-Glu-Ala-Asp) box helicase family, and the domain can bind to various RNA structures. 5′-triphosphate RNA or short dsRNA is a ligand of RIG-I, whereas long dsRNA is a ligand of MDA5 [1, 12]. However, these RIG-I-like receptors (RLR) are usually up-regulated to a sufficient level secondary to IFN stimulation, suggesting that other molecular mechanisms are responsible for the initial sensing of viral RNA.

Here, we looked for molecules that bind IPS-1 by yeast two-hybrid, and found a DEAD box helicase, DDX3 (DEAD/H BOX 3), as a component of the complex of IPS-1. DDX3 facilitated IPS-1-mediated IFN-β induction to confer high antiviral potential on early infection phase of host cells. This is the first report showing that DDX3 is an IPS-1 complement factor for antiviral IFN-β induction in host infectious cells.

Correspondence: Dr. Tsukasa Seya
e-mail: seya-tu@pop.med.hokudai.ac.jp

Results

Involvement of DDX3 in the IPS-1 complex

IPS-1 is constitutively present on the mitochondrial membrane and plays a central role in the cytoplasmic IFN-inducing pathway. We searched for proteins that bind IPS-1 in yeast. Using bait plasmids with the IPS-1 CARD region (aa 6–136), we screened a human lung cDNA library to isolate IPS-1 CARD-interacting proteins. We identified one clone, #62 that encodes the DDX3 C-terminal region (aa 276–662), which included partial DEAD box and helicase superfamily C-terminal regions (Fig. 1A). Their interaction was confirmed in HEK293FT cells by immunoprecipitation (IP), where DDX3 and IPS-1 were coupled (Fig. 1B). We confirmed that the C-terminal fragments of DDX3, at least 622-662 a.a, bound IPS-1 (data not shown). Taken together with the results of the yeast two-hybrid assay, the C-terminal portions of DDX3 directly bind the CARD-like region of IPS-1.

RIG-I and MDA5 helicases also bind the IPS-1 CARD domain [4]. In general, RNA helicases make a large molecular complex, and sometimes form homo- or hetero-oligomers. RIG-I binds to LGP2 helicase, and forms homo-oligomers during Sendai virus infection [11]. Hence, we examined whether DDX3 was associated with the RLR proteins by i.p. RIG-I and MDA5 co-precipitated with DDX3 (Fig. 2A), suggesting that DDX3 is involved in the complex of IPS-1 that interacts with RIG-I and/or MDA5. DDX3 bound the C-terminal helicase domain including the RD region of RIG-I (Fig. 2B). Thus, additional interaction may occur between DDX3 and RIG-I/MDA5. IPS-1 localizes to the membrane of mitochondria [6]. Three-color imaging analysis indicated that DDX3 in part co-localized to the IPS-1-mitochodria complex in non-stimulated resting HeLa cells, which express undetectable amounts of RLR (Fig. 2C and data not shown). These results together with accumulating evidence infer that non-infected cells harbor the complex of DDX3 and IPS-1 with minimal amounts of RIG-I/MDA5.

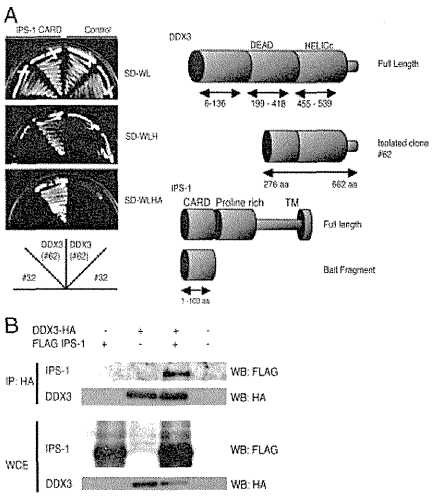

Figure 1. DDX3 binds IPS-1. (A) DDX3 partial cDNA fragment (aa 276–662) isolated by the yeast two-hybrid screening interacted with the IPS-1 CARD region (aa 1–103) in yeast. Tryptophan- and leucine-depleted synthetic dextrose medium plate (SD-WL) is non-selective, and tryptophan-, leucine- and histidine-depleted synthetic dextrose medium plate (SD-WLH) and tryptophan-, leucine-, histidine- and alanine-depleted synthetic dextrose medium (SD-WLHA) plates are selective plates. Empty bait plasmid (pGBKT7) was used for a negative control. (B) FLAG-tagged IPS-1 and HA-tagged DDX3 expression vectors were transiently transfected into HEK293FT cells by FuGeneHD reagent. 24 h after transfection, cell lysates were prepared, and IP was carried out using anti-HA Ab. The immunoprecipitates were analyzed by western blot using anti-HA or FLAG Ab. Data are representative of three independent experiments.

DDX3 promotes IPS-1-mediated IFN-β promoter activation

Forced expression of IPS-1 causes the activation of transcription from the IFN-β promoter. To ascertain the role of DDX3 in IFN-β production, we carried out reporter gene analysis to see the enhancing effect of DDX3 on IPS-1-mediated IFN-β promoter activation. Overexpression of DDX3 alone caused little activation of the promoter; however, the promoter activation was more augmented by minimal addition of DDX3 to IPS-1 than by overexpressed IPS-1 alone (Fig. 3A). This suggested that DDX3 enhanced IPS-1-mediated signaling despite the lack of RIG-I overexpression. To establish which region of DDX3 is important for IFN-β enhancer activity, partial DDX3 fragments were overexpressed with IPS-1, and IFN-β promoter activation was examined. The N-terminal region (aa 1–224, aa 224–487, aa 488–621) barely enhanced promoter activation (data not shown), but the C-terminal region (622–662) activated the promoter (Fig. 3B). These data indicated that the C-terminal region of DDX3 is important for the binding to IPS-1 and potentiation of the IPS-1 pathway.

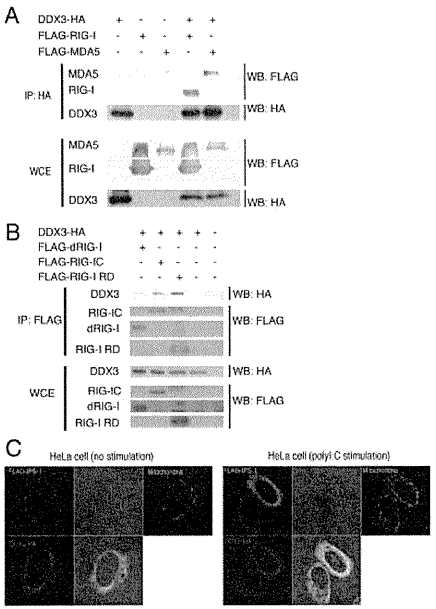

Figure 2. DDX3 joins the complex of RIG-I, MDA5 and IPS-1. (A) RIG-I and MDA5 co-precipitate with DDX3. HA-tagged DDX3 was expressed in HEK293FT cells, together with FLAG-tagged MDA5 or RIG-I, and 24 h after transfection, IP was performed using anti-HA Ab and analyzed by western blotting. (B) The C-terminal region of RIG-I participates in complex formation with DDX3. FLAG-tagged RIG-I fragments and HA-tagged DDX3 were expressed in HEK293 cells, and 24 h after transfection, IP was performed using anti-HA Ab and analyzed by western blotting. (C) DDX3 colocalizes with IPS-1. Flag-tagged IPS-1 and HA-tagged DDX3 were transfected into HeLa cells together with or without polyI:C. After 24 h, cells were fixed with formaldehyde and stained with anti-HA polyclonal and anti-FLAG monoclonal Ab. Alexa488 (DDX3-HA) or Alexa633 Ab was used for second Ab. Mitochondria was stained with Mitotracker Red. DDX-3 partially colocalized with IPS-1. Data are representative of three independent experiments.

DDX3 as a component of initial RNA sensor

RIG-I and MDA5 are IFN-inducible proteins, only traces of which exist in an early phase (<2 h) in the cytoplasm where viral RNA replicate. Previous reports showed that DDX3 binds RNA of poly rA or duplexed RNA [13, 14], and our protein analysis solidified this issue: DDX3 efficiently bound polyI:C and stem-loop RNA of viral origin in a solution (data not shown). DDX3 as well as IPS-1 were expressed even without any stimulation (Fig. 2C and 4A and B) and bound each other in the cytoplasm (Fig. 2C). Hence, DDX3 is a cytoplasmic molecule that can detect viral RNA produced in infected cells.

Knockdown studies suggested that polyI:C-mediated IFN promoter activation was abrogated in DDX3-deficient cells even in the presence of overexpressed RIG-I or MDA5 (Fig. 5). DDX3 silencing happened with two different siRNA. Thus, DDX3 may enable RIG-I and IPS-1 to confer activation of the cytoplasmic RNA-sensing pathway on virus-infected cells.

The IFN-β-inducing pathway involves IRF-3 kinases TBK1 and IKKε, which may be targets of DDX3 [15, 16]. By *in vitro* reporter analysis, increasing amounts of DDX3 barely affected IFN-β promoter activation by TBK1 and IKKε (Fig. 6A and B). Slight TBK1-enhancing activity could manage to be detected with DDX3 when decreasing amounts of TBK1 was used in the assay (Fig. 6C and D).

HeLa cells induced the mRNA of RIG-I and IFN-β in response to polyI:C stimulation within 1 h (Fig. 4A). More exactly, IFN-β induction was ~30 min faster than RIG-I induction in response to polyI:C. IFN-β mRNA induction was peaked around 3 h post stimulation, while RIG-I induction continued to increase>3 h (Fig. 4A). When HEK293 cells were infected with vesicular stomatitis virus (VSV) (a RIG-I-stimulating virus), the IFN-β mRNA was induced from 6 h, and by that time no RIG-I message was generated (Fig. 4B–D). The RIG-I message began to appear>8 h and was markedly increased (Fig. 4B and D). In either case, no up-regulation was observed with DDX3 but sufficiently present in the cytoplasm (Fig. 4C). Furthermore, overexpression of DDX3 in HeLa cells resulted in potential prevention of VSV propagation (Fig. 7). However, the distribution profiles of DDX3 and IPS-1 were barely altered in response to polyI:C stimulation (Fig. 2C). The results allow us to interpret that when viral RNA enter the cytoplasm of infected cells, the RNA first induce a small amount of IFN-β in conjunction with the complex containing trace RIG-I and then the induced IFN-β fosters intensive RIG-I/MDA5 induction. The complex is reconstituted together with upcoming RIG-I/MDA5 to amplify the cytoplasmic IFN-inducing pathway. Although the molecular reconstitution was not visible with overexpressed proteins by confocal analysis, DDX3 may act as an enhancing factor for initial RNA-sensing by the IPS-1 complex and conducts the rapid response to viral RNA to facilitate the IPS-1 signaling.

Discussion

We identified DDX3 as a protein that bound to the IPS-1 CARD region, duplexed RNA and RLR. Although the DDX3 helicase domain is a DEAD box type similar to those of RIG-I and MDA5, DDX3 does not have a signaling domain corresponding to the CARD domain. Therefore, DDX3 may not act as a signal sensor of RNA viruses, as RIG-I and MDA5 do. Considering the role of DDX3 in host RNA metabolism, it is more likely that DDX3 acts as a scaffold for RIG-I (even under the presence of low copy numbers of RIG-I) and intensifies IPS-1 signaling similar to LGP2 [11, 17]. RNA molecules usually form a complex with various

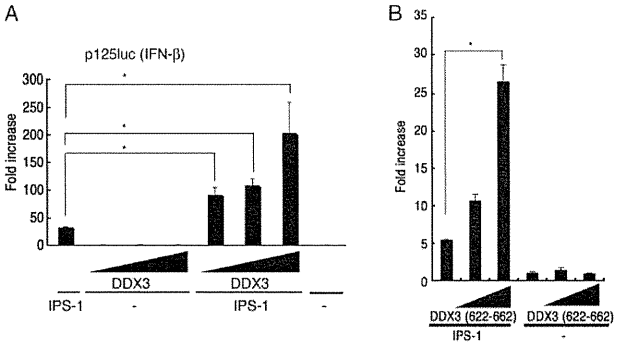

Figure 3. The C-terminal region of DDX3 participates in enhancing IPS-1-mediated IFN-β promoter activation. (A) Activation of IFN-β promoter was examined by reporter gene assay. HEK293 cells were transfected with DDX3- (100, 200 or 300 ng) and/or IPS-1 (100 ng)-encoding plasmids, together with reporter (p125luc) and control plasmids (Renilla luciferase) into 24-well plates. (B) The plasmids for expression of DDX3 (622-662 aa) and IPS-1 or the former only were transfected into HEK293 cells in 24-well plates together with p125luc reporter plasmid. After 24 h, the activation of reporter was measured. Data show mean fold induction+SD of three independent assays. *$p<0.05$, Student's t-test.

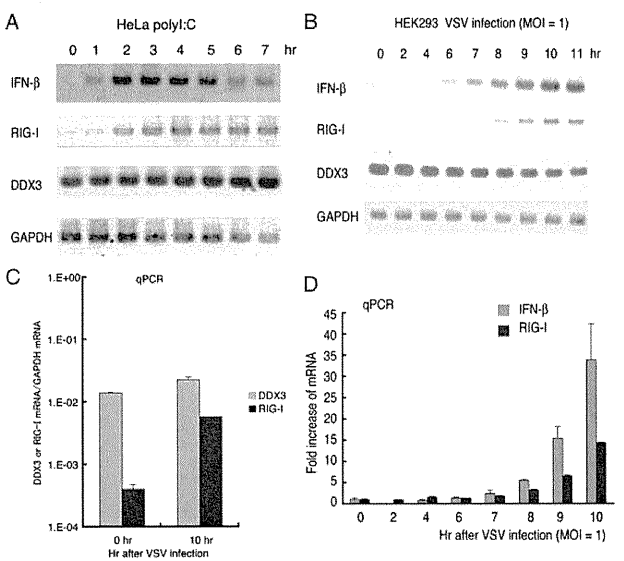

Figure 4. Earlier induction of IFN- than RIG-I in virus-infected cells. (A) Early induction of IFN-β in response to polyI:C. HeLa cells were stimulated with 50 μg/mL of polyI:C for indicated hours. Total RNA was extracted with TRIZOL and RT-PCR was carried out to examine the kinetics of expressions of DDX3, IFN-β, RIG-I and GAPDH (control). (B) IFN-β mRNA induction by VSV infection. HEK293 cell were infected with VSV at MOI = 1, and then total RNA was extracted with TRIZOL reagents at indicated times. The reverse transcription with random primers and PCR at 33 cycle were performed to detect RIG-I, DDX3 or IFN-β expression. Data are representative of three independent experiments. (C) Marked induction of RIG-I in VSV-infected cells. HEK293 cells were infected with VSV at MOI = 1, and then the total RNA was extracted with TRIZOL reagent at indicated times. The relative amounts of RIG-I or DDX3 mRNA were quantified by RT-qPCR, in which the mRNA of GAPDH was used for endogenous internal control. (D) Fold increase of IFN-β or RIG-I mRNA by VSV infection. The amount of IFN-β or RIG-I cDNA was determined by quantitative PCR. The fold increases were calculated by dividing the values of each time point by that of 0 h sample of IFN-β or RIG-I. Data show mean+SD pooled from three independent experiments.

proteins, such as 5′-end capping enzymes or translation initiation factors. Viral RNA also tends to couple with host proteins to replicate and translate RNA. DDX3 capturing RNA may function either in the molecular complex of RIG-I/MDA5/IPS-1 or in the complex of the translation machinery.

Recently, DDX3 was reported to up-regulate IFN-β induction by interacting with IKKε in the kinase complex [18]. IKKε is an NF-κB-inducible gene, whereas the DDX3-IPS-1 complex is constitutively present prior to infection. DDX3 may bind IKKε after IKKε is generated secondary to NF-κB activation [15]. Another report suggested that DDX3 interacts with TBK1 to synergistically stimulate the IFN-β promoter [16]. The report further suggested that DDX3 is recruited to the IFN promoter and acts like a transcription factor [16]. These reports also show that not C-terminal but N-terminal region of DDX3 is required for enhancing the IKKε- or TBK1-mediated IFN promoter activation. We showed that unlike these previous reports, the C-terminal region of DDX3 is important for the IPS-1 activation. These observations indicate that DDX3 is involved in RIG-I signaling at multiple steps. The involvement of DDX3 at several steps is not surprising, because DDX3 plays several roles in RNA metabolisms, such as RNA translocation or mRNA translation.

In cytoplasm, there are large amounts of DDX3 and only trace amounts of RIG-I in resting cells. Therefore, when the virus initially infects human cells, the viral RNA would encounter DDX3 before RIG-I capture the viral RNA. We demonstrated that the initial IPS-1 complex for RNA-sensing involves DDX3 in addition to trace RIG-I to cope with the early phase of infection. This IPS-1 complex activates downstream signal by involving a minute amount of viral RNA. What happens in actual viral infection is to first induce IFN-β and then RIG-I (Fig. 4B), suggesting that the initial IFN-β mRNA arises independent of the virus-induced RIG-I. Once IFN-β and RIG-I mRNA are up-regulated by viral RNA, the IPS-1 complex turns constitutionally different: the complex contains high amounts of RIG-I, which may directly capture viral RNA without DDX3. Our results indicate that the early IPS-1 complex formed in the early stages of virus-infected cells induce minute IFN-β with a mode different from the conventional IPS-1 pathway that RIG-I solely capture viral RNA and activates IPS-1. By retracting DDX3 from the complex by siRNA, only a minimal IFN-β response emerges merely with preexisting RIG-I and IPS-1, suggesting DDX3 to be a critical signal enhancer in the early IPS-1 complex. Development of a method to chase endogenous DDX3 will be required to test our interpretation.

The RIG-I generation occurring > 8 h post RNA virus challenge makes the complex direct the conventional IFN-inducing pathway harboring sufficient RIG-I/MDA5. Previous reports [13, 14] and our RNA-binding analysis also speculated that one of the RNA-capture proteins is DDX3 since DDX3 tightly binds polyI:C and dsRNA in fluid phase. These RNA-capture proteins may have a role in the IPS-1-involving molecular platform in cells with early virus infection when only a trace RIG-I protein is expressed. This interpretation fits the result that DDX3 acts predominantly on an early phase of virus infection (Fig. 4B and 7).

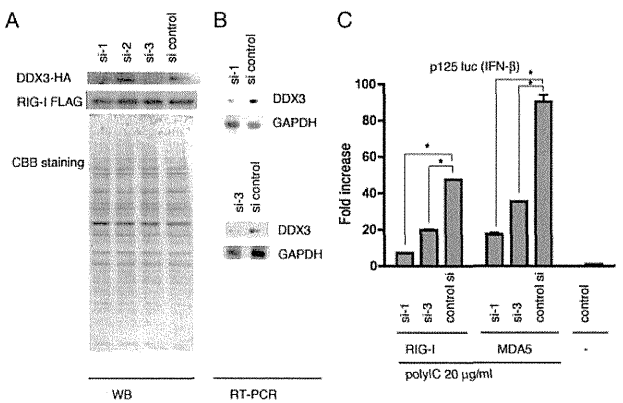

Figure 5. Knockdown of DDX3. (A) Negative control or DDX3 targeting siRNA (20 pmol), DDX3 si-1, -2 or -3, were transfected into HEK293 cells in 24-well plates, together with HA-tagged DDX3 or FLAG-tagged RIG-I expression plasmids, and after 48 h, cell lysates were prepared and analyzed by western blotting with anti-HA or anti-FLAG Ab, and the same membrane was stained with CBB. (B) DDX3 si-1, -3 or control siRNA was transfected into HEK293 cells, and after 48 h, expression of endogenous DDX3 mRNA was examined by RT-PCR. (C) DDX3 si-1, -3 or control siRNA was transfected into HEK293 cells with reporter plasmids and RIG-I- or MDA5 expression plasmid (100 ng). Forty-eight hours after transfection, cells were stimulated with polyI:C (20 μg/mL) with dextran for 4 h, and activation of the reporter was measured. siRNA for DDX3 reduced RIG-I- or MDA5-mediated p125luc activation. Data are representative of three independent experiments (A,B). Data show mean fold increase + SD pooled from three independent experiments (C). *p<0.05, Student's t-test.

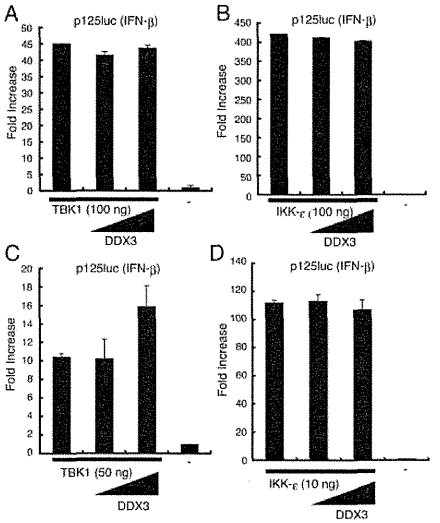

Figure 6. TBK1 and IKKε are not main targets for DDX3-mediated IFN-β up-regulation. (A–D) The activation of IFN-β promoter was examined by reporter gene assay. HEK293 cells were transfected in 24-well plates with DDX3 (0, 100 or 300 ng)-, TBK1 (0, 50 or 100 ng)- or IKKε (0, 10 or 100 ng)-encoding plasmid together with reporter (p125luc) and control plasmid. After 24 h, the cell lysate was prepared and the luciferase activities were measured. Data show mean + SD of three independent experiments.

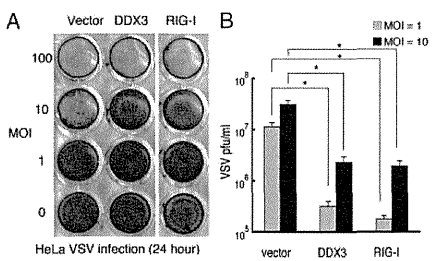

Figure 7. VSV infection is suppressed by overexpressed DDX3. (A) HeLa cells were transfected with DDX3, RIG-I or empty vector. After 24 h, the transfected cells were infected with VSV at indicated MOI. 24 h after VSV infection, the cells were fixed with formaldehyde and stained with crystal violet. (B) The VSV titers of culture supernatant of HeLa cells infected with VSV at MOI = 1 or 10 were measured by plaque assay. Data show mean + SD of three independent experiments. *p<0.05, Student's t-test.

Proteins involved in type I IFN induction are found ubiquitinated for their functional regulation. It has been reported that TRIM25 [19] and Riplet/RNF135 [20] act as ubiquitin ligases to activate RIG-I for IFN-β induction in their different sites of RIG-I ubiquitination. Another ubiquitin ligase RNF125 polyubiquitinates RIG-I through Lys48, leading to degradation of RIG-I [21]. The RIG-I level is highly susceptible to not only IFN but also ubiquitination in host cells. In addition, many viral factors may suppress the RIG-I function. It remains unknown what factor maintains a minimal level of RIG-I/MDA5 in resting cells. We favor the interpretation that DDX3 can be an alternative factor for compensating the low RLR contents in a certain infectious situation such that RIG-I is degraded or poorly up-regulated by other viral factors.

DDX3 is functionally complicated since its protective role against viruses may be modulated after the synthesis of viral proteins. DDX3 couples with the HCV core protein in HCV-infected cells and promotes viral replication [22]. This alternative function of DDX3 is accelerated by the HCV core protein, since the core protein withdraws DDX3 from the IFN-β-inducing facility, leading to suppression of IFN-β induction and positive regulation of HCV propagation in infected cells. DDX3 is also involved in HIV RNA translocation [14]. The DDX3 gene is conserved among eukaryotes, and Ded1 is a budding yeast homolog [23]. Ded1 helicase is essential for initiation of host mRNA translation, and human DDX3 can complement the lethality of Ded1-null yeast cells [24, 25]. Hence, another function of DDX3 is to bind viral RNA to modulate RNA replication and translocation. It is not surprising that DDX3 is implicated in various steps of RNA metabolism in cells with both host and viral RNA.

Materials and methods

Cell culture and reagents

HEK293 cells and HEK293FT cells were maintained in Dulbecco's Modified Eagle's low or high glucose medium (Invitrogen, Carlsbad, CA, USA) supplemented with 10% heat-inactivated FBS (Invitrogen) and antibiotics. HeLa cells were maintained in MEM (Nissui, Tokyo, Japan) supplemented with 10% heat-inactivated FBS. Anti-FLAG M2 mAb, anti-HA polyclonal Ab, were purchased from Sigma-Aldrich (St. Louis, MO, USA). Alexa Fluor® -conjugated secondary Ab were from Invitrogen.

Plasmids

DDX3 cDNA encoding the entire ORF was cloned into pCR-blunt vector using primers, DDX3N F-Xh (CTC GAG CCA CCA TGA GTC ATG TGG CAG TGG AA) and DDX3C R-Ba (GGA TCC GTT ACC CCA CCA GTC AAC CCC) from human lung cDNA library. To make an expression plasmid, HA tag was fused at the C-terminal end of the full length DDX3 (pEF-BOS DDX3-HA). pEF-BOS DDX3 (1–224 aa) vector was made by using primers DDX3 N-F-Xh and DDX3D1 (GGA TCC GGC ACA AGC CAT CAA GTC TCT TTT C).

pEF-BOS DDX3-HA (225–662) was made by using primers DDX3D2-3 (CTC GAG CCA CCA TGC AAA CAG GGT CTG GAA AAA C) and DDX3C R-Ba. To make pEF-BOS DDX3-HA (225–484) and pEF-BOS DDX3-HA (485–663), the primers DDX3D2 R-Ba (GGA TCC AAG GGC CTC TTC TCT ATC CCT C) and DDX3D3 F-Xh (CTC GAG CCA CCA TGC ACC AGT TCC GCT CAG GAA AAA G) were used, respectively. Reporter and internal control plasmids for reporter gene assay are previously described [26].

RNAi

Knockdown of DDX3 was carried out using siRNA, DDX3 siRNA-1: 5′-GAU UCG UAG AAU AGU CGA ACA-3′, siRNA-2: 5′-GGA GUG AUU ACG AUG GCA UUG-3′, siRNA-3: 5′-GCC UCA GAU UCG UAG AAU AGU-3′ and control siRNA: 5′-GGG AAG AUC GGG UUA GAC UUC-3′. Twenty picomoles of each siRNA was transfected into HEK293 cells in 24-well plates with Lipofectamin 2000 according to manufacture's protocol. Knockdown of DDX3 was confirmed 48 h after siRNA transfection. Experiments were repeated twice for confirmation of the results.

Yeast two-hybrid assay

The yeast two-hybrid assay was performed as described previously [27]. The yeast AH109 strain (Clontech, Palo Alto, CA, USA) was transformed using bait (pGBKT7) and prey (pGADT7) plasmids. The transformants were streaked onto plates and incubated for 3–5 days. The IPS-1 CARD vector was constructed by inserting IPS-1 partial fragment encoding from 6 to 136 aa region into pGBKT7 multicloning site. Yeast two-hybrid screening was performed using human lung cDNA libraries. We obtained four independent clones, and one encoded DDX3 partial cDNA. SD-WLH is a yeast synthetic dextrose medium that lacks Trp, Leu and His aa. SD-WLHA lacks adenine in addition to Trp, Leu and His. SD-WL lacks Trp and Leu and thus non-selective plate.

Reporter assay

HEK293 cells (4×10^4 cells/well) cultured in 24-well plates were transfected with the expression vectors for IPS-1, DDX3 or empty vector together with the reporter plasmid (100 ng/well) and an internal control vector, phRL-TK (Promega) (2.5 ng/well) using FuGENE (Roche) as described previously [28]. The p-125 luc reporter containing the human IFN-β promoter region (−125 to +19) was provided by Dr. T. Taniguchi (University of Tokyo, Tokyo, Japan). The total amount of DNA (500 ng/well) was kept constant by adding empty vector. After 24 h, cells were lysed in lysis buffer (Promega), and the *Firefly* and *Renella* luciferase activities were determined using a dual-luciferase reporter assay kit (Promega). The *Firefly* luciferase activity was normalized by *Renella* luciferase activity and is expressed as the fold stimulation relative to the activity in vector-transfected cells. Experiments were performed three times in duplicate (unless otherwise indicated in the legends).

PolyI:C stimulation

PolyI:C was purchased from GE Healthcare company, and solved in milliQ water. For polyI:C treatment, polyI:C (50 μg/mL) was mixed with DEAE-dextran (0.5 mg/mL) (Sigma) in the culture medium, and the cell culture supernatant was replaced with the medium containing polyI:C and DEAE-dextran. Using DEAE-dextran, polyI:C is incorporated into the cytoplasm to activate RIG-I/MDA5.

Virus preparation and infection

VSV Indiana strain or poliovirus type 1 Mahoney strain were used for virus assay. Vero derived cell (Vero-SLAM) was used for propagation and plaque assay for VSV indiana strain or poliovirus type 1 Mahoney strain. HEK293 cells were infected with viruses at MOI = 0.001 in a 24-well plate. The virus titers of culture media at indicated hours post infection in the figures were determined by plaque assay using Vero-SLAM cells. In some experiments that require rapid virus propagation, high MOI (0.1 ~ 1) was used for infection.

Immunoprecipitation

HEK293FT cells were transfected in a 6-well plate with plasmids encoding DDX3, IPS-1, RIG-I or MDA5 as indicated in the figures. Twenty-four hours after tranfection, the total cell lysate was prepared by lysis buffer (20 mM Tris-HCl (pH 7.5) containing 125 mM NaCl, 1 mM EDTA, 10% glycerol, 1% NP-40, 30 mM NaF, 5 mM Na3Vo4, 20 mM IAA and 2 mM PMSF), and the protein was immunoprecipitated with anti-HA polyclonal (Sigma) or anti-FLAG M2 mAb (Sigma). The precipitated samples were resolved on SDS-PAGE, blotted onto a nitrocellulose sheet and stained with anti-HA (HA1.1) monoclonal (Sigma), anti-HA polyclonal or anti-FLAG M2 mAb.

Confocal analysis

HeLa cells were plated onto cover glass in a 24-well plate. In the following day, cells were transfected with indicated plasmids using Fugene HD (Roch). The amount of DNA was kept constant by adding empty vector. After 24 h, cells were fixed with 3% of paraformaldehyde in PBS for 30 min, and then permeabilized with PBS containing 0.2% of Triton X-100 for 15 min. For the polyI:C stimulation, 100 ng of polyI:C were transfected into HeLa cell in 24-well plates together with IPS-1 or DDX3 expressing vectors, and 24 h after the transfection, the cells were fixed and stained for confocal microscopic analysis. Permeabilized cells were blocked with PBS containing 1% BSA and were labeled with anti-Flag M2 mAb (Sigma), anti-HA polyclonal Ab (Sigma) or Mitotracker in 1% BSA/PBS for 1 h at room temperature. The cells were then washed with 1% BSA/PBS and treated for 30 min at room temperature with Alexa-conjugated Ab (Molecular Probes). Thereafter, micro-cover glass was mounted onto slide glass using PBS containing 2.3% DABCO and 50% of glycerol. The stained cells were visualized at × 60 magnification under a FLUOVIEW (Olympus, Tokyo, Japan).

Acknowledgements: The authors thank Dr. M. Sasai, Dr. T. Ebihara, Dr. K. Funami, Dr. A. Matsuo, Dr. A. Ishii, Dr. A. Watanabe and Dr. M. Shingai in our laboratory for their critical discussions. This work was supported in part by CREST and Innovation, JST (Japan Science and Technology Corporation), the Program of Founding Research Centers for Emerging and Reemerging Infectious Diseases, MEXT, Sapporo Biocluster "Bio-S," the Knowledge Cluster Initiative of the MEXT, Grants-in-Aid from the Ministry of Education, Science, and Culture (Specified Project for Advanced Research) and the Ministry of Health, Labor, and Welfare of Japan, Mitsubishi Foundation, Mochida Foundation, NorthTec Foundation and Takeda Foundation.

Conflict of interest: The authors declare no financial or commercial conflict of interest.

References

1 **Kato, H., Takeuchi, O., Sato, S., Yoneyama, M., Yamamoto, M., Matsui, K., Uematsu, S. *et al.***, Differential roles of MDA5 and RIG-I helicases in the recognition of RNA viruses. *Nature* 2006. **441**: 101–105.

2 **Gitlin, L., Barchet, W., Gilfillan, S., Cella, M., Beutler, B., Flavell, R. A., Diamond, M. S. *et al.***, Essential role of mda-5 in type I IFN responses to polyriboinosinic:polyribocytidylic acid and encephalomyocarditis picornavirus. *Proc. Natl. Acad. Sci. USA* 2006. **103**: 8459–8464.

3 **Yoneyama, M., Kikuchi, M., Natsukawa, T., Shinobu, N., Imaizumi, T., Miyagishi, M., Taira, K. *et al.***, The RNA helicase RIG-I has an essential function in double-stranded RNA-induced innate antiviral responses. *Nat. Immunol.* 2004. **5**: 730–737.

4 **Kawai, T., Takahashi, K., Sato, S., Coban, C., Kumar, H., Kato, H., Ishii, K. J. *et al.***, IPS-1, an adaptor triggering RIG-I- and Mda5-mediated type I interferon induction. *Nat. Immunol.* 2005. **6**: 981–988.

5 **Meylan, E., Curran, J., Hofmann, K., Moradpour, D., Binder, M., Bartenschlager, R. and Tschopp, J.**, Cardif is an adaptor protein in the RIG-I antiviral pathway and is targeted by hepatitis C virus. *Nature* 2005. **437**: 1167–1172.

6 **Seth, R. B., Sun, L., Ea, C. K. and Chen, Z. J.**, Identification and characterization of MAVS, a mitochondrial antiviral signaling protein that activates NF-kappaB and IRF 3. *Cell* 2005. **122**: 669–682.

7 **Xu, L. G., Wang, Y. Y., Han, K. J., Li, L. Y., Zhai, Z. and Shu, H. B.**, VISA is an adapter protein required for virus-triggered IFN-beta signaling. *Mol. Cell* 2005. **19**: 727–740.

8 **Sasai, M., Matsumoto, M. and Seya, T.**, The kinase complex responsible for IRF-3-mediated IFN-beta production in myeloid dendritic cells (mDC). *J. Biochem.* 2006. **139**: 171–175.

9 **Ryzhakov, G. and Randow, F.**, SINTBAD, a novel component of innate antiviral immunity, shares a TBK1-binding domain with NAP1 and TANK. *EMBO J.* 2007. **26**: 3180–3190.

10 **Sasai, M., Oshiumi, H., Matsumoto, M., Inoue, N., Fujita, F., Nakanishi, M. and Seya, T.**, Cutting Edge: NF-kappaB-activating kinase-associated protein 1 participates in TLR3/Toll-IL-1 homology domain-containing adapter molecule-1-mediated IFN regulatory factor 3 activation. *J. Immunol.* 2005. **174**: 27–30.

11 **Saito, T., Hirai, R., Loo, Y. M., Owen, D., Johnson, C. L., Sinha, S. C., Akira, S. *et al.***, Regulation of innate antiviral defenses through a shared repressor domain in RIG-I and LGP2. *Proc. Natl. Acad. Sci. USA* 2007. **104**: 582–587.

12 **Hornung, V., Ellegast, J., Kim, S., Brzozka, K., Jung, A., Kato, H., Poeck, H. *et al.***, 5′-Triphosphate RNA is the ligand for RIG-I. *Science* 2006. **314**: 994–997.

13 **Franca, R., Belfiore, A., Spadari, S. and Maga, G.**, Human DEAD-box ATPase DDX3 shows a relaxed nucleoside substrate specificity. *Proteins* 2007. **67**: 1128–1137.

14 **Yedavalli, V. S., Neuveut, C., Chi, Y. H., Kleiman, L. and Jeang, K. T.**, Requirement of DDX3 DEAD box RNA helicase for HIV-1 Rev-RRE export function. *Cell* 2004. **119**: 381–392.

15 **Kravchenko, V. V., Mathison, J. C., Schwamborn, K., Mercurio, F. and Ulevitch, R. J.**, IKKi/IKKepsilon plays a key role in integrating signals induced by pro-inflammatory stimuli. *J. Biol. Chem.* 2003. **278**: 26612–26619.

16 **Soulat, D., Bürckstümmer, T., Westermayer, S., Goncalves, A., Bauch, A., Stefanovic, A., Hantschel, O. *et al.***, The DEAD-box helicase DDX3X is a critical component of the TANK-binding kinase 1-dependent innate immune response. *EMBO J.* 2008. **27**: 2135–2146.

17 **Venkataraman, T., Valdes, M., Elsby, R., Kakuta, S., Caceres, G., Saijo, S., Iwakura, Y. *et al.***, Loss of DExD/H box RNA helicase LGP2 manifests disparate antiviral responses. *J. Immunol.* 2007. **178**: 6444–6455.

18 **Schroder, M., Baran, M. and Bowie, A. G.**, Viral targeting of DEAD box protein 3 reveals its role in TBK1/IKKepsilon-mediated IRF activation. *EMBO J.* 2008. **27**: 2147–2157.

19 **Gack, M. U., Shin, Y. C., Joo, C. H., Urano, T., Liang, C., Sun, L., Takeuchi, O. *et al.***, TRIM25 RING-finger E3 ubiquitin ligase is essential for RIG-I-mediated antiviral activity. *Nature* 2007. **446**: 916–920.

20 **Oshiumi, H., Matsumoto, M., Hatakeyama, S. and Seya, T.**, Riplet/RNF135, a RING finger protein, ubiquitinates RIG-I to promote interferon-beta induction during the early phase of viral infection. *J. Biol. Chem.* 2009. **284**: 807–817.

21 **Arimoto, K., Takahashi, H., Hishiki, T., Konishi, H., Fujita, T. and Shimotohno, K.**, Negative regulation of the RIG-I signaling by the ubiquitin ligase RNF125. *Proc. Natl. Acad. Sci. USA* 2007. **104**: 7500–7505.

22 **Ariumi, Y., Kuroki, M., Abe, K., Dansako, H., Ikeda, M., Wakita, T. and Kato, N.**, DDX3 DEAD-box RNA helicase is required for hepatitis C virus RNA replication. *J. Virol.* 2007. **81**: 13922–13926.

© 2010 WILEY-VCH Verlag GmbH & Co. KGaA, Weinheim

23 Chuang, R. Y., Weaver, P. L., Liu, Z. and Chang, T. H., Requirement of the DEAD-Box protein ded1p for messenger RNA translation. *Science* 1997. 275: 1468–1471.

24 Owsianka, A. M. and Patel, A. H., Hepatitis C virus core protein interacts with a human DEAD box protein DDX3. *Virology* 1999. 257: 330–340.

25 Mamiya, N. and Worman, H. J., Hepatitis C virus core protein binds to a DEAD box RNA helicase. *J. Biol. Chem.* 1999. 274: 15751–15756.

26 Sasai, M., Shingai, M., Funami, K., Yoneyama, M., Fujita, T., Matsumoto, M. and Seya, T., NAK-associated protein 1 participates in both the TLR3 and the cytoplasmic pathways in type I IFN induction. *J. Immunol.* 2006. 177: 8676–8683.

27 Oshiumi, H., Matsumoto, M., Funami, K., Akazawa, T. and Seya, T., TICAM-1, an adaptor molecule that participates in Toll-like receptor 3-mediated interferon-beta induction. *Nat. Immunol.* 2003. 4: 161–167.

28 Matsumoto, M., Funami, K., Tanabe, M., Oshiumi, H., Shingai, M., Seto, Y., Yamamoto, A. *et al.*, Subcellular localization of Toll-like receptor 3 in human dendritic cells. *J. Immunol.* 2003. 171: 3154–3162.

Abbreviations: **CARD:** caspase recruitment domain · **DEAD:** Asp-Glu-Ala-Asp · **DDX3:** DEAD/H BOX 3 · **IKKε:** I-kappa-B kinase ε · **IRF-3:** IFN regulatory factor-3 · **IP:** immunoprecipitation · **IPS-1:** IFN-β promoter stimulator-1 · **MDA5:** melanoma differentiation-associated gene 5 · **RIG-I:** retinoic acid inducible gene-I · **RLR:** RIG-I-like receptor · **TBK1:** TANK-binding kinase 1 · **VSV:** vesicular stomatitis virus

Full correspondence: Dr. Tsukasa Seya, Department of Microbiology and Immunology, Graduate School of Medicine, Hokkaido University, Kita-ku, Sapporo 060-8638, Japan
Fax: +81-11-706-7866
e-mail: seya-tu@pop.med.hokudai.ac.jp

See accompanying Commentary:
http://dx.doi.org/10.1002/eji.201040447

Received: 30/11/2009
Revised: 8/1/2010
Accepted: 19/1/2010
Accepted article online: 1/2/2010

OPEN ACCESS Freely available online PLoS one

Development of Mouse Hepatocyte Lines Permissive for Hepatitis C Virus (HCV)

Hussein Hassan Aly[1], Hiroyuki Oshiumi[1], Hiroaki Shime[1], Misako Matsumoto[1], Taka Wakita[2], Kunitada Shimotohno[3], Tsukasa Seya[1]*

1 Department of Microbiology and Immunology, Hokkaido University Graduate School of Medicine, Sapporo, Hokkaido, Japan, **2** Department of Virology II, National Institute of Infectious Diseases, Shinjuku, Tokyo, Japan, **3** Research Institute, Chiba Institute of Technology, Narashino, Chiba, Japan

Abstract

The lack of a suitable small animal model for the analysis of hepatitis C virus (HCV) infection has hampered elucidation of the HCV life cycle and the development of both protective and therapeutic strategies against HCV infection. Human and mouse harbor a comparable system for antiviral type I interferon (IFN) induction and amplification, which regulates viral infection and replication. Using hepatocytes from knockout (ko) mice, we determined the critical step of the IFN-inducing/amplification pathways regulating HCV replication in mouse. The results infer that interferon-beta promoter stimulator (IPS-1) or interferon A receptor (IFNAR) were a crucial barrier to HCV replication in mouse hepatocytes. Although both IFNARko and IPS-1ko hepatocytes showed a reduced induction of type I interferons in response to viral infection, only IPS-1-/- cells circumvented cell death from HCV cytopathic effect and significantly improved J6JFH1 replication, suggesting IPS-1 to be a key player regulating HCV replication in mouse hepatocytes. We then established mouse hepatocyte lines lacking IPS-1 or IFNAR through immortalization with SV40T antigen. Expression of human (h)CD81 on these hepatocyte lines rendered both lines HCVcc-permissive. We also found that the chimeric J6JFH1 construct, having the structure region from J6 isolate enhanced HCV replication in mouse hepatocytes rather than the full length original JFH1 construct, a new finding that suggests the possible role of the HCV structural region in HCV replication. This is the first report on the entry and replication of HCV infectious particles in mouse hepatocytes. These mouse hepatocyte lines will facilitate establishing a mouse HCV infection model with multifarious applications.

Citation: Aly HH, Oshiumi H, Shime H, Matsumoto M, Wakita T, et al. (2011) Development of Mouse Hepatocyte Lines Permissive for Hepatitis C Virus (HCV). PLoS ONE 6(6): e21284. doi:10.1371/journal.pone.0021284

Editor: Jacques Zimmer, Centre de Recherche Public de la Santé (CRP-Santé), Luxembourg

Received May 13, 2011; **Accepted** May 24, 2011; **Published** June 22, 2011

Funding: This work was supported in part by Grants-in-Aid from the Ministry of Education, Science, and Culture (Specified Project for Advanced Research), the Ministry of Health, Labor, and Welfare of Japan, and the Hokkaido University Leader Development System in the Basic Interdisciplinary Research Areas (L station). Supports from Mitsubishi Foundation, Mochida Foundation, NorthTec Foundation Waxman Foundation and Yakult Foundation are gratefully acknowledged. The funders had no role in study design, data collection and analysis, decision to publish, or preparation of the manuscript.

Competing Interests: The authors have declared that no competing interests exist.

* E-mail: seya-tu@pop.med.hokudai.ac.jp

Introduction

Chronic hepatitis C virus (HCV) infection is a major cause of mortality and morbidity throughout the world infecting around 3.1% of the world's population [1]. The development of much needed specific antiviral therapies and an effective vaccine has been hampered by the lack of a suitable small animal model. The determinants restricting HCV tropism to human and chimpanzee hosts are unknown. Replication of HCV strain JFH1 has been demonstrated in mouse cells only upon antibody selection [2], highlighting the very limited replication efficiency. Human CD81 and occludin have been implicated as important entry receptors for retrovirus particles bearing HCV glycoproteins, HCV pseudoparticles (HCVpp), into NIH3T3 murine cells [3]. However, HCV infection, spontaneous replication and particle production by mouse cells have not yet been reported.

In mammalian cells, the host detects and responds to infection by RNA-viruses, including HCV, by primarily recognizing viral RNA through several distinct pathogen recognition receptors (PRRs), including the cell surface and endosomal RNA sensors Toll-like receptors 3 and 7 (TLR3 and TLR7), and the cytoplasmic RNA sensors retinoic acid-inducible gene I (RIG-I) and melanoma differentiation associated gene 5 (MDA5) [4]. The detection of virus infection by these receptors leads to the induction of interferons (IFNs) and their downstream IFN-inducible anti-viral genes through distinct signaling pathways [5]. Type I IFN is an important regulator of viral infections in the innate immune system [6]. Another type of IFN, IFN-lambda, affects the prognosis of HCV infection, and its response to antiviral therapy [7,8].

Mutations impairing the function of the RIG-I gene and the induction of IFN were essential in establishing HCV infectivity in human HuH7.5 cells [9]. Similarly, the HCV-NS3/4a protease is known to cleave IPS-1 adaptor molecule, inducing further downstream blocking of the IFN-inducing signaling pathway [10]. These data clearly demonstrate that the host RIG-I pathway is crucial for suppressing HCV proliferation in human hepatocytes. Using a similar strategy, we investigated whether suppressing the antiviral host innate immune system conferred any advantage on HCV proliferation in mouse hepatocytes. We examined the possibility of HCV replication in mice lacking the expression of key factors that modulate the type I IFN-inducing pathways. Only gene silencing of the IFN receptor (IFNAR) or IPS-1 was sufficient to establish spontaneous HCV replication in

mouse hepatocytes. To establish a cell line permissive for HCV replication, which is required for further *in vitro* studies of the HCV life cycle in mouse hepatocytes, we immortalized IFNAR- and IPS-1-knockout (ko) mice hepatocytes with SV40 T antigen. Upon expression of the human (h)CD81 gene, these newly established cell lines were able to support HCV infection for the first time in mouse hepatocytes. Viral factors required for HCV replication in mouse hepatocytes were also analyzed.

Results

IPS-1-mediated IFN signaling is important for HCV replication in mouse hepatocytes

As a first step in establishing HCV infection in mice, we tested the susceptibility of mouse hepatocytes to persistent expression of HCV proteins after RNA transfection. *In vitro* transcribed chimeric J6JFH1 RNA, in which the HCV structural and non-structural regions were from J6 and JFH1 isolates respectively, was transfected into hepatocytes from wild-type mice. We used a highly sensitive polyclonal antibody derived from HCV-patient serum for the detection of HCV proteins. No HCV proteins were detected five days after transfection (Fig. 1 A), suggesting that wild-type mouse hepatocytes were unable to maintain HCV replication. We then tried to find and block the pathway used by mouse hepatocytes for the detection of viral-RNA and the induction of IFN response. Mouse hepatocytes did not show the expression of either TLR3 or TLR7 as detected by RT-PCR, unlike IPS-1 and RIG-I which was fairly detected (Fig. S1), suggesting that the cytoplasmic RIG-I/IPS-1 pathway is the main pathway utilized by mouse hepatocytes for the detection of RNA viruses. We then checked the susceptibility of hepatocytes from TICAM-1ko, IPS-1ko and IFNARko mice to the prolonged expression of HCV proteins (Fig. 1B–D). Only IPS-1- and IFNARko mouse hepatocytes showed expression of J6JFH1 proteins five days after transfection (Fig. 1), indicating the importance of impaired IPS-1 and/or IFNAR receptors for HCV persistence. Similarly, the detection of the J6JFH1-RNA in transfected hepatocyte lines from various knockout mice showed higher levels in IPS-1 or IFNAR knockout cells compared to TICAM-1knockout cells in which a rapid decline of J6JFH1-RNA levels was noticed similar to the non-replicating control JFH1GND construct (Fig. S2). These data clearly suggest that the RIG-I/IPS-1 but not TLR3/TICAM-1 is the main pathway utilized for the detection of HCV-RNA and the induction of anti-viral immune response in mouse hepatocytes. Its suppression significantly improves HCV replication in mouse hepatocytes.

Establishment and characterization of immortalized mouse hepatocyte cell lines lacking expression of the IFNAR or IPS-1 gene

We further established mouse hepatocyte lines with disrupted IFNAR or IPS-1 genes through immortalization with SV40T antigen, and used these cell lines to study factors required for the HCV life cycle. Hepatocytes were transduced with SV40T-expressing lentivirus vectors. Six weeks after transduction, hepatocytes transduced with SV40T showed continuous proliferation and clonally proliferating hepatocyte lines were selected. SV40T-immortalized IFNARko and IPS-1ko clones were designated IRK (Fig. 2 A) and IPK (Fig. 2 B), respectively. 20 IRK and 19 IPK clones were picked up, of which IRK clones 2 and 4 (IRK2 and IRK4) and IPK clones 10 and 17 (IPK10 and IPK17) were most closely related to primary mouse hepatocytes in term of differentiation (Fig. 2 C) and were used in the following experiments. Expression of SV40T was confirmed by RT-PCR analysis (data not shown). IRK2, IRK4, IPK10 and IPK17, but not the non-hepatocytic NIH3T3 cells, displayed albumin and hepatocyte nuclear factor 4 (HNF4) expression similar to that observed in liver tissue, but did not express the bile duct marker, cytokeratin. IRK and IPK cells did not show expression of IFNAR and IPS-1 respectively (Fig. 2 C).

Replication of the HCV genome in IRK and IPK cells

To assess the permissiveness of the established cell lines to HCV replication, we transduced IRK4 and IPK17 cells with J6JFH1 RNA and monitored the HCV protein and RNA levels by IF (Fig. 3 A) and real time RT-PCR (Fig. 3 B). The number of cells expressing HCV proteins, as detected by IF, increased over time, indicating the continuous proliferation of J6JFH1 in these cells. However, the ratio between infected and non-infected cells did not significantly change over time for 7 days after transfection. Similarly, the amount of total J6JFH1 RNA in 1 µg of total cellular RNA was reasonably constant. By contrast, the level of

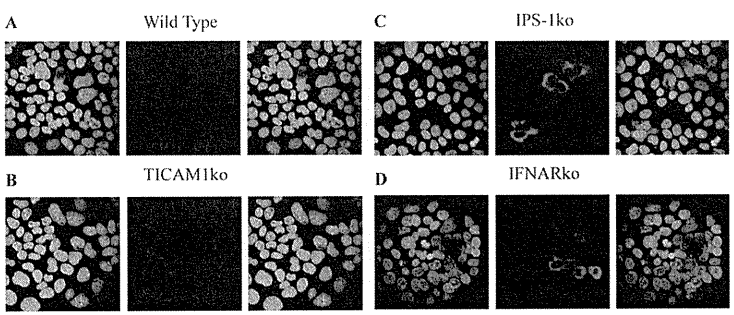

Figure 1. IF detection of of J6JFH1 proteins' expression 5 days after transfection of J6JFH1-RNA through electroporation into wild type (A), TICAM-1ko (B), IPS-1ko (C), and IFNARko (D), freshly isolated primary hepatocytes. A highly sensitive polyclonal antibody extracted from HCV-patient serum (AbS3) was used for the detection. Staining of the uninfected hepatocytes from different Ko mice was also performed and they showed negative for HCV proteins (data not shown).
doi:10.1371/journal.pone.0021284.g001

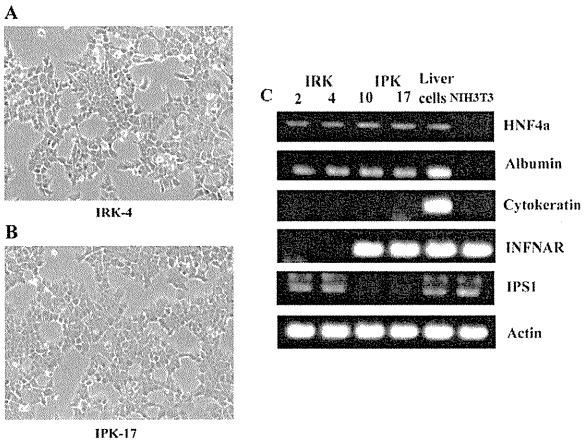

Figure 2. Morphological characteristics of IRK-4 (A) and IPK-17 (B) cells. (C) RT analysis for the expression of albumin, HNF4, cytokeratin, interferon A receptor, and IPS-1 in 2 IFNAR-KO cell lines (IRK2 and 4), 2 IPS-1-KO cell lines (IPK-10 and 17), total liver, and NIH3T3 cells.
doi:10.1371/journal.pone.0021284.g002

J6JFH1GND RNA carrying a mutation in NS5B hampering HCV replication, rapidly declined, indicating the requirement of continuous HCV replication for the maintenance of HCV positivity in the transfected mouse hepatocytes. Similar data were obtained from IRK2 and IPK10 cells (data not shown).

IPS-1-dependent/Interferon-independent pathway is responsible for HCV's cytopathic effect

In comparison to IPS-1ko hepatocytes, J6JFH1-RNA in IFNARko were lower and decreased further after its transfection, while higher stable levels of J6JFH1-RNA were maintained in IPS-1ko cells (Fig. 3 B and Fig. S2). Similarly, larger numbers of HCV-positive cells were detected in IPS-1ko hepatocytes compared with their IFNARko counterparts (Fig. 3 A), suggesting that the IPS-1 disruption benefits HCV replication in a distinct manner from IFNAR disruption. To measure the interferon induction after RNA virus infection in those cells, we used a highly infectious RNA-Virus (VSV) and measured the induction of interferon after its infection. All the interferons measured showed similar suppression of induction in IFNARko and IPS-1ko hepatocytes (Fig. 4). Surprisingly, cellular cytopathic effect that was monitored after transfection of J6JFH1-RNA was markedly reduced in IPS-1ko but not in IFNARko hepatocytes after transfection (Fig. 5A). This suppression was accompanied by an increase of J6JFH1-RNA levels in IPS-1ko cells, suggesting that minimal cellular damage induced by HCV replication in IPS-1-/- cells led to the improvement of HCV proliferation in mouse hepatocytes (Fig. 5B).Reduction of HCV-induced cellular cytotoxicity (Fig.5C), and improvement of HCV replication (Fig.5D) in wild type, and IFNAR-KO cells were found when we cultured the cells with a pan-caspase inhibitor, zVAD-fmk, 2 days before and after HCV-RNA transfection. We reasoned that the IPS-1 pathway rather than the IFNAR pathway capacitates hepatocytes to induce HCV-derived apoptotic cell death and its disruption resulted in the circumvention of cell death.

Human CD81 is required for HCV infection of mouse hepatocytes

Similar to the primary mouse hepatocytes, immortalized mouse hepatocytes showed the expression of all the mouse counterparts of human HCV entry receptors (Fig. S3). Human CD81 and hOccludin, but not other human HCV receptors such as SR-B1 or claudin1, have previously been reported to be essential for HCVpp entry into NIH3T3 mouse cells [3]. We then expressed hCD81 and/or hOccludin in IRK2 and IRK4 cells using lentivirus vectors. Using a MOI of 10, 95% transfection efficiency was achieved (Fig. S4) with lentivirus vector. We next tested the effect of these proteins on HCV particle (HCVcc) infection. Human CD81 alone was found to be required for J6JFH1 infection into all IRK and IPK cells tested (Fig. S5 and Fig. 6 A, and B). For the first time in mouse hepatocytes, HCV proteins were detected in nearly 1% of the cells used for infection. These data demonstrated the importance of hCD81 in establishing HCVcc infection in mouse hepatocytes.

Viral factors affecting HCV replication in mouse hepatocytes

After successfully establishing J6JFH1 infection in mouse hepatocytes, we attempted to infect these cells with other strains of HCV. Human CD81-expressing IPK17 cells were infected with full-length JFH1FL, however, no infection was detected (data not shown). This might be due to a problem in infection and/or replication. We further examined the replication efficiency of JFH1FL, the subgenomic JFH1 replicon and the J6JFH1 chimera in two different mouse hepatocyte lines and the HuH7.5.1 cell line. The persistent expression of HCV proteins was detected seven days after RNA transfection. Although HCV proteins were detected in HuH7.5.1 cells in all cases (Fig. 7 C), only J6JFH1 proteins were detected in the mouse hepatocyte lines, suggesting for the first time the importance of the J6 structural region for the replication of HCV in mouse hepatocytes (Fig. 7 A, and B).

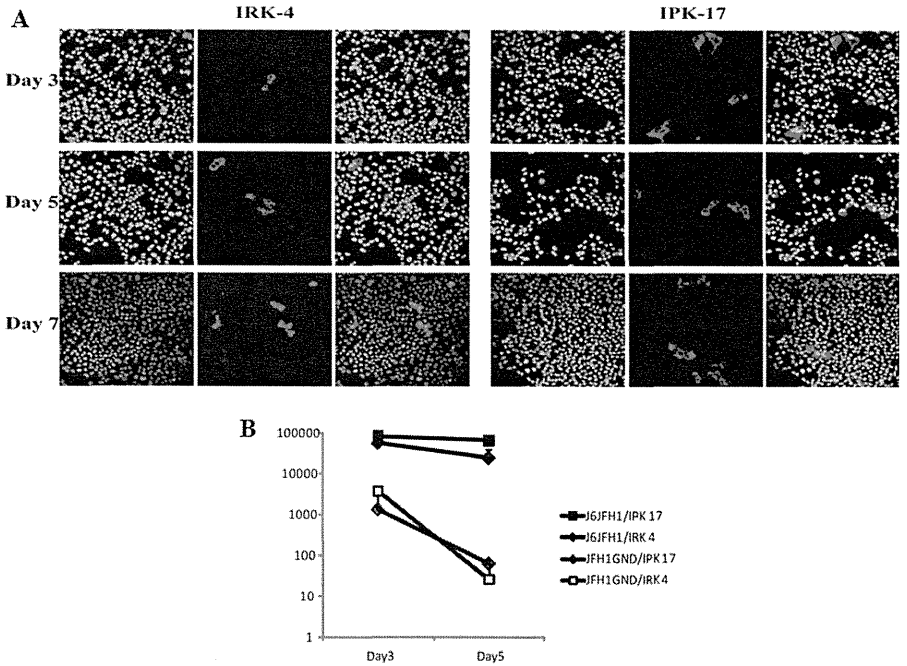

Figure 3. Proliferation of HCV in IRK4 and IPK17 cells over time as detected by immunofluorescence staining of NS5a protein using the CL1 rabbit polyclonal antibody (A) and by quantitative real-time RT-PCR analysis of HCV-RNA levels (B). JFH1GND was used as a negative control to exclude non replicating HCV-RNA. The data plotted represent the average +/− STD of 3 different experiments.
doi:10.1371/journal.pone.0021284.g003

Discussion

Gene silencing of either IPS-1 or IFNAR significantly improves HCV replication and persistence in mouse hepatocytes compared with wild-type or TICAM-1ko mice. This result demonstrated the importance of the IPS-1 pathway rather than the TICAM-1 pathway in the induction of type I IFN by HCV infection, and revealed that the IFNAR amplification pathway confers resistance to HCV in mouse hepatocytes independently of TICAM-1. In accordance with our data, HCV-NS3/4A protease is known to cleave the IPS-1 and/or RIG-I-complement molecules including DDX3 and Riplet in humans to overcome the host innate immune response, showing the importance of RIG-I/IPS-1 pathway suppression in the establishment of HCV infection [10,11,12].

To further study factors affecting the HCV life cycle in mouse hepatocytes, we established IPK and IRK immortalized mouse hepatocyte lines by transduction with SV40T antigen. The established hepatocytes cell lines showed expression of HNF4, a major hepatocyte transcription factor, required for hepatocyte differentiation and liver-specific gene expression [13]. The maintenance of hepatocellular functions was demonstrated by continuous expression of hepatocyte specific differentiation marker, albumin, and the lack of expression of the bile duct marker, cytokeratin. The close resemblance of these cell lines to primary mouse hepatocytes is crucial to ensure the physiological relevance of factors identified in these cell lines that affect the HCV life cycle.

It is worth noting that HCV replication in IPS-1ko was higher than that in IFNARko hepatocytes. Since IPS-1 is present upstream of IFNAR in the IFN-amplification pathway, this higher J6JFH1 replication efficiency in IPS-1ko hepatocytes suggested the presence of an additive factor affecting HCV replication other than the induction of IFNAR-mediated type I IFN. This enhanced replication efficiency was also not accompanied by the induction of other interferon types, but was correlated with the reduction of HCV-induced apoptosis in mouse hepatocytes. This data clearly demonstrates that IPS-1 is playing an important role in the regulation of HCV infection in mouse hepatocytes through two different pathways, the IFN-induction pathways and another new IFN-independent pathway, leading to apoptotic cell death and elimination of HCV-harboring hepatocytes. The cytopathic effect of HCV infection in human cells is still contradictory. Although, some reports showed the induction of apoptosis and cell death by HCV infection in human hepatocytes [14,15,16], others showed suppression of apoptosis by HCV proteins [17,18]. This difference may be due to the different cell lines used in the different studies. Almost all the studies reporting HCV-induced apoptosis used

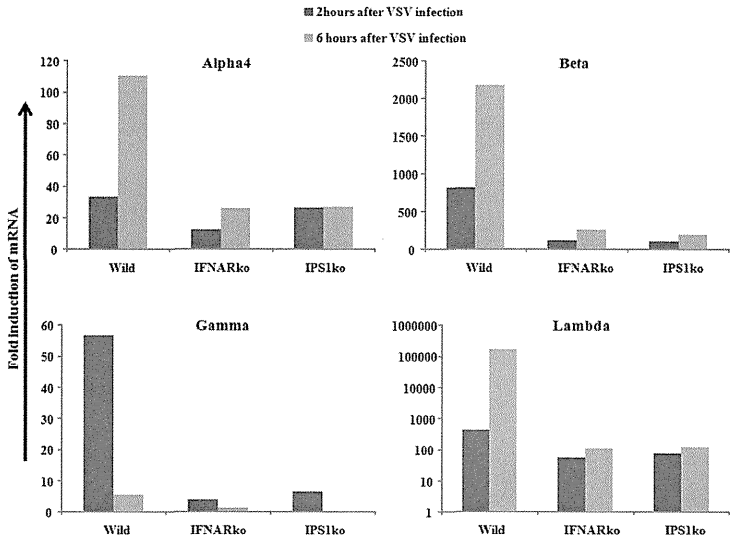

Figure 4. Wild type, IFNARko, and IPS-1ko mice hepatocytes were infected with mock or VSV virus, 2 and 6 hours later, total RNA was extracted from the cells, and interferon alpha, beta, gamma and lambda mRNA induction levels were measured by real-time RT-PCR. Similar results were obtained from 2 different experiments, each was performed in duplicates. The data plotted represent the mean duplicate readings in one of them.
doi:10.1371/journal.pone.0021284.g004

hepatocellular carcinoma cell lines. Since it has been established that the inability to undergo apoptosis is essential for the development of cancer [19,20,21], our use of immortalized, non-cancerous hepatocytes may make it possible to reproduce the physiological response of the cells to HCV infection more closely. The IPS-1 regulation of cell death following the introduction of HCV-RNA may also regulate the effector cell function. It is likely that hepatocyte debris generated secondary to intrinsic production of viral dsRNA in HCV-infected hepatocytes affect the antiviral effector response of the immune system through maturation of dendritic cells [22]. Hence, the effector cell activation may be enhanced by the induction of cell death through the IPS-1 pathway in hepatocytes which may facilitate producing dsRNA-containing debris.

In comparison to the JFH1GND construct with deficient replication that showed a rapid reduction in its RNA levels over time after transfection into mouse hepatocytes, J6JFH1 RNA was detected at four-log higher levels and was maintained at a relatively stable levels in IPS-1ko hepatocytes. Although the number of mouse cells expressing HCV proteins was found to increase over time, as detected by IF, the ratio between HCV-negative and -positive cells did not show any significant change for 7 days after transfection and increased after 10 days (data not shown). This indicates a negative selection of HCV-bearing cells over time which may be due to slower cellular replication, or loss of HCV replication. Another possibility may be that HCV infection is affected by the presence of an inhibitory factor possibly triggered by HCV replication or the lack of a human host factor required for HCV replication. Due to the initial replication of HCV in the transfected IPK and IRK mouse hepatocytes for the first 7 days and the establishment of infection, we favor the presence of a possible inhibitory factor that may be triggered by HCV replication. Another factor that also limits HCV spread in mouse hepatocytes is the failure of HCV to produce infectious particles in these cells (data no shown).

Using this newly established immortalized mouse hepatocyte line, we found that although J6JFH1, JFH1FL and the subgenomic JFH1 replicon all share a similar non-structural region derived from isolate JFH1 that is required for HCV replication, and although all of these constructs can replicate efficiently in HuH7.5.1 cells, strikingly, only J6JFH1 carrying the J6 structural region replicated in mouse hepatocytes. This indicates the importance of the J6 structural region and/or the chimeric construct between J6 and JFH1 for HCV replication in mouse hepatocytes. Structural regions are known to be important for HCV entry and/or particle formation [23], but this is the first time that their importance in replication in HCV-bearing cells has been demonstrated. This finding clearly shows the importance of non-hepatoma cell lines with less genetic abnormalities and mutations for the discovery of new aspects of the life cycle of HCV.

Although, the co-expression of human CD81 and Occludin genes was found to be important for HCVpp entry into murine NIH3T3 cells [3], the expression of hCD81 alone was sufficient for J6JFH1 entry into mouse hepatocytes. This may be explained by the different cell lines used in the different studies. In contrast to NIH3T3 cells, we used immortalized hepatocytes that showed close physiological resemblance to primary mouse hepatocytes and showed the expression of all the mouse counterparts of HCV entry

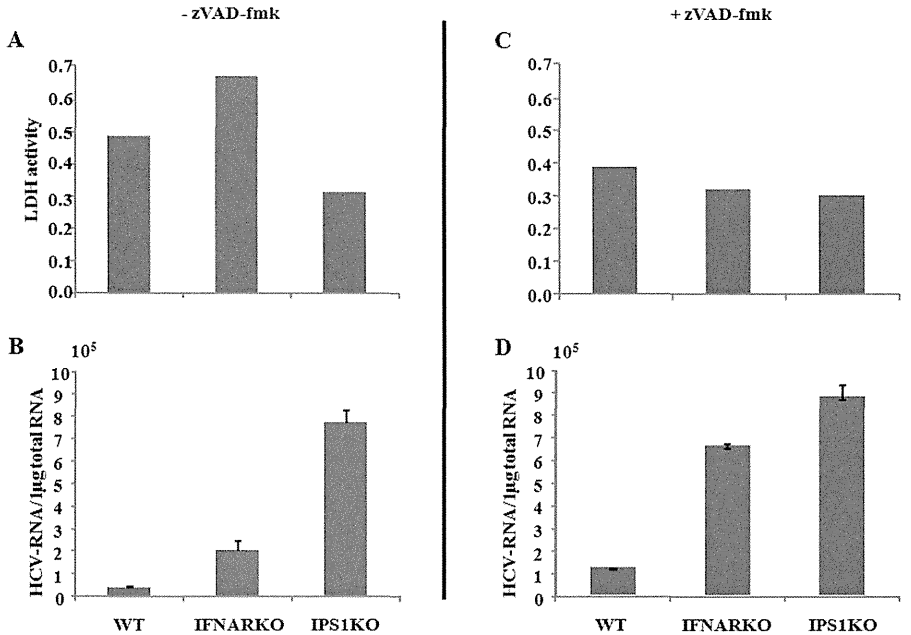

Figure 5. Measurement of J6JFH1 mediated cytopathic effect in wild type, IFNARko, and IPS-1ko mouse hepatocytes. Culture medium were left untreated (A;B) or treated with 20 μM of zVAD-fmK (C;D) 2 days before and after J6JFH1-RNA transfection. One day after transfection of J6JFH1-RNA, culture medium was discarded and cells were washed with PBS. A new medium was added and cells were cultured for another 24 hours. The LDH activity in the culture medium was measured in 2 different experiments in duplicates and showed similar results, the average levels of a duplicate from a single experiment was plotted (A, C). HCV-RNA titers in the cells were also measured using real-time RT-PCR (B, D), the data shown represent the mean +/− STD of 3 different experiments.
doi:10.1371/journal.pone.0021284.g005

receptors. A study from a different group showed that adaptive mutations in HCV envelope proteins allowing its interaction with murine CD81 is enough for efficient HCVpp entry without the expression of any human entry receptors in murine cells [24]. This report, together with ours, suggest that CD81 is the main human host restriction factor for HCV entry, and that overcoming this problem either by HCV adaptation to murine CD81, or the expression of human CD81 in murine hepatocytes is essential for HCV entry. Although our lentivirus transfection efficiency with CD81 was around 95% in IPK and IRK clones, only 1% of the cells were prone to infection with HCVcc. Also, HCVpp showed lower entry levels in those cells compared to HuH7.5.1 cells (Fig. S6). This suggests that hCD81 expression is the minimum and most crucial requirement for HCV entry into mouse hepatocytes. The discovery and expression of other co-receptors facilitating HCV entry in human cells is still required for efficient and robust HCV infection.

In summary, the suppression of IPS-1 is important for the establishment of HCV infection and replication in mouse hepatocytes through the suppression of both interferon induction and interferon independent J6JFH1-induced cytopathic effect. We have established hepatocytes lines from IPS-1 and IFNARko mice that support HCV replication and infection. These cell lines will be very useful in identifying other species restriction factors and viral determinants required for further establishment of a robust and efficient HCV life cycle in mouse hepatocytes. Using those cells, we showed for the first time the importance of HCV structural region for viral replication. IRF3ko mouse embryo fibroblasts (MEFs) were previously shown to support HCV replication more efficiently than wild MEFs [25]. Since the knockout of IPS-1 mainly suppresses signaling in response to virus RNA detection, and maintains an intact IFN response to other stimulants, it may result in minimum interference to adaptive immune responses as compared to IRF3 or IFNARko. Therefore, further development of hCD81-transgenic IPS-1ko mice may serve as a good model for the study of immunological responses against HCV infection. This mouse model can be used as a backbone for any further future models supporting robust HCV infectivity for the study of HCV pathogenesis, propagation and vaccine development.

Material and Methods

Cell culture

HuH7.5.1 cells were cultured in high-glucose Dulbecco's modified Eagle's medium (DMEM; Gibco/Invitrogen, Tokyo, Japan) supplemented with 2 mM L-glutamine, 100 U of penicillin/ml, 100 μg of streptomycin/ml and 10% fetal bovine serum. Mouse primary hepatocytes were isolated from the liver using collagenase perfusion through the inferior vena cava (IVC), while clamping the animal's intrathoracic extension. Hepatocyte isolation and perfusion control were performed as previously described [26]. Primary and immortalized hepatocytes were cultured in a similar medium supplemented with: HEPES (Gibco/Invitrogen), 20 mmol/L; L-proline, 30 μg/mL; insulin (Sigma, St. Louis, MO, USA), 0.5 μg/mL; dexamethasone (Wako, Osaka, Japan), 1×10^{-7} mol/L; $NaHCO_3$, 44 mmol/L; nicotinamide (Wako), 10 mmol/L; EGF (Wako), 10 ng/mL; L-ascorbic acid 2-phosphate (Wako), 0.2 mmol/L; and MEM-non essential amino acids (Gibco/Invitrogen), 1%.

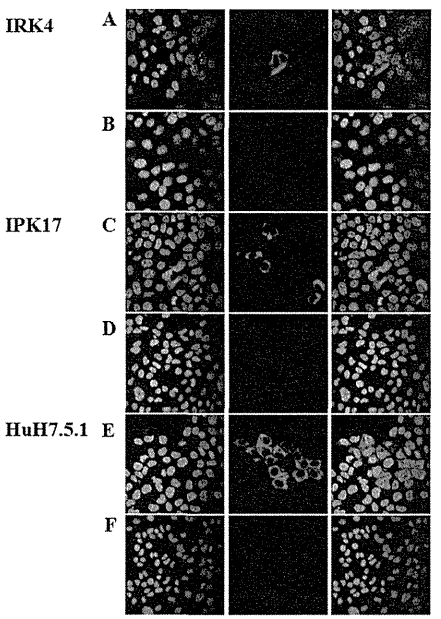

Figure 6. J6JFH1 infection into IRK-4 and IPK17 cells. HCV-NS5A protein detection in mouse IRK4 (A,B) and IPK17 (C,D) and human 7.5.1 cells (E,F). The cells were transduced with lentivirus expressing human CD81 gene at 10 MOI. 48 hours later the cells were infected with 100 times concentrated supernatant medium, collected during 1 week after transfection of HuH7.5.1 cells with J6JFH1-RNA (A, C, and E) or JFH1GND-RNA (B, D, and F).
doi:10.1371/journal.pone.0021284.g006

Gene-disrupted mice

All mice were backcrossed with C57BL/6 mice more than seven times before use. Toll-like receptor adaptor molecule 1 (TICAM-1) ko [27] and IPS-1ko mice [28] were generated in our laboratory (detailed information regarding the IPS-1 mice will be presented elsewhere). All mice were maintained under specific-pathogen-free conditions in the animal facility of the Hokkaido University Graduate School of Medicine (Japan).

RNA extraction, reverse transcriptase polymerase chain reaction (RT-PCR) and real-time RT-PCR

RNA was extracted from cultured cells using Trizol reagent (Invitrogen, San Diego, CA, USA) according to the manufacturer's protocol. Using 1 μg of total RNA as a template, we performed RT-PCR and real-time RT-PCR as previously described [29,30].

In vitro RNA transcription, transfection and preparation of J6JFH1 and Jfh1 viruses

In vitro RNA transcription, transfection into HuH7.5.1 or mouse hepatocytes, and preparation of J6JFH1 and JFH1 viruses, were all performed as previously reported [31]. RNA transfection into human and mouse hepatocytes was performed by electroporation using a Gene Pulser II (Bio-Rad, Berkeley, California) at 260 V and 950 Cap.

HCV infection

J6JFH1 and JFH1 concentrated medium were adjusted to contain a similar RNA copy number by real-time RT-PCR. 2×10^4 cells/well were cultured in 8-well glass chamber slides. After 24 hours, the medium was removed and replaced by concentrated medium containing JFH1 or J6JFH1 viruses. After three hours, the concentrated medium was removed, cells were washed with PBS and incubated in fresh medium for 48 hours, before the detection of infection.

Lentivirus construction, titration and infection

The gene encoding T antigen from simian virus was cloned from plasmid CSII-EF-SVT [32]. The genes encoding human CD81 and occludin were cloned from HuH-7.5.1 cells using the Zero Blunt TOPO PCR Cloning Kit (Invitrogen) according to the manufacturer's protocol. These genes were then inserted into the GFP reporter gene-containing lentiviral expression (pLBIG) vector using the *Eco*RI and *Xho*I restriction sites for SV40T and hCD81, and the *Xba*I and *Xho*I restriction sites for hOccludin. Lentivirus expression vectors were then constructed as previously described [27]. GFP expression was used for the titration of lentivirus vectors, and a multiplicity of infection (MOI) of 10 was used for the infection of mouse cells. Forty-eight hours after the transfection of hCD81 and/or hOccludin, cells were trypsinized and counted. Then, 2×10^4 cells/well were cultured in 8-well glass chamber slides for HCV infection and 5×10^4 cells/well were cultured in 12-well plates, along with 1 ml of medium containing HCVpp, for HCV entry experiments.

HCVpp construction and the detection of luciferase expression

HCVpp containing the E1 and E2 proteins from HCV isolate J6 and expressing the luciferase reporter gene were a kind gift from Dr. Thomas Pietschmann at the TWINCORE Center for Experimental and Clinical Infection Research, Germany. The production of HCVpp and the measurement of luciferase levels were performed as previously described [33].

Indirect immunofluorescence (IF)

IF expression of HCV proteins was detected in the infected cells using antibodies in the serum of chronic HCV patients or rabbit IgG anti-NS5A antibody (Cl-1) (both kind gifts from K. Shimotohno, Chiba Institute of Technology, Japan). Goat anti-human IgG Alexa 594 and goat anti-rabbit Alexa 594 (Invitrogen) were used as secondary antibodies, respectively. Fluorescence

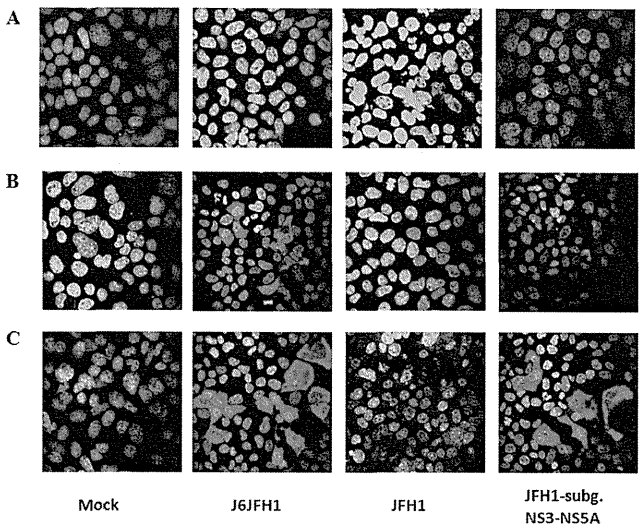

Figure 7. Detection of HCV-NS5A protein in IRK-2 (A), IRK-4 (B) and HuH-7.5 cells (C) by IF 5 days after transfection with J6JFH1, FL-JFH1 or subgenomic JFH1-RNA.
doi:10.1371/journal.pone.0021284.g007

detection was performed on a ZEISS LSM 510 Meta confocal microscope (Zeiss, Jena, Germany).

Detection of cell death

Culture medium was collected from HCV infected and control cells and used for measuring lactate dehydrogenase (LDH) levels using an LDH cytotoxicity detection kit (Takara Biomedicals, Tokyo, Japan). Light absorbance was then measured according to the manufacturer's protocol.

Ethic Statement

This study was carried out in strict accordance with the recommendations in the Guide for the Care and Use of Laboratory Animals of the National Institutes of Health. The protocol was approved by the Committee on the Ethics of Animal Experiments in the Animal Safety Center, Hokkaido University, Japan. All mice were used according to the guidelines of the institutional animal care and use committee of Hokkaido University, who approved this study as ID number: 08-0243, " Analysis of immune modulation by toll-like receptors".

Supporting Information

Figure S1 RT detection of TLR3, TLR7, RIG-I, and IPS-1 expression in mouse hepatocytes. GAPDH expression was used as internal control, and RNA from CD11c+ spleenocytes (dendritic cells) was used as positive control.
(TIF)

Figure S2 Proliferation of HCV in IPS-1, TICAM-1(TRIF) and IFNAR-knockout mouse hepatocytes over time as detected by quantitative real-time RT-PCR analysis of HCV-RNA levels. JFH1GND transfection into IPS-1 knockout cells was used as a negative control to exclude non replicating HCV RNA. The data plotted represent the average +/− STD of 3 different experiments.
(TIF)

Figure S3 RT detection of CD81, Occludin, Claudin 1, SRB1, and LDL receptor expression in primary, IRK4 and IPK17 mouse hepatocytes. GAPDH expression was used as internal control.
(TIF)

Figure S4 Estimation of the transfection efficiency of lentivirus vector expressing green fluorescent protein (GFP) as a reporter, together with hCD81 or hOccludin. 48 hours after transfection with the lentivirus vector, cells were trypsinized and GFP positive cells were detected by BD FACSCalibur (BD Biosciences).
(TIF)

Figure S5 HCV infection of IRK2 cells transfected with lentivirus expressing hCD81 and/or hOccludin. IRK2 cells were transfected with lentivirus expressing empty vector (A), hCD81 (B), hOccludin (C) or hCD81 and hOccludin (D) at a MOI of 10. After 48 hours, the cells were infected with concentrated J6JFH1 transfected 7.5.1 culture medium. After a further three hours, cells were washed with PBS and incubated in fresh medium. After another 48 hours, HCV infection was examined through the detection of HCV-NS5a protein expression by immunofluorescence staining.
(TIF)

Figure S6 HCVpp entry into mouse cells. A similar number of IPK17 and HuH7.5.1 were cultured in triplicate. IPK17 cells were only transfected with lentivirus expressing hCD81, while HuH7.5.1 cells were transfected with empty vector at a MOI of 10. After 48 hours, the medium was replaced with a new medium containing mock VSVG-pp or HCVpp expressing luciferase. After another 48 hours, pseudoparticles entry was determined by measuring the luciferase activity. In order to compare the HCVpp entry between IPK17 and HuH7.5.1 cells, the luciferase expression from VSV-Gpp entry was used an internal control, while that from HCVpp was plotted relatively.
(TIF)

Acknowledgments

We want to thank Dr. Michinori Kohara (Tokyo Metropolitan Institute for Medical Science, Tokyo, Japan); Dr. Tadatsugu Taniguchi (University of Tokyo, Yokyo, Japan); Dr. Thomas Pietschmann (Division of Experimental Virology, TWINCORE, Hannover, Germany); and Dr. Makoto Hijikata (The Institute for Virus Research, Kyoto University, Japan) for their generous supply of research material. Dr. Hussein H. Aly was supported by a JSPS postdoctoral fellowship from the Japan Society for the Promotion of Science.

Author Contributions

Conceived and designed the experiments: HHA TS. Performed the experiments: HHA HO. Analyzed the data: HHA MM HO HS TS. Contributed reagents/materials/analysis tools: KS TW. Wrote the paper: HHA.

References

1. Seto WK, Lai CL, Fung J, Hung I, Yuen J, et al. (2010) Natural history of chronic hepatitis C: Genotype 1 versus genotype 6. J Hepatol.
2. Uprichard SL, Chung J, Chisari FV, Wakita T (2006) Replication of a hepatitis C virus replicon clone in mouse cells. Virol J 3: 89.
3. Ploss A, Evans MJ, Gaysinskaya VA, Panis M, You H, et al. (2009) Human occludin is a hepatitis C virus entry factor required for infection of mouse cells. Nature 457: 882–886.
4. Diamond MS (2009) Mechanisms of evasion of the type I interferon antiviral response by flaviviruses. J Interferon Cytokine Res 29: 521–530.
5. O'Neill LA, Bowie AG (2010) Sensing and signaling in antiviral innate immunity. Curr Biol 20: R328–333.
6. Platanias LC (2005) Mechanisms of type-I- and type-II-interferon-mediated signalling. Nat Rev Immunol 5: 375–386.
7. Tanaka Y, Nishida N, Sugiyama M, Kurosaki M, Matsuura K, et al. (2009) Genome-wide association of IL28B with response to pegylated interferon-alpha and ribavirin therapy for chronic hepatitis C. Nat Genet 41: 1105–1109.
8. Thompson AJ, Muir AJ, Sulkowski MS, Ge D, Fellay J, et al. (2010) Interleukin-28B polymorphism improves viral kinetics and is the strongest pretreatment predictor of sustained virologic response in genotype 1 hepatitis C virus. Gastroenterology 139: 120–129. e118.
9. Sumpter R, Jr., Loo YM, Foy E, Li K, Yoneyama M, et al. (2005) Regulating intracellular antiviral defense and permissiveness to hepatitis C virus RNA replication through a cellular RNA helicase, RIG-I. J Virol 79: 2689–2699.
10. Foy E, Li K, Sumpter R, Jr., Loo YM, Johnson CL, et al. (2005) Control of antiviral defenses through hepatitis C virus disruption of retinoic acid-inducible gene-I signaling. Proc Natl Acad Sci U S A 102: 2986–2991.
11. Oshiumi H, Ikeda M, Matsumoto M, Watanabe A, Takeuchi O, et al. (2010) Hepatitis C virus core protein abrogates the DDX3 function that enhances IPS-1-mediated IFN-beta induction. PLoS One 5: e14258.
12. Oshiumi H, Miyashita M, Inoue N, Okabe M, Matsumoto M, et al. (2010) The ubiquitin ligase Riplet is essential for RIG-I-dependent innate immune responses to RNA virus infection. Cell Host Microbe 8: 496–509.
13. Ishiyama T, Kano J, Minami Y, Iijima T, Morishita Y, et al. (2003) Expression of HNFs and C/EBP alpha is correlated with immunocytochemical differentiation of cell lines derived from human hepatocellular carcinomas, hepatoblastomas and immortalized hepatocytes. Cancer Sci 94: 757–763.
14. Berg CP, Schlosser SF, Neukirchen DK, Papadakis C, Gregor M, et al. (2009) Hepatitis C virus core protein induces apoptosis-like caspase independent cell death. Virol J 6: 213.
15. Deng L, Adachi T, Kitayama K, Bungyoku Y, Kitazawa S, et al. (2008) Hepatitis C virus infection induces apoptosis through a Bax-triggered, mitochondrion-mediated, caspase 3-dependent pathway. J Virol 82: 10375–10385.
16. Zhu H, Dong H, Eksioglu E, Hemming A, Cao M, et al. (2007) Hepatitis C virus triggers apoptosis of a newly developed hepatoma cell line through antiviral defense system. Gastroenterology 133: 1649–1659.
17. Ray RB, Meyer K, Ray R (1996) Suppression of apoptotic cell death by hepatitis C virus core protein. Virology 226: 176–182.
18. Mankouri J, Dallas ML, Hughes ME, Griffin SD, Macdonald A, et al. (2009) Suppression of a pro-apoptotic K+ channel as a mechanism for hepatitis C virus persistence. Proc Natl Acad Sci U S A 106: 15903–15908.
19. Ladu S, Calvisi DF, Conner EA, Farina M, Factor VM, et al. (2008) E2F1 inhibits c-Myc-driven apoptosis via PIK3CA/Akt/mTOR and COX-2 in a mouse model of human liver cancer. Gastroenterology 135: 1322–1332.
20. Lowe SW, Lin AW (2000) Apoptosis in cancer. Carcinogenesis 21: 485–495.
21. Schulze-Bergkamen H, Krammer PH (2004) Apoptosis in cancer–implications for therapy. Semin Oncol 31: 90–119.
22. Ebihara T, Shingai M, Matsumoto M, Wakita T, Seya T (2008) Hepatitis C virus-infected hepatocytes extrinsically modulate dendritic cell maturation to activate T cells and natural killer cells. Hepatology 48: 48–58.
23. Mateu G, Donis RO, Wakita T, Bukh J, Grakoui A (2008) Intragenotypic JFH1 based recombinant hepatitis C virus produces high levels of infectious particles but causes increased cell death. Virology 376: 397–407.
24. Bitzegeio J, Bankwitz D, Hueging K, Haid S, Brohm C, et al. (2010) Adaptation of hepatitis C virus to mouse CD81 permits infection of mouse cells in the absence of human entry factors. PLoS Pathog 6: e1000978.
25. Lin LT, Noyce RS, Pham TN, Wilson JA, Sisson GR, et al. (2010) Replication of subgenomic hepatitis C virus replicons in mouse fibroblasts is facilitated by deletion of interferon regulatory factor 3 and expression of liver-specific microRNA 122. J Virol 84: 9170–9180.
26. Ishigami A, Fujita T, Handa S, Shirasawa T, Koseki H, et al. (2002) Senescence marker protein-30 knockout mouse liver is highly susceptible to tumor necrosis factor-alpha- and Fas-mediated apoptosis. Am J Pathol 161: 1273–1281.
27. Akazawa T, Ebihara T, Okuno M, Okuda Y, Shingai M, et al. (2007) Antitumor NK activation induced by the Toll-like receptor 3-TICAM-1 (TRIF) pathway in myeloid dendritic cells. Proc Natl Acad Sci U S A 104: 252–257.
28. Ebihara T, Azuma M, Oshiumi H, Kasamatsu J, Iwabuchi K, et al. (2010) Identification of a polyI:C-inducible membrane protein that participates in dendritic cell-mediated natural killer cell activation. J Exp Med 207: 2675–2687.
29. Aly HH, Qi Y, Atsuzawa K, Usuda N, Takada Y, et al. (2009) Strain-dependent viral dynamics and virus-cell interactions in a novel in vitro system supporting the life cycle of blood-borne hepatitis C virus. Hepatology 50: 689–696.
30. Aly HH, Shimotohno K, Hijikata M (2009) 3D cultured immortalized human hepatocytes useful to develop drugs for blood-borne HCV. Biochem Biophys Res Commun 379: 330–334.
31. Wakita T, Pietschmann T, Kato T, Date T, Miyamoto M, et al. (2005) Production of infectious hepatitis C virus in tissue culture from a cloned viral genome. Nat Med 11: 791–796.
32. Aly HH, Watashi K, Hijikata M, Kaneko H, Takada Y, et al. (2007) Serum-derived hepatitis C virus infectivity in interferon regulatory factor-7-suppressed human primary hepatocytes. J Hepatol 46: 26–36.
33. Haid S, Windisch MP, Bartenschlager R, Pietschmann T (2010) Mouse-specific residues of claudin-1 limit hepatitis C virus genotype 2a infection in a human hepatocyte cell line. J Virol 84: 964–975.

Cyclosporin A Associated Helicase-Like Protein Facilitates the Association of Hepatitis C Virus RNA Polymerase with Its Cellular Cyclophilin B

Kengo Morohashi[1☯], Hiroeki Sahara[2*], Koichi Watashi[3☯], Kazuki Iwabata[1], Takashi Sunoki[1], Kouji Kuramochi[1], Kaori Takakusagi[1], Hiroki Miyashita[4], Noriyuki Sato[4], Atsushi Tanabe[2], Kunitada Shimotohno[5], Susumu Kobayashi[1], Kengo Sakaguchi[1], Fumio Sugawara[1]

1 Genome and Drug Research Center, Tokyo University of Science, Noda, Chiba, Japan, **2** Laboratory of Biology, Azabu University School of Veterinary Medicine, Sagamihara, Kanagawa, Japan, **3** Department of Virology II, National Institute of Infectious Diseases, Shinjuku-ku, Tokyo, Japan, **4** Department of Pathology, Sapporo Medical University School of Medicine, Sapporo, Hokkaido, Japan, **5** Research Institute, Chiba Institute of Technology, Narashino, Chiba, Japan

Abstract

Background: Cyclosporin A (CsA) is well known as an immunosuppressive drug useful for allogeneic transplantation. It has been reported that CsA inhibits hepatitis C virus (HCV) genome replication, which indicates that cellular targets of CsA regulate the viral replication. However, the regulation mechanisms of HCV replication governed by CsA target proteins have not been fully understood.

Principal Findings: Here we show a chemical biology approach that elucidates a novel mechanism of HCV replication. We developed a phage display screening to investigate compound-peptide interaction and identified a novel cellular target molecule of CsA. This protein, named CsA associated helicase-like protein (CAHL), possessed RNA-dependent ATPase activity that was negated by treatment with CsA. The downregulation of CAHL in the cells resulted in a decrease of HCV genome replication. CAHL formed a complex with HCV-derived RNA polymerase NS5B and host-derived cyclophilin B (CyPB), known as a cellular cofactor for HCV replication, to regulate NS5B-CyPB interaction.

Conclusions: We found a cellular factor, CAHL, as CsA associated helicase-like protein, which would form trimer complex with CyPB and NS5B of HCV. The strategy using a chemical compound and identifying its target molecule by our phage display analysis is useful to reveal a novel mechanism underlying cellular and viral physiology.

Citation: Morohashi K, Sahara H, Watashi K, Iwabata K, Sunoki T, et al. (2011) Cyclosporin A Associated Helicase-Like Protein Facilitates the Association of Hepatitis C Virus RNA Polymerase with Its Cellular Cyclophilin B. PLoS ONE 6(4): e18285. doi:10.1371/journal.pone.0018285

Editor: Robyn Klein, Washington University, United States of America

Received April 15, 2010; **Accepted** March 2, 2011; **Published** April 29, 2011

Funding: This work was supported by The Promotion and Mutual Aid Corporation for Private Schools of Japan, Grant-in-Aid for Matching Fund Subsidy for Private Universities. The funders had no role in study design, data collection and analysis, decision to publish, or preparation of the manuscript.

Competing Interests: The authors have declared that no competing interests exist.

* E-mail: sahara@azabu-u.ac.jp

☯ These authors contributed equally to this work.

Introduction

Cyclosporin A (CsA) possesses immunosuppressive effects and is widely used for allogeneic transplantation [1]. These therapeutic effects of CsA, in particular downregulation of interleukin 2 (IL-2) production by T cells, are considered to be responsible for the suppression of immunological events via cellular immunology [2,3]. Its mechanism is widely believed to include CsA binding to its primary cytoplasmic receptor cyclophilin A (CyPA). This CsA/CyPA complex inhibits the phosphatase activity of calcineurin, which is essential for the activation of nuclear factor of activated T cells (NFAT) transcription factors and their downstream cytokine production [2–5]. The cyclophilins (CyP), identified as cytoplasmic receptors for CsA are a family of peptidylprolyl cis-trans isomerases (PPIase) and include more than ten subtypes [6–8]. Recently, it was reported that several CyPs regulated hepatitis C virus (HCV) replication; CyPA binds to HCV NS5A and NS5B proteins. CyPB also interacted with HCV NS5A and NS5B [9–11]. The interaction of CyPB stimulates the RNA binding activity of NS5B. These viral-cellular interaction mechanisms were revealed by a chemical biological analysis focusing on an anti-viral characteristic of CsA. However, it has not been fully understood how a series of CsA-target proteins regulate HCV replication. We obtained the data suggesting the possibility that CsA target factor(s) other than CyP family also modify HCV replication.

To exploit a novel drug target is a challenging but a powerful strategy to elucidate unknown aspects of cellular physiology that are modified by the compound. In this study, we identify a CsA binding factor by a phage display method. There are various methods to isolate targets of small molecules. Most of the methods, however, require tagged small molecules for screening to separate the drug and protein complex. The steps to synthesize tagged small molecules are technically limited in the case of complicated molecules such as CsA. To overcome this limitation, we recently developed a labeling method that can be theoretically utilized for any chemical substance [12]. A highly reactive carbene induced by UV irradiation reacts with CsA, resulting in the production of immobilized CsA in a nonspecific manner. By using the photoaffinity method, we successfully immobilized CsA on resins and performed phage display screening. This method cloned a CsA associated helicase-like protein, which we termed CAHL, and this protein was shown to interact with HCV replication machinery. Our result presents an example for the chemical biological method that could facilitate to reveal a mechanism of viral-cellular interaction.

Results

Phage display screening with immobilized CsA isolated CsA associated helicase-like protein, CAHL

To explore CsA binding proteins, we applied a chemical biology approach. In general, small molecule is necessary to be chemically modified such as biotinylated to be immobilized on solid surface for isolation of binding proteins. However, due to the structural complexity of CsA, it is technically challenging to chemically modify a certain residue of CsA. Therefore, we took advantage of photoaffinity coupling method, which we previously developed [12]. The highly reactive carbene induced by UV irradiation reacted with CsA, resulting in the production of immobilized CsA on solid surface in a nonspecific manner (Fig. 1A). We performed phage display screening with multiple cycles that consist of binding, washing, recovery and amplification (Fig. 1B). We used phage particles randomly displayed 12 amino acids as a library [13]. Through the screening cycles, the ratios of eluted phage particles associated with CsA-immobilized resins comparing to input were dramatically increased (Fig. 1C). We randomly picked up 22 single phage clones from the sixth panning elution (Table S1). Five out of the 22 phage clones were identical, and we called it phage #13. In order to validate the binding specificity of the phage, we amplified phage #13 and measure the ratio of eluted phage titer with CsA and mock resins, which were treated with MeOH to block photoaffinity reaction. The ratio of the phage #13 was 3.75, whereas randomly picked up phage was 1.00. These results indicated that the phage #13 specifically associated with CsA-immobilized resins.

CAHL has an RNA-dependent ATP hydrolysis activity

Phage #13 was predicted to display amino acids, LVFGTLLGQLRA, in the carboxyl terminus of its phage-coat protein, which is responsible for interaction with CsA. We searched the protein database to find proteins that showed similarities to the LVFGTLLGQLRA sequence. As a result of the search, we found a protein with a sequence identical to LLGQLRA, encoded by a gene accession number NM_022828 in the NCBI database. NM_022828 is predicted to encodes 1430 amino acid protein that has a couple of conserved domains, such as DEXHc helicase, RNA-dependent ATPase and ankyrin repeat (Fig. 2A; Fig S1). LLGQLRA sequence is located in the middle region of the protein (amino acids 940–946), where is no known conserved motif is found (Fig. 2A). Since it has not been reported on its biological functions, hereafter we refer to the NM_022828 as CsA-associated helicase-like protein, CAHL. To confirm the interaction between CAHL and CsA, we prepared a recombinant C-terminal protein of CAHL (named CAHL-C) that consisted of amino acids 761 to 1430 (Fig. 2B) including LLGQLRA motif, and performed surface plasmon resonance (SPR) analysis. It was difficult to use a full-length CAHL for *in vitro* pull-down assays since obtaining enough amount of full-length CAHL for SPR was technically challenging due to high insolubility. Considering that CsA binding sequence found by the phage display screening is located C-terminus of CAHL, we used CAHL-C protein. A specific binding response with CsA was observed ($KD = 1.2\times10^{-7}$ M), whereas those with FK506, which is an immunosuppressant and has no HCV-inhibitory activity, were significantly weak ($KD = 2.5\times10^{-6}$ M) (Fig. 2C). Since CAHL was predicted to be RNA-dependent ATPase based on conserved domains (Fig. 2A), we measured the ATPase activity of CAHL in the presence and absence of RNA. As shown in Fig.2D, RNA-dependent ATP hydrolytic activity of CAHL-C was clearly observed, and this activity was suppressed in

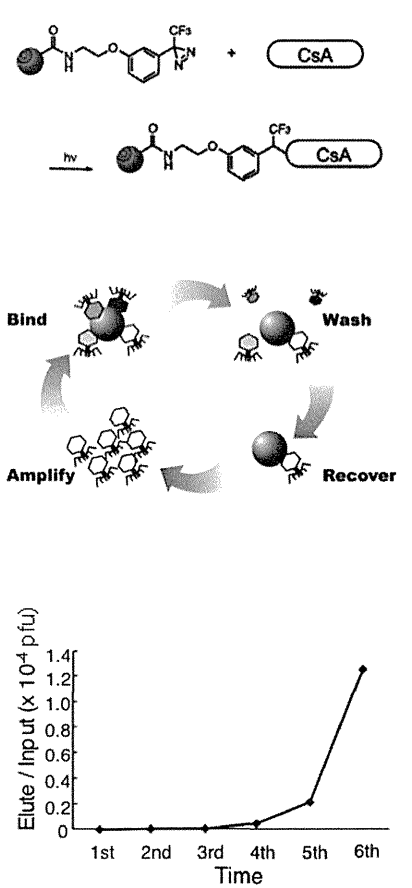

Figure 1. Immobilization of CsA and phage display screening. (A) A schematic diagram of CsA immobilization on photoaffinity resins. (B) Procedure of phage display screening. (C) Relative enrichment of phage particles. Relative enrichment was determined by the relationship between phage titer of elution from a CsA immobilized resins and input.
doi:10.1371/journal.pone.0018285.g001

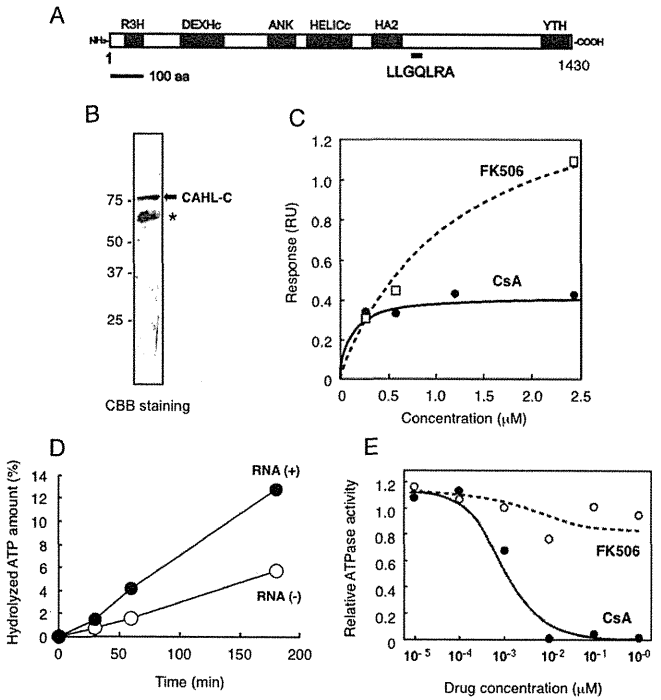

Figure 2. Cloning of CsA associated helicase-like protein (CAHL) by phage display screening. (A) Schematic representation of CAHL protein. R3H (*cd*02325), DEXHc (*cd*00269), ANK (*cd*00204), HELICc (*smart*00490), HA2 (*pfam*04408) and YTH (*pfam*04146) motifs were found by a CD search (http://www.ncbi.nlm.nih.gov/Structure/edd/wrpsb.cgi). Underline indicates a region of the LLGQRA amino acid sequence identical to the CsA-associated sequence displayed on phage #13. (B) Purified recombinant CAHL-C protein was confirmed by SDS-PAGE analysis (arrow). Asterisk indicates degraded products. (C) A kinetic plot and binding isotherm for binding of CsA (closed circle) and FK506 (opened square) to CAHL-C sensor chips in concentrations ranging from 0.25 to 2.5 mM. The estimated KD value of interaction between CAHL-C and CsA or FK506 was 1.2×10^{-7} or 2.5×10^{-6} M, respectively. (D) RNA-dependent ATP hydrolytic activities of CAHL. Filled and open circles indicate ATP hydrolytic activities of CAHL in the presence (closed circle) or absence (opened circle) of total RNA extracted from liver cells, respectively. (E) CsA inhibitory effects on ATP hydrolytic activities of CAHL. Filled and open circles indicate ATP hydrolytic activities with CsA (closed circle) or FK506 (opened circle), respectively.
doi:10.1371/journal.pone.0018285.g002

a dose-dependent manner when CsA, but not FK506 (Fig. 2E). A difference of inhibitory effects of CsA and FK506 on CAHL-C hydrolytic activity is more than 2-orders of magnitude. Considering that the difference of *KD*s of CsA and FK506 values measured by SPR, CsA association with CAHL would significantly affect on the activity. These results indicate that CAHL had RNA-dependent ATPase activity and was specifically inhibited by CsA.

CAHL is localized in ER and its expression is up-regulated by TNF-α treatment

Since biological functions of CAHL were unknown, we investigated the biological background of the CAHL gene. We first performed RNA blotting analysis and RT-PCR using normal human tissues and tumor cells. As shown in Fig. 3A, CAHL-transcripts with approximately 1.6 kbp were detected in both human hepatoma Huh-7 cells and MH-14 cells, which do not and do carry the HCV subgenome replicon, respectively, whereas much less was detected in normal liver tissues. RT-PCR analysis revealed that in other normal tissues (though not testis) little or no expression of CAHL was observed as compared the house-keeping gene G6PDH, whereas clear expression of it was detected in all the tumor cell lines examined (Fig. 3B). Since the CAHL expression was very little in the normal liver tissues, a question was arisen: how is CAHL expression regulated? It is possible that CAHL could be induced by inflammation caused by virus infections. To test the hypothesis, we observed whether CAHL expressions are induced by inflammatory signals. Indeed, CAHL in normal liver cells was upregulated in the presence of a proinflammatory cytokine, tumor necrosis factor (TNF)-α with dose dependent manner (Fig. 3C), suggesting that CAHL can express to some extent in the liver under chronic hepatitis. Next, we observed CAHL subcellular localization in Huh-7 and MH-14 cells using an anti-CAHL antibody (Fig. 3D). Fluorescence derived from CAHL

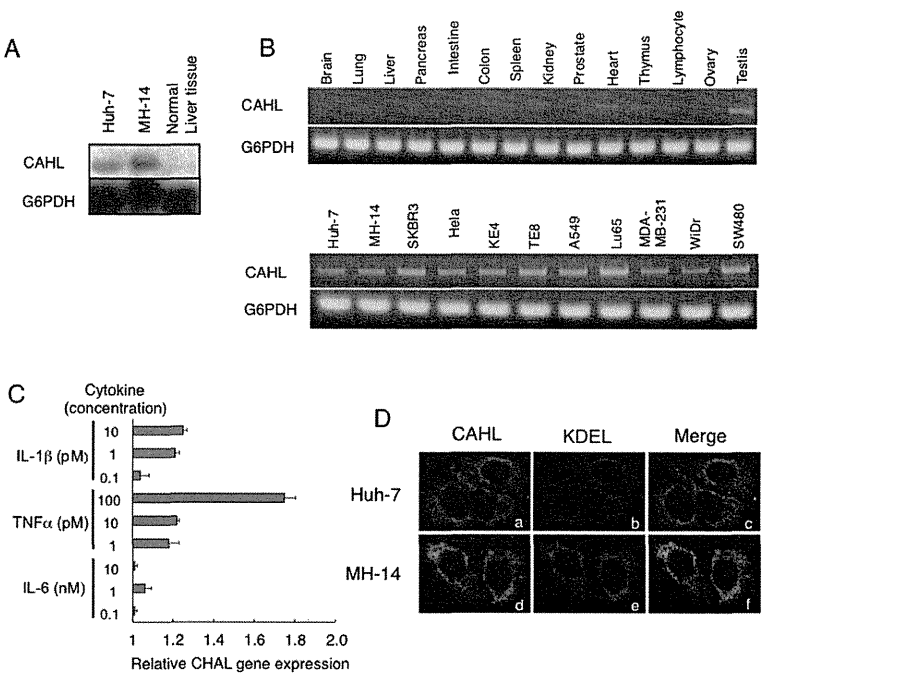

Figure 3. Expression profile of CAHL. (A) For Northern blot analysis, CAHL and G6PDH as an internal control were detected in RNAs derived from Huh-7 and MH-14 cells, as well as normal liver tissues. (B) RT-PCR analysis for CAHL, and G6PDH as an internal control, were performed using RNAs derived from normal human tissues and tumor cells. (C) CAHL in normal liver cells was upregulated by TNF-α. Normal liver cells were cultured in the presence of proinflammatory cytokines, IL-1β, TNF-α, and IL-6 at the indicated concentrations for 8 h. Subsequently, cells were harvested, and measurement of these cells derived-CAHL gene expression by quantitative analysis by was performed using the LightCycler system. These data represent as relative rates (1 = non-treated cells). Error bars represent the standard error of the mean. (D) Colocalization of CAHL with KDEL as an endoplasmic reticulum (ER) marker. Indirect immunofluorescence analysis was performed on Huh-7 and MH-14 cells. Cells stained with anti-CAHL (panels a and d, green) and an anti-KDEL mAb (panels b and e, red) for ER identification as a marker used as a primary antibody followed by Alexa Fluor 488-conjugated goat anti-rabbit and 594-conjugated goat anti-mouse antibodies, respectively. Merged images of green and red signals are shown in panels c and f.The optically merged image is representative of most cells examined by laser confocal microscopy. Original magnification: x1000.
doi:10.1371/journal.pone.0018285.g003

demonstrated that CAHL was co-localized with KDEL protein as a marker for endoplasmic reticulum (ER) in both the presence (MH-14 cells) and absence (Huh-7 cells) of the HCV subgenome, indicating that CAHL could localize in ER with HCV independent manner. Moreover, it was observed that CAHL also colocalized with HCV-derived proteins such as NS3, NS4A, NS4B, NS5A and NS5B localized in ER (Fig. S2). Thus, these data strongly suggested that CAHL would localize in ER.

Association of CAHL, NS5B and CyPB

Since CAHL interacts CsA, which has inhibitory effects to HCV replication, it is interesting to investigate the molecular interactions of CAHL and HCV-derived molecules involving the replication machinery. Intriguingly, the purified full-length CAHL fused to GST was coprecipitated with NS5B but not NS3, NS4B or NS5A protein, as shown in Fig. 4A. To determine a regions of NS5B responsible for binding with CAHL, various dissected NS5B proteins were subjected to pull-down assays, resulting in that two separated regions (1–200 aa or 401–520 aa) of NS5B were sufficient for the interaction with CAHL (Fig. 4B). In addition to the CAHL and NS5B interaction, we found interaction between CAHL and CyPB, but not CyPA (Fig. 4C). The interaction of CAHL and CyPB was disrupted with presence of CsA, whereas the association of CAHL with NS5B was not (Fig. 4D). These results suggest that trimer complex consisting of CAHL, CyPB and NS5B could form.

CAHL has a main role in HCV-replication via NS5B

The finding that CAHL structurally associated with the CyPB/NS5B complex in cell-free assessment prompted us to examine whether this trimer complex could act for HCV genome replication *in vivo*. First, five small interference RNAs (siRNA)